2011

The Role of Nogo-A in Memory and Neuronal Plasticity in the Aged Rodent Brain

Rebecca Lynn Gillani
Loyola University Chicago

LOYOLA UNIVERSITY CHICAGO

THE ROLE OF NOGO-A IN MEMORY AND NEURONAL PLASTICITY IN THE AGED RODENT BRAIN

A DISSERTATION SUBMITTED TO

THE FACULTY OF THE GRADUATE SCHOOL

IN CANDIDACY FOR THE DEGREE OF

DOCTOR OF PHILOSOPHY

PROGRAM IN NEUROSCIENCE

BY

REBECCA LYNN GILLANI

CHICAGO, ILLINOIS

MAY 2011

ACKNOWLEDGEMENTS

I would like to thank my family and friends for their support and encouragement, especially my husband Khurram.

I would also like to thank the members of Dr. Greenough's and Dr. Gold's laboratories for providing me with valuable laboratory experience before entering graduate school.

The Kartje laboratory has been a wonderful environment for me to learn and develop as a researcher, and I thank all of its members for their assistance and encouragement. I especially thank Dr. Kartje for her mentorship.

Additionally, I thank my committee members for their valuable help in designing and completing this dissertation.

Finally, I thank the support that has made these experiments possible. This work was supported by the Department of Veterans Affairs, NINDS grant 40960, NINDS grant F30NS060560, the Loyola University Chicago Neuroscience Institute, and the Illinois Regenerative Medicine Institute. I thank Novartis Pharma AG for the gift of the monoclonal antibodies.

TABLE OF CONTENTS

LIST OF FIGURES

LIST OF ABBREVIATIONS

AAV	Adeno-Associated Virus
ALS	Amyotrophic Lateral Sclerosis
APP	Amyloid Precursor Protein
BACE1	β-site APP Cleaving Enzyme 1
BAEP	Brainstem Auditory Evoked Potentials
BOLD	Blood Oxygenation Level Dependent
CCA	Common Carotid Artery
CNS	Central Nervous System
DRG	Dorsal Root Ganglia
EAE	Experimental Autoimmune Encephalomyelitis
EGFR	Epidermal Growth Factor Receptor
EMG	Electromyogram
FGF	Fibroblast Growth Factor
fMRI	Functional Magnetic Resonance Imaging
GAP-43	Growth-Associated Protein-43
GFAP	Glial Fibrillary Acidic Protein
GPI	Glycosylphosphatidyl Inositol
IEE	Integration Efficiency Element
IU	Infectious Units

kD	kiloDalton
LIMK1	Lin-11, Isl-1, Mec-3 Kinase 1
LTD	Long Term Depression
LTP	Long Term Potentiation
MAG	Myelin-Associated Glycoprotein
MCAO	Middle Cerebral Artery Occlusion
miRNA	MicroRNA
MTP	Matching-to-Place
NEP1-40	Nogo-66 (1-40) Antagonist Peptide
NGF	Nerve Growth Factor
NgR1/NgR	Nogo-66 Receptor
NGS	Normal Goat Serum
OMgp	Oligodendrocyte-Myelin Glycoprotein
PBS	Phosphate Buffered Saline
PirB	Paired Immunoglobulin-Like Receptor B
PKC	Protein Kinase C
PNS	Peripheral Nervous System
PPI	Prepulse Inhibition
Rho-GDI	Rho-Guanine Dissociation Inhibitor
ROCK	Rho Kinase
RISC	RNA-Induced Silencing Complex
RNAi	RNA Interference
SG	Stratum Granulosum

shRNA	Small Hairpin RNA
siRNA	Short Interfering RNA
SL	Stratum Lucidum
SLM	Stratum Lacunosum-Moleculare
SM	Stratum Moleculare
SO	Stratum Oriens
SP	Stratum Pyramidale
SR	Stratum Radiatum
STAIR	Stroke Therapy Academic Industry Roundtable
TNFR	Tumor Necrosis Factor Receptor
tPA	Tissue-Type Plasminogen Activator
TTC	2,3,5-triphenyl-2H-tetrazolium chloride
TX100	Triton-X 100

ABSTRACT

The long-term effects of stroke often include cognitive impairments, but other than cognitive rehabilitation, which is often not fully successful, there is no intervention to treat cognitive impairments in stroke survivors. Our laboratory has previously shown that immunotherapy directed against the Nogo-A protein, which is enriched on oligodendrocytes, improves recovery of skilled forelimb sensorimotor function in adult and aged rats after an ischemic stroke lesion to the sensorimotor cortex. Furthermore, this recovery was correlated with axonal sprouting from intact pathways to denervated areas, as well as dendritic sprouting and increased dendritic spine density in the contralateral sensorimotor cortex. In the present project we aimed to investigate whether anti-Nogo-A immunotherapy improves performance on a spatial memory task after a sensorimotor cortical stroke in aged rats. We found that rats with ischemic stroke and treated with anti-Nogo-A immunotherapy performed better on the reference memory portion of the Morris water maze than control antibody treated rats. In the hippocampus, a brain area important for spatial memory, we found a decrease in dendritic complexity on the same side as the stroke when compared to normal aged rats. However, anti-Nogo-A immunotherapy did not prevent this decrease in dendritic complexity in the hippocampus on the same side as the stroke lesion. To further investigate whether Nogo-A plays a role in dendritic structural plasticity, and specifically the Nogo-A found in neurons, we used RNA interference to reduce the levels of Nogo-A in hippocampal CA1 pyramidal cells in aged

rats. We did not detect any changes in dendritic spine density and morphology. Taken together this suggests that anti-Nogo-A immunotherapy may be a successful treatment for cognitive impairments caused by stroke, although the potential neuroanatomical basis for this recovery is still under investigation.

CHAPTER ONE

OVERVIEW AND HYPOTHESIS

Each year in the United States 795,000 people have a new or recurrent stroke (Lloyd-Jones et al., 2009). In ischemic stroke survivors over the age of 65, nearly 50% have cognitive deficits six months post-stroke (Kelly-Hayes et al., 2003). Furthermore, stroke patients without dementia at a baseline evaluation had a faster decline in memory performance as compared to aged individuals without stroke (Reitz et al., 2006). Cognitive rehabilitation is currently the only treatment for the long-term cognitive impairments caused by stroke and is often not successful. With the burdens that cognitive impairment places on survivors of stroke and their care-givers, it is important to develop new treatments for cognitive impairments after stroke.

A promising novel treatment for stroke is anti-Nogo-A immunotherapy, which is directed against Nogo-A, the myelin associated inhibitor of axonal growth (Gonzenbach et al., 2008). After sensorimotor cortical stroke in adult and aged rats anti-Nogo-A immunotherapy given one week later improved performance on a skilled forelimb reaching task (Papadopoulos et al., 2002a; Markus et al., 2005b; Seymour et al., 2005a; Tsai et al., 2007). The improved performance was correlated in adult rats with axonal sprouting across the midline from intact pathways to denervated areas (Papadopoulos et al., 2002a; Seymour et al., 2005a), and with dendritic sprouting and increased dendritic spine density in the contralesional sensorimotor cortex (Papadopoulos et al., 2006).

Anti-Nogo-A immunotherapy has been shown to improve cognitive performance on a spatial memory task after traumatic brain injury in adult rats (Lenzlinger et al., 2005b; Marklund et al., 2007a), and to induce recovery from severe neglect caused by a cortical lesion (Brenneman et al., 2008b). Whether anti-Nogo-A immunotherapy improves cognitive performance in aged rats after a stroke has not yet been investigated. Additionally, the role that Nogo-A plays in dendritic structural plasticity in the aged hippocampus, an area important for spatial memory, has not yet been investigated.

HYPOTHESIS

Neutralizing the Nogo-A protein will improve memory performance after stroke in the aged by enhancing neuronal plasticity.

Specific Aim 1: Determine whether anti-Nogo-A immunotherapy will improve performance on a spatial memory task after stroke in the aged. Aged rats will be tested on the Morris water maze after stroke and intracerebroventricular treatment with anti-Nogo-A immunotherapy or a control antibody.

Specific Aim 2: Determine whether anti-Nogo-A immunotherapy will induce dendritic plasticity in the hippocampus after stroke in the aged. The brains from the animals from aim 1 will be processed for Golgi-Cox staining, and CA3 and CA1 pyramidal neurons, and dentate gyrus neurons will be analyzed for dendritic complexity and dendritic spine density and morphology.

Specific Aim 3: Determine whether knockdown of *neuronal* Nogo-A will induce structural changes in dendritic spines in the hippocampus of aged rats. Aged rats will be injected with either a control virus carrying the EGFP reporter transgene, or a virus carrying genes for a small hairpin RNA (shRNA) directed against Nogo-A and EGFP, and four weeks later CA1 pyramidal cells will be analyzed for dendritic spine density and morphology.

CHAPTER TWO

REVIEW OF LITERATURE

NEURONAL PLASTICITY IN THE DEVELOPING AND ADULT CNS

Kennard Principle

In the 1930's Margaret Kennard showed that non-human primates given motor cortical injury during development had better functional recovery than monkeys given motor cortical injury as adults (Kennard, 1936, 1938). The idea that there is improved recovery from CNS damage in the young as compared to adults became known as the "Kennard Principle," though recovery in the young after CNS damage seems to depend upon the location and age (Schneider, 1979; Kolb et al., 1989). Improved functional recovery in the young after CNS damage seems to be based upon neuroanatomical plasticity, or changes in the structure of dendrites and axons (Kolb and Whishaw, 1989). For example, after unilateral sensorimotor cortical lesions in neonatal rats axons from the intact corticospinal tract sprouted across the midline to innervate denervated areas, and these axons were functionally connected to the intact hemisphere (Kartje-Tillotson et al., 1987; Barth et al., 1990). Neuronal plasticity does occur in the adult CNS, but it is very limited (Cotman et al., 1981; Darian-Smith et al., 1995; Goldman et al., 1997; Bareyre et al., 2004; Schaechter et al., 2006).

GROWTH INHIBITORY ENVIRONMENT OF THE ADULT CNS

The Discovery of Nogo-A

After injury to the adult CNS axons are unable to regenerate or sprout more than a couple of mm, but after injury to the adult peripheral nervous system (PNS) axons grow long distances (Davies et al., 1996). In a landmark experiment, Aguayo and his colleague took a segment of sciatic nerve from a rat and positioned one end of the graft at the medulla and the other end at the thoracic spinal cord. After 5.5-7.5 months the rats were sacrificed, and axons of brain stem and spinal cord neurons were found to have grown more than 30 millimeters into the sciatic nerve graft (David et al., 1981). This experiment suggested that the environment of the PNS allows for axonal growth, while the environment of the CNS does not. The lack of axonal growth in the CNS as opposed to the PNS could be due to differences in availability of trophic factors, or to a non-permissive substrate in the CNS. To differentiate between these possibilities, Schwab et al. cultured neurons in the center of a three-compartment chamber in the presence of nerve growth factor (NGF) with a sciatic nerve segment extending from the center to one side chamber and a optic nerve segment extending from the center to the other side chamber. After 10 to 20 days in culture axons were found extending through the sciatic nerve and entering the side chamber, but no axons were found in the optic nerve, and the same results were shown even when the nerve segments were dead (Schwab et al., 1985). This experiment suggests that the lack of axonal growth in the CNS is due to a non-permissive substrate rather than a lack of trophic factors, because axons did not grow into the optic nerve segment even with the presence of nerve growth factor.

Schwab and his colleagues went on to show that differentiated oligodendrocytes and spinal cord myelin, but not astrocytes and immature oligodendrocytes, are non-permissive for neurite growth and fibroblast spreading (Schwab et al., 1988). Next they isolated 35- and 250-kD membrane bound proteins (NI-35/250) from rat myelin that are non-permissive for neurite growth and fibroblast spreading (Caroni et al., 1988c). The IN-1 monoclonal antibody raised against the NI-35 and NI-250 proteins in part neutralized the non-permissive properties of CNS myelin for neurite growth and fibroblast spreading *in vitro* (Caroni et al., 1988a).

A bovine homologue of NI-250 called bNI-220 was isolated and it was found that the IN-1 monoclonal antibody in part neutralized the neurite growth and fibroblast spreading properties of bNI-220 (Spillmann et al., 1998). Six peptide sequences were obtained during the purification of bNI-220, and from this information in 2000 the gene encoding NI-220/250 was cloned independently by three groups and named Nogo-A (Chen et al., 2000b; GrandPre et al., 2000; Prinjha et al., 2000).

The Signaling Pathway of Nogo-A

Three splice variants, Nogo-A, -B, and –C, are produced from the Nogo gene by alternative splicing and alternate promoter usage (Chen et al., 2000b; GrandPre et al., 2000; Prinjha et al., 2000). Nogo-A has three active sites as follows: a Nogo-A/-B N-terminal region that inhibits fibroblast spreading; a Nogo-A specific region that inhibits neurite outgrowth, induces growth cone collapse, and inhibits fibroblast spreading; and a C-terminal region, Nogo-66, common to all three is forms that induces growth cone

collapse (Oertle et al., 2003). Nogo-A is an integral membrane protein that has a di-lysine endoplasmic reticulum retention signal at the C terminus but no signal sequence at the N-terminus (Chen et al., 2000b; GrandPre et al., 2000; Prinjha et al., 2000). Nogo-A is highly enriched in the endoplasmic reticulum, but is also found in the cell membrane with all three active sites exposed to the extracellular space (GrandPre et al., 2000; Dodd et al., 2005).

Additional molecules contribute to the growth inhibitory environment of the adult CNS, including chondroitin sulfate proteoglycans (Niederost et al., 1999; Schmalfeldt et al., 2000), myelin-associated glycoprotein (MAG, McKerracher et al., 1994; Mukhopadhyay et al., 1994), oligodendrocyte and myelin glycoprotein (OMgp, Wang et al., 2002b), and the repulsive axon guidance molecules Ephrin B3 (Benson et al., 2005), and Semaphorin 4D (Moreau-Fauvarque et al., 2003). With the exception of the chondroitin sulfate proteoglycans, which are extracellular matrix molecules, all of these growth inhibitory molecules can be found in myelin (Yiu et al., 2006). The CNS of adult higher vertebrates loses the capacity to regenerate concurrently with the onset of myelination (Ferretti et al., 2003). This suggests the importance of myelin proteins in inhibiting neuronal plasticity and regeneration in the CNS.

A common receptor was identified called the Nogo-66 receptor (NgR1) that bound to the Nogo-66 domain common to all three isoforms of Nogo, along with MAG, and OMgp (Fournier et al., 2001; Domeniconi et al., 2002; Wang et al., 2002b). With this discovery it was hypothesized that myelin growth inhibitors converged on the NgR1 to inhibit growth (Fig 1, Giger et al., 2008). However, evidence has revealed that it is

more likely that myelin growth inhibitors signal through multiple receptor systems, and the contribution of each receptor system may vary depending upon the type of neuron (Giger et al., 2008). Indeed an additional receptor called paired immunoglobulin-like receptor B (PirB) has been found to bind Nogo-66, MAG and OMgp to inhibit neurite outgrowth (Atwal et al., 2008).

The NgR1 contains eight leucine rich repeat domains, and is linked to the membrane by a glycosylphosphatidyl inositol (GPI) anchor (Fournier et al., 2001). The NgR1 does not cross the membrane so it requires co-receptors for signal transduction. Several co-receptor molecules have been identified, including p75 (Wang et al., 2002a) and TROY (Park et al., 2005), members of the tumor necrosis factor receptor (TNFR) family, and LINGO-1 (Mi et al., 2004).

Several pathways have been identified in the intracellular signaling of myelin inhibitors (Fig 1). First, Nogo-A and MAG activate the small GTPase RhoA (Lehmann et al., 1999; Niederost et al., 2002; Fournier et al., 2003) by releasing it from the inhibitory regulator Rho-guanine dissociation inhibitor (Rho-GDI, Yamashita et al., 2003). RhoA activates Rho Kinase (ROCK), and it is thought that ROCK activates Lin-11, Isl-1, Mec-3 Kinase 1 (LIMK1) by phosphorylation (Hsieh et al., 2006). The activated LIMK1 then phosphorylates and inactivates cofilin, an actin depolymerization factor (Hsieh et al., 2006). Secondly, Nogo and MAG cause an increase in intracellular calcium (Bandtlow et al., 1993; Wong et al., 2002; Hasegawa et al., 2004) and activation of Protein Kinase C (PKC, Hasegawa et al., 2004; Sivasankaran et al., 2004). Finally, NgR1 activation also

leads to phosphorylation and transactivation of the epidermal growth factor receptor (EGFR) by calcium signaling (Koprivica et al., 2005).

Interestingly, it has been demonstrated that the Nogo-A specific region, also known as the Amino-Nogo domain, can regulate RhoA independent of the NgR1/p75 pathway, suggesting that the Nogo-A specific region has a distinct binding site (Schweigreiter et al., 2004). Recently it was found that the Amino-Nogo domain of Nogo-A may inhibit integrin signaling to inhibit neurite growth (Hu et al., 2008).

Analysis of gene and protein changes after Nogo-A neutralization gives further insight into Nogo-A signaling. In rat hippocampal slice cultures the anti-Nogo-A antibodies 11C7 and 7B12 cause changes in RNA transcripts for genes related to growth, including genes function in the extracellular matrix, cell adhesion, neurogenesis, GTPase signal transduction, and growth factors (Craveiro et al., 2008b). In genetically modified mice lacking Nogo-A samples from unlesioned spinal cords showed changes in protein expression in proteins related to the cytoskeleton, signaling, neuroprotection, metabolism and transport as compared to wild-type mice (Montani et al., 2009).

Signaling Pathways of Myelin Inhibitors

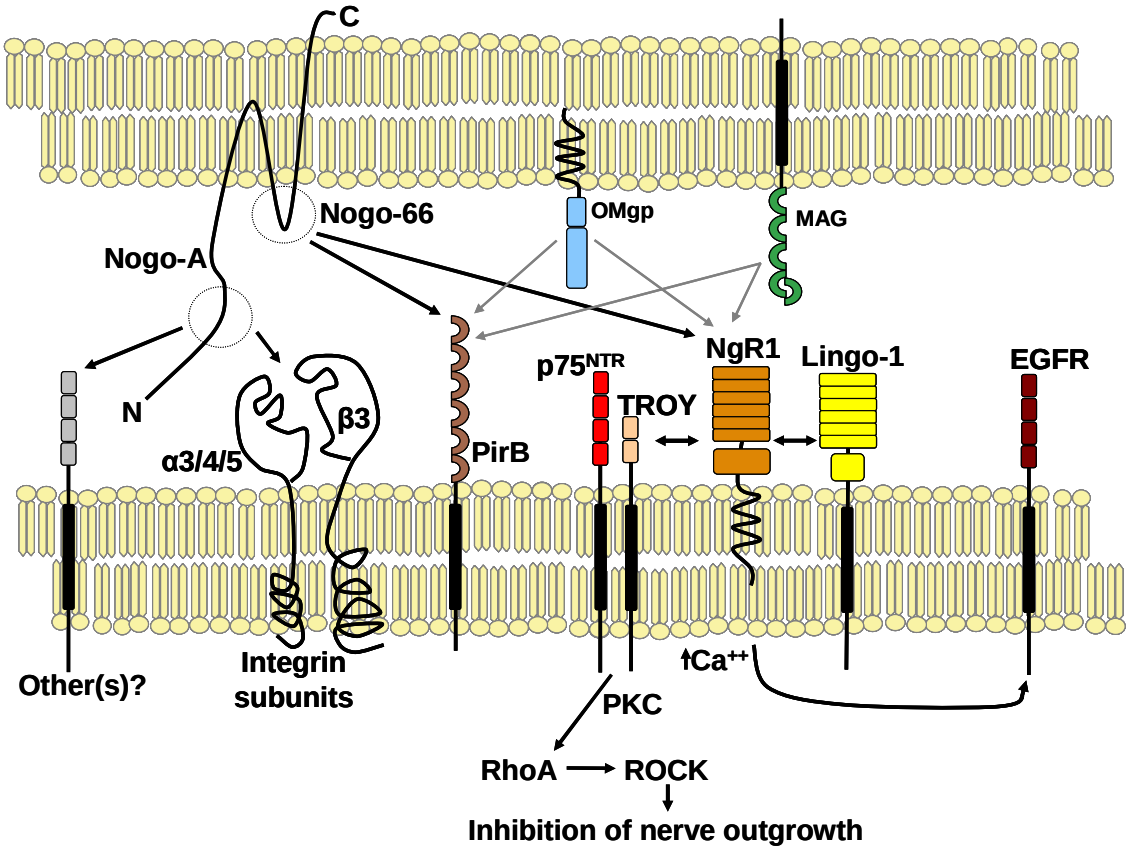

Compliments of Alicia Case

Figure 1. Signaling Pathways of Myelin Inhibitors.

ANTI-NOGO-A IMMUNOTHERAPY, AND OTHER METHODS TO NEUTRALIZE NOGO-A, ENHANCE FUNCTIONAL RECOVERY AND NEURONAL PLASTICITY AND REGENERATION AFTER CNS INJURY

Cortical Lesions, Stroke and Traumatic Brain Injury in Rodents

In the 1990's Schwab and his colleagues showed that the IN-1 anti-Nogo-A antibody induced functional recovery, axonal regeneration, and axonal plasticity after lesion to the corticospinal tract at the level of the spinal cord or the medullary pyramid (Schnell et al., 1990, 1993; Bregman et al., 1995; Thallmair et al., 1998; Z'Graggen et al., 1998). The corticospinal tract originates from layer V pyramidal cells in the sensorimotor cortex, so a logical next step was to examine whether anti-Nogo-A antibodies would enhance functional recovery and neuronal plasticity after lesions to the sensorimotor cortex. Indeed, when adult rats underwent a sensorimotor cortical aspiration lesion and treatment with the IN-1 anti-Nogo-A antibody, they had improved performance on a skilled forelimb reaching task and on a skilled forelimb walking test as compared to control antibody treated rats (Emerick et al., 2003; Emerick et al., 2004). This behavioral recovery became statistically significant 4 weeks after the sensorimotor cortical lesion and antibody treatment. The functional recovery was correlated with neuronal plasticity in the intact corticospinal tract, in which fibers were found to have sprouted across the midline into denervated areas at the level of the spinal cord, red nucleus and basilar pontine nuclei (Fig 2, Wenk et al., 1999; Emerick and Kartje, 2004). In addition, after sensorimotor cortical lesion and treatment with the anti-Nogo-A antibody the intact cortex sent more projections to the contralateral striatum as compared to control antibody treated rats (Fig 2, Kartje et al., 1999). The neuronal plasticity in projections from the

intact sensorimotor cortex was shown to be functional, because intracortical microstimulation of the intact cortex caused increased ipsilateral forelimb movements as compared to control antibody treated rats (Emerick et al., 2003).

In the more physiologically relevant model of stroke, adult rats underwent a middle cerebral artery occlusion (MCAO) that resulted in an ischemic stroke in the sensorimotor cortex and were treated with the IN-1 anti-Nogo-A antibody. These animals also had improved performance on a skilled forelimb reaching task as compared to control antibody treated rats (Papadopoulos et al., 2002a). In this experiment behavioral recovery became statistically significant at 6 weeks after the MCAO and antibody treatment.

In these studies of cortical aspiration lesion and MCAO, the anti-Nogo-A antibody treatment was given starting at the same time as the lesion. However, in the clinical setting it would be advantageous for a stroke treatment to be effective when given after a CNS insult. Therefore, studies were undertaken to evaluate anti-Nogo-A immunotherapy as a delayed treatment for stroke, and it was found that the anti-Nogo-A antibodies were effective up to one week after stroke in inducing functional recovery in skilled forelimb reaching in adult rats (Wiessner et al., 2003b; Seymour et al., 2005b). Experiments were also undertaken to evaluate more clinically relevant delivery routes. Initial studies on treatment of stroke with anti-Nogo-A immunotherapy used hybridoma cells secreting the IN-1 antibody (Papadopoulos et al., 2002b; Seymour et al., 2005b), and then researchers began to use mini-osmotic pumps to deliver purified monoclonal anti-Nogo-A antibodies intracerebroventricularly (Wiessner et al., 2003b; Markus et al.,

2005b). More recently it has been shown that intrathecal delivery is also effective in enhancing functional recovery in adult rats after stroke (Tsai et al., 2007).

Similar to the neuronal plasticity after sensorimotor cortical aspiration lesion and treatment with anti-Nogo-A immunotherapy, after stroke in adult rats and treatment with anti-Nogo-A immunotherapy fibers from the intact corticospinal tract were found to have sprouted across the midline into denervated areas at the level of the spinal cord and the red nucleus (Fig 2, Papadopoulos et al., 2002b; Wiessner et al., 2003b; Seymour et al., 2005b). Additionally, after stroke in adult rats and treatment with anti-Nogo-A immunotherapy thalamic activation was reported as increased as indicated by functional magnetic resonance imaging (fMRI) after stimulation of the impaired forepaw as compared to control antibody treated rats (Markus et al., 2005b). In addition to this reported axonal plasticity, dendritic plasticity has also been shown after stroke and treatment with anti-Nogo-A immunotherapy. Layer V pyramidal neurons in the contralesional sensorimotor cortex had increased dendritic branching, dendritic arbor length, and dendritic spine density after MCAO and anti-Nogo-A immunotherapy (Fig 2, Papadopoulos et al., 2006). Two additional important observations were made in this study. First, treatment of unlesioned adult animals with the anti-Nogo-A antibody caused a transient increase in dendritic complexity in layer II/III neurons in the occipital cortex, and layer V pyramidal neurons of the sensorimotor cortex at two weeks, but by six weeks the dendritic arbors had returned to baseline levels. Secondly, in animals with a stroke, lasting increases in dendritic arbor complexity after anti-Nogo-A immunotherapy were specific to the contralesional sensorimotor cortex, because layer II/III neurons in the

occipital cortex showed no changes in dendritic complexity six weeks after stroke and anti-Nogo-A immunotherapy. Due to the correlation of neuroanatomical changes and behavioral results it is thought that axonal and dendritic reorganization of the brain is responsible at least in part for the improved functional recovery after cortical injury and treatment with anti-Nogo-A immunotherapy.

Several other methods have been used to manipulate Nogo-A signaling in studies of experimental stroke. First, mice genetically modified to lack the NgR1 or Nogo-A and Nogo-B have improved performance on a skilled reaching task after a stroke lesion, and increased fiber sprouting from intact pathways across the midline into denervated areas at the level of the spinal cord and red nucleus (Lee et al., 2004). Secondly, rats treated with the NgR(310)Ecto-Fc protein one week after stroke, which binds to the ligands of the NgR1 and thereby blocks receptor activation, had improved performance on a skilled reaching task and increased fiber sprouting from intact pathways across the midline into denervated areas at the level of the spinal cord and red nucleus (Lee et al., 2004).

Stroke is more prevalent in the aged human population (Lloyd-Jones et al., 2009) so preclinical studies on potential treatments for stroke should include aged animal subjects (1999; Grotta et al., 2008). Therefore, aged rats underwent MCAO and were treated with anti-Nogo-A immunotherapy beginning one week post-stroke. These rats had improved functional recovery on a skilled forelimb reaching task (Markus et al., 2005b). However, in this experiment behavioral recovery became statistically significant at 9 weeks after the MCAO, which was a longer time period for recovery as compared to adult rats with stroke and anti-Nogo-A immunotherapy.

Another clinically relevant brain injury model in which anti-Nogo-A immunotherapy has been tested is traumatic brain injury. Adult rats underwent a left lateral fluid percussion brain injury and 24 hours later treatment with anti-Nogo-A immunotherapy or a control antibody. The composite neuroscore, a test of motor function, showed a lesion induced deficit, but there was no difference between the anti-Nogo-A antibody treated rats and the control antibody treated rats (Lenzlinger et al., 2005b; Marklund et al., 2007a). Four weeks after the traumatic brain injury rats were tested on the Morris water maze place task for spatial memory, and rats treated with the anti-Nogo-A antibody performed better than the control antibody treated rats (Lenzlinger et al., 2005b; Marklund et al., 2007a). After completion of the place task, rats were tested on a probe trial and again the rats with traumatic brain injury and treated with the anti-Nogo-A antibody performed better than the control antibody treated rats (Marklund et al., 2007a). In addition, rats with traumatic brain injury and treated with the anti-Nogo-A antibody had higher growth-associated protein-43 (GAP-43) expression, an axonal growth marker, in CA1 of the hippocampus than control antibody treated rats (Marklund et al., 2007a).

Anti-Nogo-A immunotherapy has also been tested in a cortical injury model causing severe neglect. Rats underwent aspiration of the medial agranular cortex and immediately delivery of anti-Nogo-A immunotherapy or a control antibody was started (Brenneman et al., 2008b). Lesioned animals exhibited contralesional neglect to visual, tactile and auditory stimuli. Lesioned animals treated with anti-Nogo-A immunotherapy recovered from the neglect more quickly and more completely than control antibody

treated rats. Additionally, after knife cut surgery to sever the corpus collosum, the recovered anti-Nogo-A antibody treated rats once again exhibited neglect, suggesting that the contralesional hemisphere was involved in the initial recovery.

Neuronal Plasticity after Sensorimotor Cortical Lesion and Anti-Nogo-A Immunotherapy

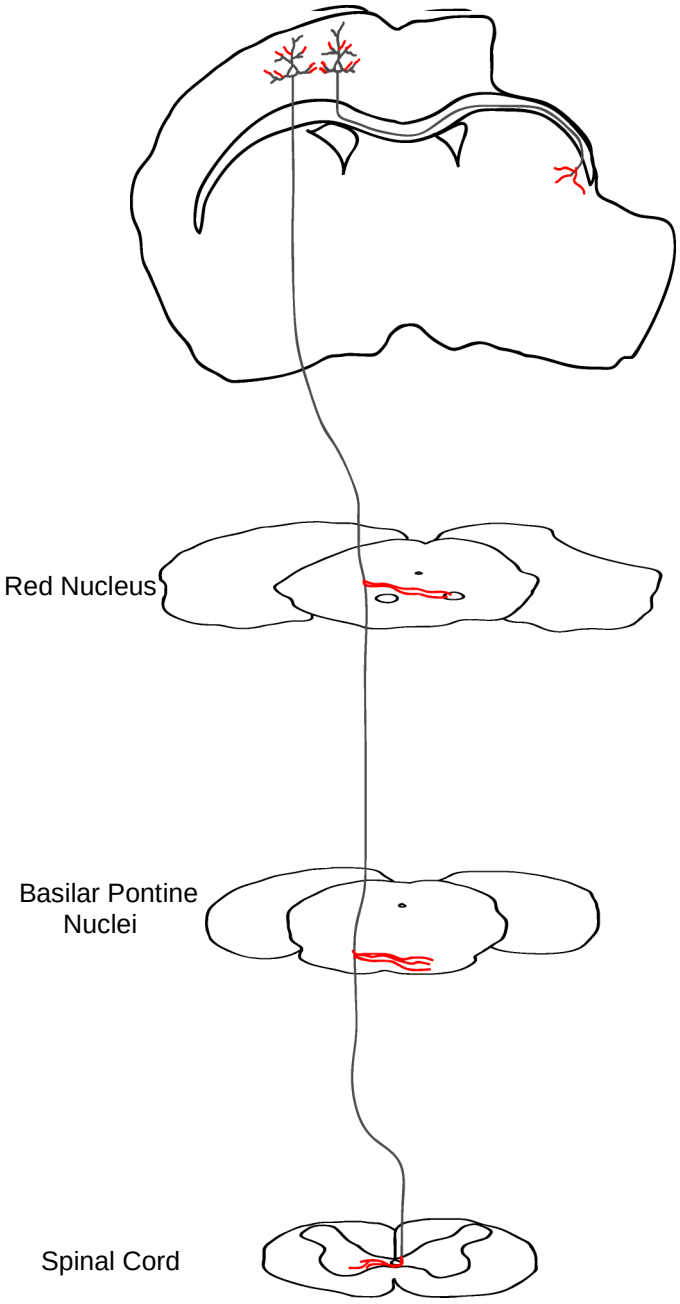

Figure 2. Neuronal Plasticity after Sensorimotor Cortical Lesion and Anti-Nogo-A Immunotherapy. The intact corticospinal tract sprouts across the midline into denervated areas at the level of the red nucleus, basilar pontine nuclei and spinal cord. Layer V pyramidal neurons in the intact sensorimotor cortex have increased dendritic branching, and dendritic arbor length. The intact cortex sends more projections to the contralateral striatum. Axonal and dendritic sprouting are shown in red.

Pyramidotomy and Spinal Cord Injury in Rodents and Primates

At the same time that anti-Nogo-A immunotherapy was being evaluated for the treatment of cortical injury and stroke it was also being evaluated for the treatment of spinal cord injury using several models.

In the first model, dorsal hemisection, the spinal cord is cut dorsally so that the dorsal columns and most of the corticospinal tract are severed. When rats underwent a mid-thoracic dorsal hemisection and were treated with anti-Nogo-A immunotherapy, they showed improved performance on reflex and motor function tests as compared to control antibody treated rats (Bregman et al., 1995; Merkler et al., 2001; Liebscher et al., 2005). This recovery was correlated with regeneration of cut axons though spared tissue bridges and past the lesion site (Schnell and Schwab, 1990, 1993; Bregman et al., 1995). Similar axon regeneration is seen after dorsal hemisection in rats and treatment with a Fab fragment (IN-1 Fab) with the variable domains of the anti-Nogo-A antibody IN-1 (Brosamle et al., 2000). In control antibody treated rats the cut axons regenerated less than 1 millimeter past the lesion, while in anti-Nogo-A antibody treated rats the cut axons regenerated up to 11 millimeters past the lesion (Schnell and Schwab, 1990). When the hindlimb was administered sensory stimulation, the anti-Nogo-A antibody treated rats, but not the control antibody treated rats, showed cortical activation as measured by blood oxygenation level dependent (BOLD) fMRI (Liebscher et al., 2005). Raphespinal (serotonergic) and coeruleospinal (noradrenergic) axons were also shown to have increased sprouting or regeneration caudal to the lesion as compared to control antibody treated rats (Bregman et al., 1995).

Similar recovery of motor function and axonal regeneration after dorsal hemisection has been demonstrated after treatment with a competitive antagonist of the NgR1, the Nogo-66 (1-40) antagonist peptide (NEP1-40, GrandPre et al., 2002; Li et al., 2003), and NgR(310)ecto-Fc protein (Li et al., 2004; Li et al., 2005b). Blocking the binding between NgR1 and its co-receptor LINGO-1 with the LINGO-1-Fc after dorsal hemisection also improves functional recovery and enhances axon regeneration (Ji et al., 2006). In another approach, blocking the intracellular signal molecules downstream of Nogo-A, including RhoA with C3 transferase and ROCK with Y-27632, after dorsal hemisection also leads to improved functional recovery and enhanced axonal regeneration (Dergham et al., 2002; Fournier et al., 2003).

Studies with non-human primates have further supported the effectiveness of anti-Nogo-A immunotherapy for the treatment of spinal cord injury. Adult Macaque monkeys underwent unilateral lesion of the spinal cord at the C7-C8 border and then were treated with anti-Nogo-A immunotherapy or a control antibody. Monkeys with anti-Nogo-A immunotherapy recovered ipsilesional hand manual dexterity as measured by the modified Brickman board task more quickly and to a greater extent than control antibody treated monkeys (Freund et al., 2006; Freund et al., 2009). Additionally, the monkeys with anti-Nogo-A immunotherapy recovered ipsilesional capacity to generate force with the digits as measured by the reach and grasp drawer test faster than control antibody treated monkeys (Freund et al., 2006). This recovery was correlated with increased regeneration and sprouting of corticospinal tract neurons both rostral and caudal to the lesion (Freund et al., 2006; Freund et al., 2007a). However, the anti-Nogo-A

immunotherapy did not prevent shrinkage and loss of neurons in the contralesional magnocellular part of the red nucleus (Wannier-Morino et al., 2008), nor the shrinkage of neurons in the affected motor cortex (Beaud et al., 2008). Sprouting and regeneration of corticospinal neurons after anti-Nogo-A immunotherapy has also been shown in Marmoset monkeys after midthoracic unilateral lesion of the spinal cord (Fouad et al., 2004).

Genetically modified mice that lack Nogo-A, Nogo-A and -B, or Nogo-A, -B, and –C have also been evaluated after spinal cord injury for functional recovery and axonal regeneration and sprouting. The results from these studies have been conflicting, most likely due to different lesion models (Cafferty et al., 2006), different genetic backgrounds of the mice (Dimou et al., 2006), and compensatory upregulation of Nogo-B (Simonen et al., 2003). After dorsal hemisection, Nogo-A knockout mice showed enhanced axonal regeneration (Simonen et al., 2003). After dorsal hemisection, Nogo-A and –B knockout mice showed improved motor recovery and enhanced axonal regeneration in one study (Kim et al., 2003) and no enhanced axonal regeneration in another study (Zheng et al., 2003). After dorsal hemisection, Nogo-A, -B, and –C knockout mice showed no enhanced axonal regeneration (Zheng et al., 2003). Further experiments are needed to determine the basis of these conflicting results.

Another model that was used to evaluate anti-Nogo-A immunotherapy for the treatment of spinal cord injury was pyramidotomy. Pyramidotomy involves surgically severing the corticospinal tract at the level of the medullary pyramids. Pyramidotomy allows for unilateral lesion by using the basilar artery as a landmark, and also largely

spares other descending and ascending systems (Thallmair et al., 1998). After a unilateral pyramidotomy and treatment with the anti-Nogo-A antibody IN-1, rats showed improved performance on a skilled forelimb reaching task, a grip strength test, the grid walking task, and a sensory test as compared to control antibody treated rats (Thallmair et al., 1998; Z'Graggen et al., 1998). This recovery was correlated with neuronal plasticity with fibers from the affected corticospinal tract being found to have sprouted across the midline at the level of the red nucleus and basilar pontine nuclei (Thallmair et al., 1998; Z'Graggen et al., 1998). At the level of the basilar pontine nuclei these sprouting fibers made asymmetric synaptic contacts (Blochlinger et al., 2001). Fibers from the spared corticospinal tract were found to have sprouted across the midline at the level of the spinal cord into denervated areas (Thallmair et al., 1998). The lesioned corticospinal tract also was found to regenerate to innervate the dorsal column nuclei (Thallmair et al., 1998).

Similar results have been shown in genetically modified mice that lack the NgR1 or Nogo-A and Nogo-B. After unilateral pyramidotomy these mice showed improved performance on a skilled forelimb reaching task and increased fiber sprouting from the intact corticospinal tract across the midline into the denervated spinal cord as compared to wild-type mice (Cafferty and Strittmatter, 2006). It is important to note that this same corticospinal tract fiber sprouting was not observed after dorsal hemisection in NgR1 knockout mice (Kim et al., 2004; Zheng et al., 2005) and in one study in Nogo-A, -B knockout mice (Zheng et al., 2003). However, after dorsal hemisection in NgR1 knockout mice there is improved motor function and sprouting of rubrospinal and raphespinal

axons (Kim et al., 2004). Therefore, the results from genetic neutralization of the NgR1 and Nogo-A and –B appear to be dependent on the lesion model, pyramidotomy vs. dorsal hemisection, and fiber systems studied.

When rats underwent bilateral pyramidotomy and were treated with the anti-Nogo-A antibody IN-1, they also showed improved performance on a skilled forelimb reaching task as compared to control antibody treated rats (Raineteau et al., 2001). In these rats the unlesioned rubrospinal tract sprouted to increase its innervation of the spinal cord. Additionally, the sensorimotor cortex was functionally reconnected because stimulation of the sensorimotor cortex elicited electromyogram (EMG) responses in the trunk, shoulder, biceps and in some cases the proximal and medial muscles of the forelimb in rats with pyramidotomy and treated with the anti-Nogo-A antibody, but not in rats treated with a control antibody (Raineteau et al., 2001).

Axon Regeneration after Nogo-A Neutralization is Not Limited to Descending Pathways

Axonal regeneration is well described after spinal cord injury and treatment with anti-Nogo-A immunotherapy, but it has also been described within the neocortex, hippocampus and cranial nerves.

There are two reports of axonal regeneration after anti-Nogo-A immunotherapy in cholinergic fibers. In the first, adult rats underwent aspiration lesions to the sensorimotor cortex, transplantation of fetal neocortical tissue into the lesion site and treatment with either an anti-Nogo-A antibody or a control antibody. Three months later the grafts were analyzed for the ingrowth of host cholinergic fibers, and rats treated with the anti-Nogo-

A antibody had more axonal regeneration/sprouting of cholinergic fibers into the transplant than control antibody treated rats (Schulz et al., 1998). Therefore, anti-Nogo-A immunotherapy enhanced the connectivity between the host neocortical tissue and the fetal neocortical graft. In the second report, 3 week old rats underwent unilateral aspiration of the dorsal fornix and fimbria to lesion the septohippocampal pathway. At the time of the septohippocampal lesion a bridge was placed between the septum and rostral hippocampus consisting of a nitrocellulose strip and human placental extracellular matrix material soaked in NGF. In control antibody treated rats cholinergic fibers only regenerated 0.2-1 millimeter into the hippocampus, while in anti-Nogo-A antibody treated rats cholinergic fibers regenerated 2-4 millimeters into the hippocampus. Furthermore, the regenerated axons grew into sites corresponding to their original innervation pattern (Cadelli et al., 1991b).

There have been two reports of axonal regeneration in hippocampal slice cultures after treatment with an anti-Nogo-A antibody. In the first report, the perforant pathway was severed in mice hippocampal slice cultures and then the cultures were treated with an anti-Nogo-A antibody or control antibody. In cultures treated with the anti-Nogo-A antibody after 7-10 days there were more entorhinal axons growing into the hippocampus than in cultures treated with control antibody. However, the axons did not grow only into their original innervation locations, but also grew into ectopic hippocampal layers (Mingorance et al., 2004a). In the second report, the Schaffer collaterals were severed in rat hippocampal slice cultures and then the cultures were treated with an anti-Nogo-A antibody or control antibody. In cultures treated with anti-Nogo-A antibody after 5 days

there were more axons growing across the lesion than in cultures treated with control antibody. Additionally, stimulation of CA3 generated higher amplitude evoked potentials recorded in CA1 in cultures treated with anti-Nogo-A antibody as compared to cultures treated with control antibody. Interestingly, this study also observed axonal growth/sprouting in intact hippocampal slice cultures after treatment with an anti-Nogo-A antibody, but no dendritic growth/sprouting (Craveiro et al., 2008b).

In cranial nerves there have been several reports of axonal regeneration after Nogo-A neutralization. After the optic nerve is lesioned in rats by freeze-crush, treatment with an anti-Nogo-A antibody in the presence of fibroblast growth factor (FGF) enhances axonal regeneration past the lesion as compared to a control antibody (Weibel et al., 1994). In another approach, the optic nerve was crushed in rats overexpressing the NgR1 or expressing a dominant negative form of NgR1 and at the same time the lens was injured to stimulate macrophages to release factors favorable to axon regeneration. Rats overexpressing the NgR1 had impaired axon regeneration, while rats expressing a dominant negative form of NgR1 had enhanced axon regeneration (Fischer et al., 2004). In another study, the cochlear nerve was cut in rats between the brain stem and the internal acoustic meatus. In this model treatment with a Fab fragment (IN-1 Fab) with the variable domains of the anti-Nogo-A antibody IN-1 enhanced axonal regeneration past the lesion as compared to control antibody. Additionally, rats treated with IN-1 Fab showed functional recovery as measured by Brainstem Auditory Evoked Potentials (BAEP), while animals treated with the control antibody did not recover (Tatagiba et al., 2002).

Anti-Nogo-A Immunotherapy Distribution and Mechanism of Action after Intracerebroventricular Infusion

Commonly used antibodies against Nogo-A include the monoclonal antibody IN-1 which recognizes Amino-Nogo, and the more specific monoclonal antibodies 11C7 and 7B12 which recognize short amino acid sequences in Amino-Nogo (Fig 3). When the 11C7 and 7B12 anti-Nogo-A antibodies are infused into the lateral ventricle or intrathecally in non-lesioned rats or in rats with spinal cord injury or stroke, the antibodies reach the entire spinal cord and brain including the hippocampus. Additionally, the anti-Nogo-A antibodies are at high levels near spinal cord lesions or stroke lesions. Anti-Nogo-A immunotherapy binds to surface Nogo-A on neurons and oligodendrocytes and causes internalization and degradation of Nogo-A. Indeed, after 7 days of intrathecal infusion of anti-Nogo-A antibodies, the levels of Nogo-A in the spinal cord were reduced (Weinmann et al., 2006). Therefore, one of anti-Nogo-A immunotherapy's mechanisms of action appears to be downregulation of cell surface Nogo-A. Additionally, anti-Nogo-A antibodies that bind to Amino-Nogo could block the binding of Nogo-A with an as of yet unidentified Amino-Nogo receptor. Finally, these antibodies could sterically block the Nogo-A-NgR1 binding (Gonzenbach and Schwab, 2008).

Monoclonal Antibody Binding Sites on Nogo-A

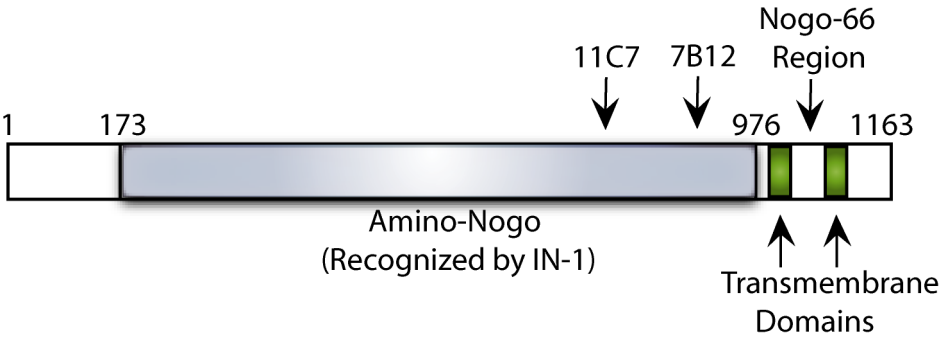

Figure 3. Monoclonal Antibody Binding Sites on Nogo-A. An illustration of the Nogo-A protein with amino acid locations of interest marked. The N-terminus is on the left and the C-terminus is on the right. The monoclonal 1N-1 antibody recognizes the Amino-Nogo portion of Nogo-A. The monoclonal antibodies 11C7 and 7B12 recognize short amino acid sequences within Amino-Nogo.

NOGO-A AND NEUROLOGICAL DISORDERS

Alzheimer's Disease

There is evidence that Nogo proteins and NgR may play a role in the pathophysiology of Alzheimer's disease, possibly by modulating amyloid precursor protein (APP)/ Aβ metabolism (Park et al., 2007). Nogo-A expression is increased in the hippocampus and frontal cortex of aged subjects with Alzheimer's disease (Gil et al., 2006a). In addition, Nogo-A immunoreactivity can be found in neuritic plaques (Gil et al., 2006a), as well as NgR immunoreactivity (Park et al., 2006b). An additional report showed increased NgR expression in hippocampal neurons in subjects with Alzheimer's disease (Zhu et al., 2007). Additionally, in Alzheimer's disease Nogo-A expression is enhanced in neuronal cell bodies, while NgR expression is decreased in cell bodies (Park et al., 2006b).

The NgR was found to physically interact with APP. Studies with APPswe/PSEN-1(ΔE9) double transgenic mice demonstrate that NgR affects Aβ accumulation and dystrophic neurite formation. When the double transgenic mice are also modified to lack the NgR, the levels of Aβ, and Aβ plaques are increased and there are also increased dystrophic neurites. On the other hand, if NgR(310)ecto-Fc was infused into the cerebral ventricle of the double transgenic mice, the levels of Aβ, and Aβ plaques were decreased and there were also fewer dystrophic neurites (Park et al., 2006b). In another approach, NgR(310)ecto-Fc was delivered subcutaneously to the double transgenic mice, and the levels of Aβ, and Aβ plaques were decreased and there were also fewer dystrophic

neurites, less astrocytosis and improved performance on a spatial memory task (Park et al., 2006a).

In addition, members of the reticulon family, including Nogo proteins which are reticulon 4, interact with β-site APP cleaving enzyme 1 (BACE1) to inhibit the enzyme's activity (He et al., 2004; He et al., 2006). Reticulon proteins and BACE1 interact via an amino acid sequence within the C-terminus of reticulon proteins in the reticulon homology domain (He et al., 2006).

Motor Neuron Diseases

Nogo-A may be a disease marker for amyotrophic lateral sclerosis (ALS), and it may also play a role in the pathogenesis of ALS (Teng et al., 2008). In 2002 researchers found that ALS transgenic mice (G86R SOD1 overexpression) had higher Nogo-A mRNA expression in the lumbar spinal cord and the gastrocnemius muscle than wild-type mice. They went on to show that muscle biopsies from ALS patients have elevated levels of Nogo-A, but there was no elevation of Nogo-A in muscle biopsies from patients with primary muscle disease or polyneuropathy (Dupuis et al., 2002). Further research showed that Nogo-A/B expression levels correlated with ALS disease severity (Jokic et al., 2005). A prospective study of patients with lower motor neuron syndrome revealed that Nogo-A in muscle biopsies detected by western blot could be used to identify patients who would progress to ALS (Pradat et al., 2007). However, this finding was disputed by another group who found elevated Nogo-A in muscle biopsies from other forms of

myopathy and peripheral neuropathies (Wojcik et al., 2006). Therefore the usefulness of Nogo-A as a biomarker for ALS remains controversial.

An additional study suggests that Nogo-A may be involved in the pathogenesis of ALS. When ALS transgenic mice (G86R SOD1 overexpression) were also genetically modified to lack Nogo-A, the mice survived longer, had attenuated loss of motor neurons and less muscle denervation. Furthermore, overexpression of Nogo-A in wild-type mice led to disruption of the neuromuscular junction with postsynaptic shrinkage and presynaptic retraction (Jokic et al., 2006). However, in a somewhat contradictory report a NgR agonist Pep4 and a NgR antagonist NEP1-40 both can attenuate motor neuron loss after neonatal sciatic nerve lesion (Dupuis et al., 2008). Therefore, the role of Nogo-A and the NgR in the pathogenesis of ALS remains unclear.

Psychiatric Disorders

There is evidence that decreased NgR1 signaling may increase the risk for schizophrenia (Budel et al., 2008). The NgR1 gene is located within the 22q11 locus which has been linked to schizophrenia risk, and polymorphisms in the NgR1 gene are associated with schizophrenia (Liu et al., 2002; Sinibaldi et al., 2004; Hsu et al., 2007; Budel et al., 2008). However, in the Chinese population there appears to be no association between NgR1 gene variation and schizophrenia (Chen et al., 2004). The variants in the NgR1 gene associated with schizophrenia are rare, but may affect the functioning of the receptor. Four NgR1 variants were evaluated for their functional properties, and it was shown that the variants were not able to inhibit growth cone

collapse and acted as dominant-negatives (Budel et al., 2008). Mice genetically modified to lack the NgR1 were tested for behaviors affected by schizophrenia. The mice lacking NgR1 showed impairment on a working memory task in one study (Budel et al., 2008) but not in another study (Hsu et al., 2007). Sensorimotor gating as measured by prepulse inhibition (PPI) was unaltered in mice lacking the NgR1 (Hsu et al., 2007; Budel et al., 2008), though a subset of these mice lacked a PPI response (Budel et al., 2008).

In 2002 Nogo was also implicated as being involved in schizophrenia when Nogo mRNA was found to be overexpressed in the frontal cortex of schizophrenic individuals (Novak et al., 2002). In this study no distinction was made between Nogo-A, -B and –C, so a further study was undertaken which found that Nogo-C was overexpressed in schizophrenia but not Nogo-A or –B. Furthermore Nogo-B was found to be underexpressed in depression, and there were no changes in Nogo-A, -B or –C in bipolar disorder (Novak et al., 2006). Some studies have shown an association between polymorphisms in the gene for Nogo with schizophrenia (Novak et al., 2002; Tan et al., 2005), while other studies have not replicated this result (Covault et al., 2004; Gregorio et al., 2005; Xiong et al., 2005). Therefore, Nogo and NgR may be involved in several psychiatric disorders and in particular schizophrenia, possibly by modifying the genetic risk.

Epilepsy

Nogo-A protein levels have been shown to be increased in the hippocampus in individuals with temporal lobe epilepsy (Bandtlow et al., 2004; Gil et al., 2006a). This

result has also been replicated in several experimental models of epilepsy. After kainate-induced seizures in rats Nogo-A mRNA expression was increased in hippocampal neurons (Meier et al., 2003). However, another study of kainate-induced seizures in rats showed a transient downregulation of Nogo and NgR mRNA in the hippocampus (Mingorance et al., 2004a), and another study showed no change in Nogo mRNA in the hippocampus (Josephson et al., 2001). In these two studies no distinction was made between Nogo-A, -B and –C. In a mouse genetic model of temporal lobe epilepsy (*mceph/mceph*) there was an upregulation of Nogo-A and NgR mRNA in the hippocampus (Lavebratt et al., 2006). In another study with amygdala kindling, rats showed increased Nogo-A and Ng-R protein expression in the ipsilateral hippocampus (Takeda et al., 2007). Therefore, Nogo-A and NgR expression may be regulated by epilepsy but it is unclear what role this may play in the pathogenesis of the disease.

Multiple Sclerosis

Nogo-A and NgR have been investigated as disease markers for multiple sclerosis. One study showed that a soluble Nogo-A product was present in the cerebral spinal fluid of individuals with multiple sclerosis, but not in control subjects (Jurewicz et al., 2007). However, another study disputed this claim and concluded that the detected protein was a immunoglobulin light chain and not a soluble Nogo-A product (Lindsey et al., 2008).

There is also evidence that Nogo-A and NgR may be involved in the pathogenesis of multiple sclerosis. Autoantibodies against the N-terminus of Nogo-A (IgM) are

detectable in the serum and are elevated in patients with multiple sclerosis as compared to controls. In addition, autoantibodies against the N-terminus of Nogo-A (IgG) are detectable in the cerebral spinal fluid and are higher in relapsing-remitting multiple sclerosis than in chronic progressive multiple sclerosis (Reindl et al., 2003). Autoantibodies against the Nogo-66 sequence and the NgR (IgG) have also been identified in the serum of patients with multiple sclerosis, though they were also found in controls (Onoue et al., 2007). These autoantibodies may simply be a consequence of the disease, they may mediate further injury, or they may play a role in repair (Reindl et al., 2003).

A further study suggested that anti-Nogo-A antibodies may be protective in multiple sclerosis. Mice underwent vaccination with Nogo-A, or were injected with an anti-Nogo-A IgG and then experimental autoimmune encephalomyelitis (EAE), a model of multiple sclerosis, was induced. Mice with antibodies against Nogo-A had decreased incidence and severity of EAE. Additionally, in genetically modified mice that lacked Nogo-A,-B and –C, EAE was delayed, less severe, and shorter in duration (Karnezis et al., 2004). Taken together, this suggest Nogo-A may be a therapeutic target in multiple sclerosis.

Nogo-A and NgR1 signaling may play a role in multiple sclerosis via immune cells. One study reported that Nogo-A was upregulated in oligodendrocytes, and NgR1 was upregulated in reactive astrocytes and microglia/macrophages in multiple sclerosis demyelinating lesions (Satoh et al., 2005). A recent report showed that NgR1 is found in

human B cells, T cells and monocytes and that NgR1 can affect the motility of immune cells in the presence of myelin (Pool et al., 2009).

Nogo-A is also involved in oligodendrocyte differentiation. In mice genetically modified to lack Nogo-A a delay in oligodendrocyte differentiation was observed in the optic nerve and cerebellum. Additionally, at P15 the Nogo-A knock-out mice had hypomyelinated optic nerves with axons of decreased caliber, but myelination and axon caliber reached normal levels by P28. In Nogo-A knock-out mice myelin structure and the nodes of Ranvier were not disrupted (Pernet et al., 2008). The role that Nogo-A plays in oligodendrocyte differentiation could have implications for remyelination in multiple sclerosis.

EXPRESSION OF NOGO-A IN NEURONS

Nogo-A is often thought of as a myelin associated protein, but Nogo-A mRNA and protein is also found in many neurons (Josephson et al., 2001; Huber et al., 2002; Hunt et al., 2003; Meier et al., 2003; Mingorance et al., 2004a). In the human hippocampus, Nogo-A protein is expressed by pyramidal neurons, non-pyramidal neurons and granule cells (Buss et al., 2005; Gil et al., 2006a). In the human cerebral cortex neurons in all layers express Nogo-A protein (Buss et al., 2005). In the rat hippocampus, Nogo-A protein is expressed by pyramidal neurons, non-pyramidal neurons and granule cells (Huber et al., 2002; Hunt et al., 2003). In the rat hippocampus the expression of Nogo-A appears to be related to the location of different afferent terminations. For example, in locations where the lateral entorhinal cortex has

terminations like in the stratum lacunosum-moleculare of the CA1 and subiculum border and CA3, Nogo-A expression is higher (Mingorance et al., 2004a). In the rat cerebral cortex neurons in all layers express Nogo-A protein (Huber et al., 2002; Hunt et al., 2003). Nogo-A expression in neurons is also found at many other locations such as the retina, red nucleus and cerebellum (Huber et al., 2002; Hunt et al., 2003).

POTENTIAL FUNCTIONS OF NEURONAL NOGO-A

Axonal Growth

Nogo-A in oligodendrocytes as been implicated in inhibiting axonal growth for some time (Gonzenbach and Schwab, 2008), but new evidence suggests that neuronal Nogo-A may also inhibit axonal growth (Montani et al., 2009). Dorsal root ganglia (DRG) neurons were isolated from mice genetically modified to lack Nogo-A and wild-type mice. DRG neurons from mice lacking Nogo-A had larger and more motile growth cones than wild-type mice. Additionally, in DRG neurons from Nogo-A knock-out mice there was increased phosphorylation of LIMK1 and increased activated Rho (RhoGTP). This is significant because the RhoGTP/LIMK1/Cofilin pathway regulates actin dynamics (Montani et al., 2009).

Synaptic Plasticity

Further evidence points to a role in the adult for neuronal Nogo-A in synaptic plasticity. Nogo-A is located at the post-synaptic density of spinal cord motor neurons (Liu et al., 2003), and is located presynaptically at the neuromuscular junction (Dodd et

al., 2005). Genetic manipulation to specifically overexpress Nogo-A in Purkinje cells led to the retraction and loss of inhibitory Purkinje cell terminals, suggesting a role for neuronal Nogo-A in the maintenance of inhibitory synapses (Aloy et al., 2006). Nogo-A has also been shown to inhibit integrin signaling (Hu and Strittmatter, 2008), and integrins have been implicated in regulating dendritic spine morphology (Webb et al., 2007). The NgR1 has also been shown to be involved in synaptic plasticity. In the cortex the NgR1 is located both pre and post-synaptically (Wang et al., 2002c), and mutant mice without NgR1 have a shift of dendritic spine morphologies in the apical CA1 pyramidal cell dendritic tree so there are more stubby spines and fewer mushroom and thin spines as compared to heterozygous controls (Lee et al., 2008). This represents a shift towards more immature dendritic spine morphologies. In this study, mice lacking NgR1 had enhanced FGF2-dependent long term potentiation (LTP) and attenuated long term depression (LTD) at hippocampal Schaffer collateral-CA1 synapses. Taken together, these studies suggest that neuronal Nogo-A and its receptor NgR1 play a role in synaptic plasticity.

Structure of the Endoplasmic Reticulum

Nogo-A, like all of the reticulon proteins, is highly localized to the endoplasmic reticulum (GrandPre et al., 2000; Oertle et al., 2003). Immunogold staining of Nogo-A shows Nogo-A localized at the rough endoplasmic reticulum (Jin et al., 2003b). Although Nogo-A is located in the peripheral endoplasmic reticulum, it is absent from the nuclear envelope. A report showed that Nogo-A plays a role in the shaping of tubular

endoplasmic reticulum (Voeltz et al., 2006). The authors speculated that Nogo-A may stabilize highly curved membranes.

Central Nervous System Development

Growing evidence points to a role for Nogo-A in CNS development. During development the expression of Nogo-A in the brain precedes that of the NgR (Wang et al., 2002c). Additionally, Nogo-A is more highly expressed during development than during adulthood in many neuronal populations, with the exception of the hippocampus (Huber et al., 2002; Meier et al., 2003). In mice genetically modified to lack Nogo-A,-B and –C, developing cortical cells *in vitro* showed early polarization and increased branching (Mingorance-Le Meur et al., 2007), suggesting Nogo-A is involved in cortical development. Additionally, during development large projection neurons of the chick optic tectum express Nogo-A during the process of neuritogenesis (Caltharp et al., 2007). Another study showed that Nogo-A is expressed in developing olfactory receptor neurons during axonal growth (Richard et al., 2005). We have previously reported that knocking down Nogo-A during development in neocortical pyramidal neurons led to decreased dendritic spine density and an increased percentage of immature dendritic spine morphologies (Pradhan, 2007). Taken together, these studies of Nogo-A during development support the idea that neuronal Nogo-A has a role in CNS development, circuit formation, and structural synaptic plasticity.

There is also evidence that Nogo-A and NgR signaling consolidate neural pathways after development. Mice genetically modified to lack Nogo-A and –B demonstrate ocular dominance plasticity after the critical period (McGee et al., 2005).

Further support for a role for Nogo-A in development of the CNS comes from behavioral characterization of mice genetically modified to lack Nogo-A. Adult mice lacking Nogo-A had improved motor coordination and balance, increased locomotion in the dark phase of the light-dark cycle, and increased locomotor response to amphetamine treatment (Willi et al., 2008b). These findings suggest that Nogo-A may play a role in the development of the cerebellum and the dopaminergic system.

Peripheral Nerve Development and Regeneration

Evidence has emerged that Nogo-NgR signaling may be involved in peripheral nerve axon pathfinding by acting as a negative guidance cue. Zebrafish, like mammals, express three splice variants of Nogo known as Nogo-α, -β, and -γ, and they are conserved only at the C-terminus where the reticulon homology domain containing Nogo-66 is located. They are not conserved at the Nogo-A, and –B specific N terminal domains. When protein synthesis for NgR or Nogo-γ was disrupted in zebrafish embryos, CNS development was grossly unaffected, but peripheral nerves were shorter, thinner, defasciculated and branched into aberrant locations (Brosamle et al., 2009). In rats during development and adulthood, Nogo-A is expressed in peripheral ganglia such as the dorsal root ganglion (Josephson et al., 2001; Huber et al., 2002), and peripheral nerve fibers (Huber et al., 2002). Expression of Nogo-A in peripheral ganglia in fetal and adult human

tissue has also been demonstrated (Josephson et al., 2001). Though Nogo-A mRNA was restricted to neuron cell bodies, suggesting that Schwann cells and the perineurium in peripheral nerves do not express Nogo-A (Huber et al., 2002). Additionally, after the sciatic nerve is transected in rats, Nogo-A protein is highly expressed in the regenerating/sprouting axons (Hunt et al., 2003). Taken together, these studies suggest that Nogo-A and NgR is involved in the development and regeneration/sprouting of peripheral axons.

RNA INTERFERENCE IN THE RAT BRAIN *IN VIVO*

RNA Interference

In 1998 Andrew Fire and his colleagues showed that injection of double-stranded RNA into *Caenorhabditis elegans* could cause specific interference to endogenous mRNA with complementary sequences (Fire et al., 1998). Then in 2001 RNAi was demonstrated in mammalian cells *in vitro* (Elbashir et al., 2001). This experiment showed that short interfering RNA (siRNA) duplexes 21-nucleotides in length could specifically interfere with endogenous mRNA, while longer double stranded RNA cause non-specific and specific interference. Then in 2002 specific RNAi was demonstrated in adult mice either using siRNA or *in vivo* expression of a shRNA (McCaffrey et al., 2002).

RNAi using synthetic siRNA or shRNA utilizes molecular machinery for endogenous gene silencing by microRNA (miRNA). In the RNAi endogenous pathway primary miRNA is processed by Drosha and DGCR8 to produce precursor miRNA. This process occurs in the nucleus, and precursor miRNA is transported to the cytoplasm by

exportin 5. In the cytoplasm miRNA is further processed by Dicer, and then one of the strands, known as the guide strand, is incorporated into the RNA-induced silencing complex (RISC). The guide strand binds to a complementary sequence in mRNA, and, if the sequences perfectly match, then the mRNA is degraded by AGO2. However, if the sequences match imperfectly, then translational repression occurs and the mRNA may be degraded in processing bodies in a non-sequence specific way. For this to occur there must be at least matching in the seed region, which is at nucleotides 2-8 of the miRNA. An additional mechanism for gene silencing, which involves transcriptional gene silencing, can occur when siRNA is found in the nucleus. For this mechanism to occur the siRNA must be complementary to the gene in the promoter region (for review see Castanotto et al., 2009b).

Synthetic siRNA enters the endogenous RNAi pathway by being incorporated into RISC. Alternatively, plasmids can be delivered to the cell that express a shRNA under control of a polymerase II or III promoter. This shRNA then enters the endogenous RNAi pathway by being processed by Drosh and/or Dicer (Castanotto and Rossi, 2009b).

There are several possible complications when using synthetic siRNA. The synthetic siRNA could disrupt the endogenous RNAi. Synthetic siRNA can also cause specific off-target interference in mRNA other than the target if the siRNA is complementary to other mRNA (Castanotto and Rossi, 2009b). Additionally, synthetic siRNA can also activate the immune system and production of type I interferon (Hornung et al., 2005; Castanotto and Rossi, 2009b).

Viral Delivery by Adeno-Associated Virus

For long-term expression of a siRNA *in vivo* viral delivery is used. In this approach a vector is used to deliver a gene for a shRNA under the control of a polymerase II or III promoter (Castanotto and Rossi, 2009b). Adeno-associated virus (AAV) vectors are well suited for gene delivery because they can support persistent transgene expression for chronic experiments, and the host immune response to AAV is minimal (Daya et al., 2008).

AAV viruses belong to the *Parvoviridae* family and *Dependovirus* genus. They are small non-enveloped viruses with a single strand of DNA. AAV requires a helper virus, either adenovirus or herpesvirus, for productive infection. AAVs are unique in that they can integrate into the chromosome at a specific location 19q13.4. The genome contains two open reading frames flanked by two inverted terminal repeats. The open reading frames contain the Rep and Cap genes (Daya and Berns, 2008).

For AAV use as a gene transfer vector the viral genes are removed and in addition an integration efficiency element (IEE) is removed. This makes AAV vectors unable to replicate or integrate in a site specific manner. The inverted terminal repeats are retained because they are required for packaging of the vector. A common approach to modify tissue transduction specificity is to package the inverted terminal repeats of one AAV serotype into the capsids of different serotypes. There have been 12 human serotypes identified and greater than 100 serotypes from non-human primates identified (Daya and Berns, 2008).

STROKE

Introduction

Ischemic stroke occurs when a blood vessel in the brain is occluded. Ischemic stroke is most often caused by atherosclerotic disease, hypertension and emboli, though there are many other conditions that can cause ischemic strokes. These fall into classifications of vasculitis, connective tissue disorders, angiopathies, metabolic disorders, hematologic and oncologic, pregnancy related, substance abuse, infections, and migrainous infarctions (Tarulli, 2007).

Occlusion of a cerebral artery with resultant lack of blood flow causes damage to the brain, and this damage leads to neurological impairments such as hemiparesis, cognitive deficits, aphasia, and sensory deficits (Kelly-Hayes et al., 2003). To some extent spontaneous recovery from neurological impairments usually occurs after stroke. For the motor system most improvements occur during the first 3 months after a stroke. For cognitive impairments significant improvements can occur past 3 months after a stroke (Cramer, 2008). After this more rapid recovery, slower spontaneous recovery can occur for years after a stroke (Hankey et al., 2007). Patients who are less severely disabled recover more rapidly (Hankey et al., 2007).

Incidence and Prevalence

There are 6,500,000 people in the United States who have experienced a stroke, and every year 795,000 people have a new or recurrent stroke. Stroke is the third leading cause of death in the United States, and in addition stroke is the #1 cause of serious long-

term disability. 87% of strokes are ischemic, 10% are hemorrhagic and 3% are subarachnoid hemorrhage. Stroke is more prevalent in the aged population and increasing age is a significant risk factor for stroke. In the age group of 20-39 the prevalence of stroke in men is 0.2% of the population, while for women it is 0.3%. In the age group of 80+ the prevalence of stroke in men is 17.1% of the population while for women it is 13.5% (Lloyd-Jones et al., 2009).

Stroke in the Aged

Stroke is a disease of the aged, and 60% of people who have had a stroke are over the age of 65 (Pleis et al., 2007). In a study of disability 6 months following an ischemic stroke in subjects 65-94 years old, older age was associated with greater disability (Kelly-Hayes et al., 2003). In ischemic stroke survivors over the age of 65, nearly 50% have cognitive deficits 6 months post-stroke (Kelly-Hayes et al., 2003). Furthermore, stroke patients without dementia at a baseline evaluation had a faster decline in memory performance as compared to aged individuals without stroke (Reitz et al., 2006). Therefore, age is a risk factor for stroke, and increasing age is associated with greater disability following ischemic stroke.

Experiments in rodent models have demonstrated that the response of an aged subject to stroke is different than the response of a younger subject (Popa-Wagner et al., 2007b). Aged rodents functionally recover from a cortical stroke more slowly and to a lesser extent than younger rodents (Badan et al., 2003a; Brown et al., 2003; Markus et al., 2005b; Rosen et al., 2005; Zhang et al., 2005; Popa-Wagner et al., 2007c). The extent of

recovery from stroke depends upon an interplay of factors causing tissue damage, factors inhibiting repair, and factors promoting repair, and in the aged brain these factors appear to be dysregulated in magnitude and timing (Popa-Wagner et al., 2007b). For example, in aged rats the ischemic infarct develops more quickly and amount of apoptotic cells in the infarct core is higher at earlier time points as compared to younger rats (Popa-Wagner et al., 2007c). Additionally, the glial scar forms earlier in aged animals as compared to young animals (Badan et al., 2003a). In aged rats most growth-promoting genes increase after stroke, but this increase is delayed as compared to younger animals (Li et al., 2006).

Current Approved Therapies for Stroke

Recombinant tissue-type plasminogen activator (tPA) is the only approved therapy for acute ischemic stroke and is effective up to 4.5 hours after the onset of symptoms (Hacke et al., 2008). After this short time window, the therapies for stroke are limited. Rehabilitation is often utilized and may include physical therapy, speech pathology, occupational therapy, and neuropsychological and cognitive rehabilitation (Adams et al., 2006). The effectiveness of cognitive rehabilitation to improve memory impairments after stroke is unclear because there have been few randomized controlled trials (das Nair et al., 2007). Therefore, there is a great need for therapies to improve stroke outcome.

SPATIAL MEMORY

Brain Structures Involved and Connectivity

In 1981 Richard Morris described the Morris water maze as a test of spatial memory (Morris, 1981). In this report the hidden platform test was described as a test for the ability to use distal cues to locate a particular location, specifically the location of a submerged escape platform in a pool of water. Subsequently, it has been shown that performance on the Morris water maze is sensitive to disruption in many different brain regions (D'Hooge et al., 2001b). This disruption could be in the form of a lesion, but disconnecting the brain region, pharmacological manipulation or electrophysiological manipulation can also cause deficits in performance on the Morris water maze. The hippocampus, and more specifically the dorsal hippocampus, is a key brain structure in performance on the Morris water maze, and afferents and efferents of principal cells in the trisynaptic pathway are described in Fig 4. Other brain regions where disruption leads to Morris water maze impairments include but are not limited to the striatum, basal forebrain, cerebellum, entorhinal cortex, perirhinal cortex, prefrontal cortex, anterior cingulated cortex, and insular cortex (D'Hooge and De Deyn, 2001b). Therefore, it appears that a network of brain areas contribute to performance on the Morris water maze.

One way that the brain may represent spatial information is through the firing of "place cells," which fire when the organism is in a specific location in space. Cells that fire in response to place were first identified in the hippocampus, but they have also been

found in the medial entorhinal cortex, subiculum, striatum, presubiculum, parasubiculum and lateral septum (Knierim, 2006).

Hippocampus Afferents and Efferents (Principal Cells)

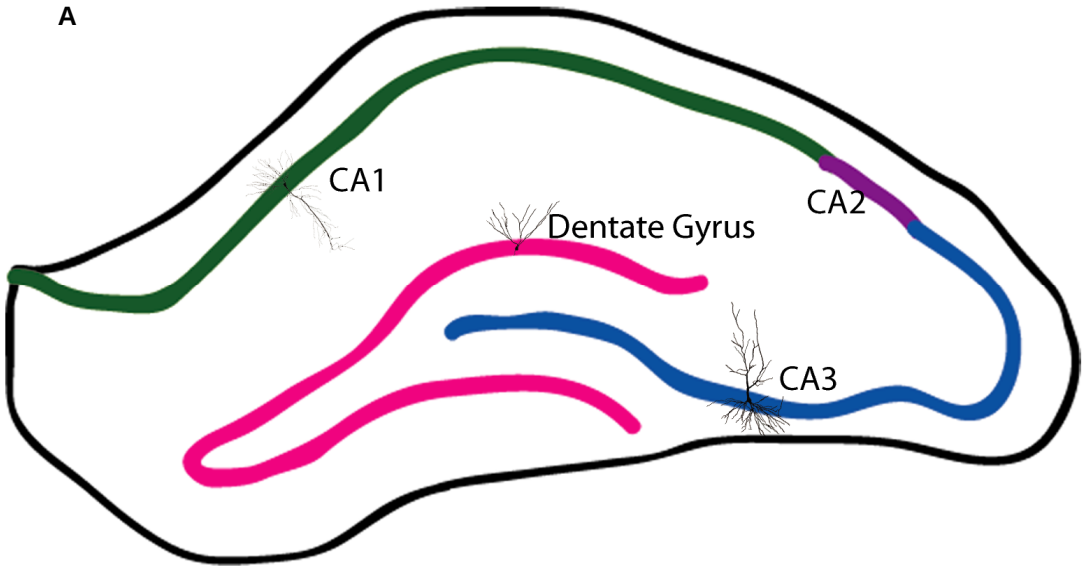

Figure 4. Hippocampus Afferents and Efferents. (A) Unilateral diagram of the rat hippocampus in a coronal section. (B) CA1 pyramidal cell, (C) CA3 pyramidal cell and (D) Dentate Gyrus granule cell afferents (red) and efferents (green arrows and green type) (Spruston et al., 2006). s.p.=stratum pyramidale, s.o.=stratum oriens, s.r.=stratum radiatum, s.l.m.=stratum lacunosum-moleculare, s.l.=stratum lucidum, s.m.=stratum moleculare, s.g.=stratum granulosum

Hippocampus Afferents and Efferents (CA1 Pyramidal Cell)

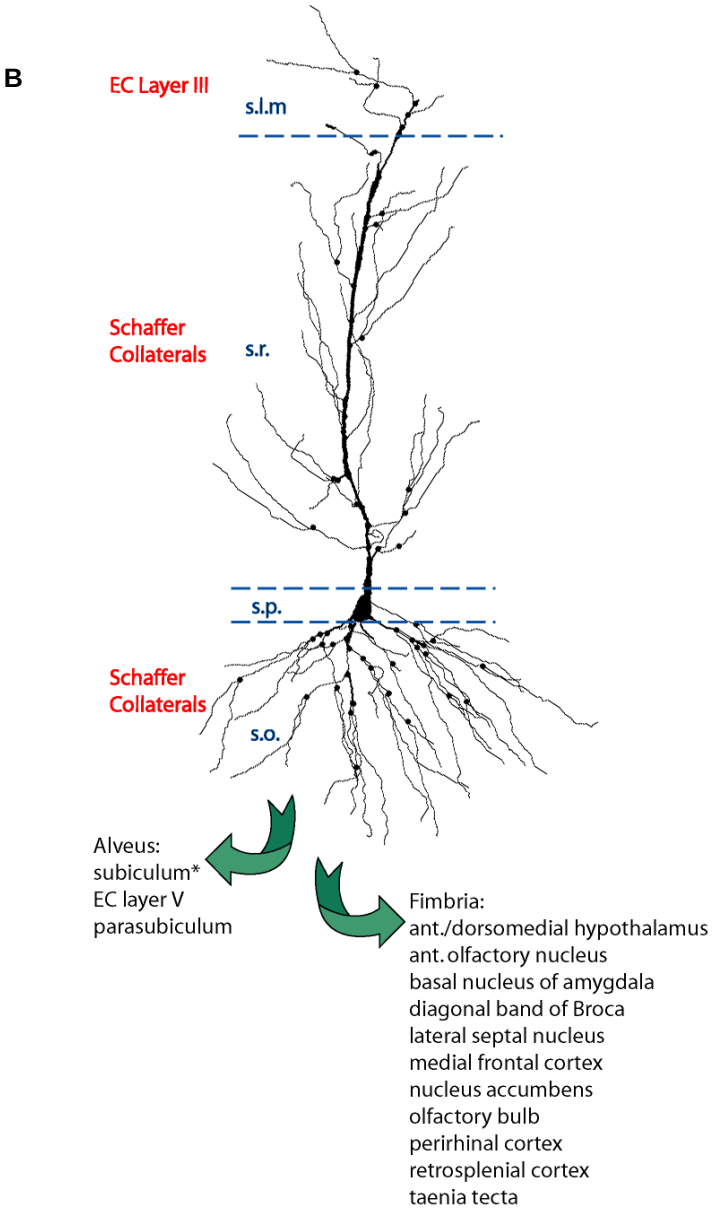

Other Afferents:
nucleus reuniens of thalamus
basolateral nucleus of the amygdala
cholinergic afferents from septum
noradrenergic inputs from locus coeruleus
serotonergic inputs from raphe nuclei
dopaminergic inputs from ventral tegmental area

inhibitory interneurons

Other Efferents:
interneurons

Hippocampus Afferents and Efferents (CA3 Pyramidal Cell)

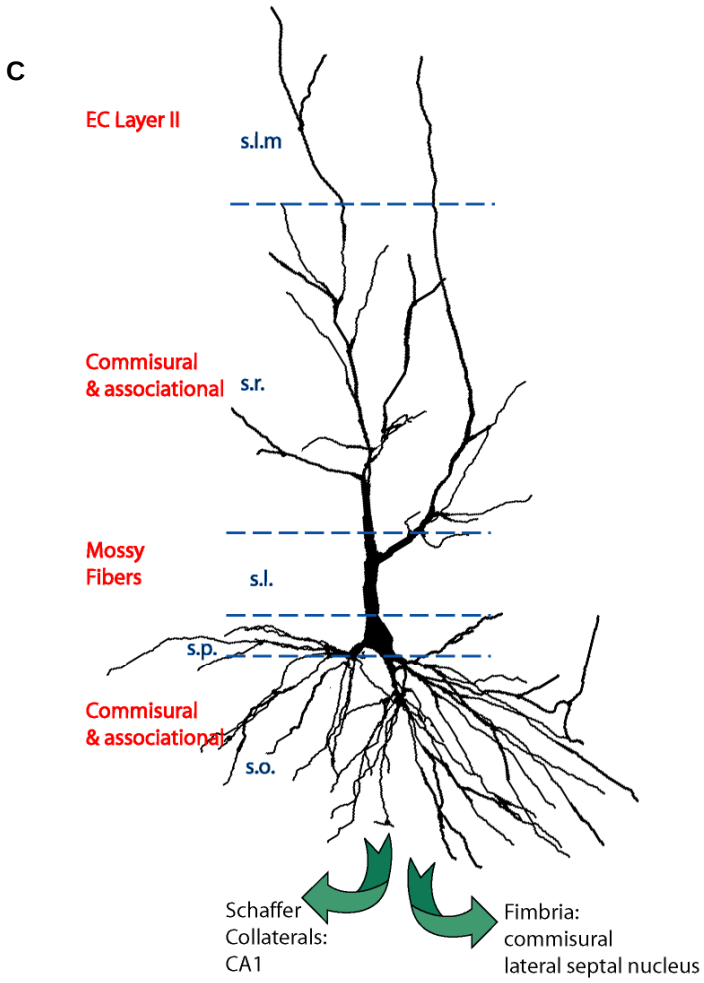

Other Afferents
cholinergic afferents from septum
and nucleus of the diagonal band of Broca

inhibitory interneurons

Other Efferents:
interneurons

Hippocampus Afferents and Efferents (Dentate Gyrus Granule Cell)

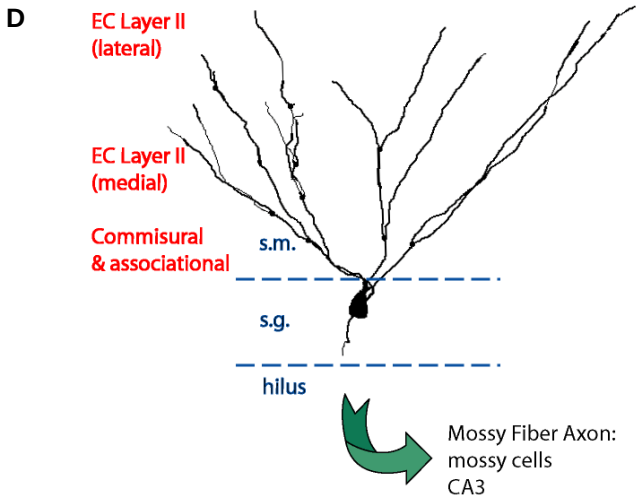

Other Afferents
cholinergic afferents from septum
noradrenergic inputs from locus coeruleus
dopaminergic inputs from ventral tegmental area
hypothalamus supramammillary region

inhibitory interneurons

Other Efferents:
interneurons

Cognitive Processes Involved in Performance on the Morris Water Maze

Performance on the Morris water maze involves several different cognitive processes. The most obvious is the learning of the location of the hidden platform in relation to distal cues. Additionally, at the start of testing rats must acquire the procedural aspects of the task. For example, rats must learn that there is no escape in the periphery of the pool or via the wall of the pool, and that there is an escape platform located in the central part of the pool. Additionally, at the start of testing when the environment is novel, rats use a process called "dead reckoning" to spatially navigate. With dead reckoning rats keep track of their location in relation to the start location by using self-movement cues (Whishaw, 1998; Wallace et al., 2008). Manipulations that impair Morris water maze performance could be related to deficits in any of these cognitive processes.

DENDRITIC SPINES

Structure of Dendritic Spines as it Relates to Function

Dendritic spines are small protrusions from dendrites that are the postsynaptic sites of most excitatory synapses in the brain. Dendritic spines can be categorized by their shape (Fig 5). Mushroom, thin and 2-headed spines have distinct heads, while stubby spines by definition have a head diameter that is approximately equal to the width of the neck. Filopodia are dendritic protrusions that are abundant during development. Filopodia may have no synapses or multiple synapses, and that can develop into either dendritic spines or retract to form synapses on the dendritic shaft. Filopodia are also present in the adult, but are much more scarce (Bourne et al., 2008).

Dendritic spine morphology is of interest because the shape of a spine indicates the strength of the synapse. Therefore, observing changes in the morphology and number of dendritic spines is a way to observe changes in the organization and strength of excitatory synaptic connections (Tada et al., 2006). Mushroom spines have large heads and narrow necks, and are thought to be stronger and more stable. Mushroom spines have larger post-synaptic densities, more AMPA receptors, are more likely to contain smooth endoplasmic reticulum and polyribosomes, and are more likely to be associated with astroglial processes (Bourne and Harris, 2008). Thin spines on the other hand are thought to be more plastic because they can form and change size readily and are less stable. Mushroom spines can last for months, while thin spines can turnover in several days. One way to conceptualize this idea is to think of mushroom spines as “memory spines” and thin spines as “learning spines” (Bourne et al., 2007).

The morphology of dendritic spines depends upon the actin cytoskeleton (Bourne and Harris, 2008). Interestingly, several of the molecules downstream of Nogo-A signaling act on the actin cytoskeleton and affect the morphology of dendritc spines. It has been demonstrated that RhoA and ROCK shortens spines (Tashiro et al., 2008), LIMK1 promotes enlargement of spines (Meng et al., 2002; Schratt et al., 2006), and cofilin promotes shrinkage of spines (Chen et al., 2007).

Common Dendritic Spine Morphologies

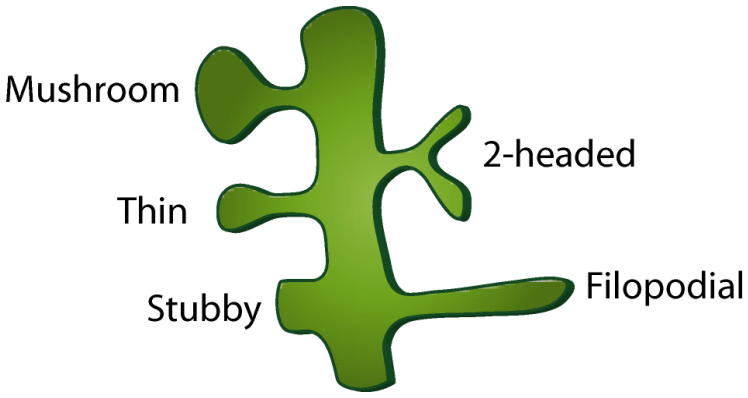

Figure 5. Common Dendritic Spine Morphologies. These classifications are made based upon the relationship between the head diameter and neck width. For example, mushroom spines have head diameters that are much larger than the neck width. On the other hand in stubby spines the head diameter is the same as the neck width. Filopodial protrusions are not considered to be dendritic spines, but instead may act as precursors to dendritic spines.

CHAPTER THREE

IMPROVED PERFORMANCE ON THE MORRIS WATER MAZE AFTER STROKE AND ANTI-NOGO-A IMMUNOTHERAPY IN AGED RATS

ABSTRACT

We have previously shown that immunotherapy directed against the protein Nogo-A leads to recovery on a skilled forelimb reaching task in rats after sensorimotor cortex stroke and this improvement correlated with axonal and dendritic plasticity. Here we investigated anti-Nogo-A immunotherapy as an intervention to improve performance on a spatial memory task in aged rats after stroke, and whether cognitive recovery was correlated with structural plasticity. Aged rats underwent a unilateral permanent MCAO and one week later were treated with an anti-Nogo-A or control antibody. Nine weeks post-stroke, treated rats and normal aged rats were tested on the Morris water maze task. Following testing rats were sacrificed and brains processed for the Golgi-Cox method. Hippocampal CA3 and CA1 pyramidal and dentate gyrus granule cells were examined for dendritic length and number of branch segments, and CA3 and CA1 pyramidal cells were examined for spine density and morphology. Anti-Nogo-A immunotherapy given one week following stroke in aged rats improved performance on the reference memory portion of the Morris water maze task. However, this improved performance was not correlated with structural changes in hippocampal CA3 and CA1 pyramidal or dentate gyrus granule cells. Our finding of improved performance on the Morris water maze in aged rats after stroke and treatment with anti-Nogo-A immunotherapy demonstrates the

promising therapeutic potential for anti-Nogo-A immunotherapy to treat cognitive deficits after stroke.

INTRODUCTION

Each year 795,000 people in the United States have a new or recurrent stroke, and 87% of these events are caused by blockage of a cerebral artery (Lloyd-Jones et al., 2009), leading to ischemic brain damage. Such brain damage often results in long-term neurological deficits in various functions including cognition. The risk of stroke increases with age (Lloyd-Jones et al., 2009) and in the elderly population more advanced age is associated with greater disability after ischemic stroke (Kelly-Hayes et al., 2003). This is thought to be due at least in part to the differential response of the aged brain to ischemia, including increased neuronal degeneration and apoptosis (Popa-Wagner et al., 2007c), faster onset of inflammation and scar formation (Badan et al., 2003b), and increased DNA damage and oxidative stress (Li et al., 2005a; Popa-Wagner et al., 2007a). Therefore, in order to best investigate the therapeutic potential of emerging therapies for stroke recovery, using the appropriate age group in animal models of stroke is important and recommended by the Stroke Therapy Academic Industry Roundtable (STAIR, 1999) and the Stroke Progress Review Group (Grotta et al., 2008).

Spontaneous recovery of function after stroke is thought to be limited by the growth inhibitory environment in the adult CNS, which includes the myelin-associated inhibitors (Gonzenbach and Schwab, 2008). The potent myelin inhibitor Nogo-A was first identified as a neurite growth inhibitory protein *in vitro* (Caroni et al., 1988b; Caroni and Schwab, 1988a; Chen et al., 2000a; GrandPre et al., 2000; Prinjha et al., 2000) and then as an inhibitor of axonal regeneration and compensatory growth and recovery of function in models of spinal cord injury (Gonzenbach and Schwab, 2008). Subsequently

we have shown that anti-Nogo-A immunotherapy after focal ischemic stroke leads to functional recovery in a skilled sensorimotor test in adult and aged rats (Papadopoulos et al., 2002a; Markus et al., 2005a; Seymour et al., 2005a; Tsai et al., 2007). The functional recovery in adult rats was correlated with axonal compensatory growth (Papadopoulos et al., 2002a; Markus et al., 2005a; Seymour et al., 2005a), and increased dendritic arborization and spine density in the contralesional sensorimotor cortex (Papadopoulos et al., 2006), indicating that recovery of sensorimotor function after cortical injury may be achieved by dis-inhibiting sprouting in axons and dendrites by strategies to neutralize the Nogo-A protein.

Importantly, ischemic stroke can lead to other types of neurologic deficits other than sensorimotor impairment, including cognitive disorders. Therefore, we investigated the therapeutic potential of anti-Nogo-A immunotherapy on cognitive recovery after ischemic stroke in aged animals. We found that anti-Nogo-A immunotherapy given one week after stroke in aged rats improved performance on a spatial memory task, but was not correlated with increased dendritic complexity or increased spine density in hippocampal neurons.

METHODS

Animal Subjects

Experiments were approved by the Institutional Animal Care and Use Committee of Hines Veterans Affairs Hospital. Aged male Long Evans black-hooded rats (18 months of age at start of the study) were divided into three groups: (1) Normal aged (n=10), (2)

MCAO/control antibody treatment (n=13), and (3) MCAO/anti-Nogo-A antibody treatment (n=12). Rats were double housed, except in the case of three rats in which one rat's cage-mate died after surgery, and two rats were cage-mates and had to be separated due to fighting. Rats were maintained in a 12 hour light/dark cycle, with free access to food and water. Behavioral testing was performed during the light phase. Rats in both stroke groups and the normal aged rats were weighed and evaluated on a 3 point score for activity level (1=sick, 2=low activity, 3=normal activity) and for coat condition (1=dirty and rough, 2=moderate, 3= smooth and shiny) at least once per week.

Stroke Surgery

MCAO was performed as in Chen et al. (Chen et al., 1986), and as in our previous work (Papadopoulos et al., 2002a; Markus et al., 2005a; Seymour et al., 2005a; Papadopoulos et al., 2006; Tsai et al., 2007). Briefly, rats were anesthetized with isoflurane inhalant anesthesia (3% in oxygen). Through an anterior cervical incision the bilateral common carotid arteries (CCA) were isolated. Rats were placed in a stereotaxic frame and a 2 cm vertical incision was made between the right eye and right ear and the temporalis muscle retracted. A burr hole exposed the MCA and the artery was ligated with a 10-0 suture and transected above the suture with microscissors. The right CCA was permanently ligated with 5-0 chromic gut suture, and the left CCA was occluded for 60 minutes with an aneurysm clip. The surgical wound was closed and the rats were returned to pervious housing for one week until antibody infusion as below.

Antibody Intracerebroventricular Infusion

The experimental design is depicted in Fig 6. One week post-stroke, rats were randomized and anesthetized with isoflurane inhalant anesthesia (3% in oxygen). Rats were placed in a stereotaxic frame and a midline incision was made in the scalp. A burr hole on the same side as the stroke lesion exposed the cortex. A cannula was placed into the right lateral cerebral ventricle at coordinates 1.3 mm lateral, 0.8 mm posterior, and 3.8 mm ventral (relative to bregma) and secured to the skull with cyanoacrylate gel. Through a mid-scapular incision an Alzet osmotic minipump (model 2ML2; Durect Corporation, Cupertino, CA, USA) was implanted subcutaneously posterior to the scapulae and connected to the cannula with polyethylene tubing. Either purified mouse monoclonal anti-Nogo-A antibody (11C7, IgG1) or control antibody (anti-wheat auxin, IgG1) was infused at a rate of 15 μg/hr (2.5 mg/ml) for two weeks, after which the animals are again anesthetized and the pumps removed.

Morris Water Maze

Morris water maze testing started 9 weeks post-stroke. Experimenters were blinded to antibody treatment. Rats were handled for five consecutive days, excluding weekends, prior to stroke surgery and then once weekly until one week before Morris water maze testing when they were again handled for five consecutive days. The apparatus consisted of a galvanized steel circular tank with a diameter of 6 feet and a depth of 2 feet filled halfway with water (20-22º) colored white with tempura paint. A 4 inch by 4 inch topped plexiglass platform covered in a white sock for traction was located just below the

surface of the water. Prominent distal cues in the room including posters, cabinets, and blacked out windows remained constant throughout testing.

PLACE TASK. During days 1-7 of testing the hidden platform was always located in the same position in the NE quadrant of the pool. Rats were given four trials per day starting from each of the four cardinal locations (N, E, S and W) in a random order. Trials were separated by at least five minutes. When rats reached the platform, they were allowed to remain there for 30 seconds, and then removed. If rats did not find the platform in 2 minutes then the experimenter guided the rat to the platform with her hand. In between trials rats were dried with a towel and returned to their home cages. The place task evaluates the rats' ability to learn about the environmental cues to guide movement toward the hidden platform.

PROBE TRIAL. On day 8 of testing the platform was removed from the pool and the rats were given one probe trial lasting 2 minutes and starting from the west start location. The probe trial tests whether the rats prefer the pool quadrant where the platform was previously located during the place task.

MATCHING-TO-PLACE TASK. On days 9-13 of testing the platform location was moved each day in the sequence as follows: SE, NW, SW, NE, and SW quadrants. Rats were given two trials per day from the W start location, and trials were separated by 20 seconds. Rats remained on the platform for 30 seconds. If rats did not find the platform in

4 minutes then the experimenter guided the rat to the platform with her hand. In between trials rats were placed in a bucket on the floor of the testing room. The matching-to-place task evaluates the rats' ability to update their representations of the hidden platform.

Behavioral Analysis

All water maze trials were recorded to DVD using an overhead bullet camera. Ethovision 3.1 (Noldus Information Technology, Leesbug, VA, USA) video tracking software was used to digitize the trials.

PLACE TASK. Both time and distance to locate the platform from each of the four trials per day were averaged for statistical analysis.

PROBE PREFERENCE SCORE. For the probe trials the probe preference score was calculated as [(T-A)+(T-B)+(T-C)]/3, where T is the swim time in the quadrant that contained the platform during the place task and A, B, and C are the swim times in the other three quadrants (Brown et al., 2000).

THIGMOTAXIS. Time spent and distance swam in the outer 50% of the pool were generated from Ethovision 3.1 software for each rat on each of the four trials on seven days of hidden platform testing. Thigmotaxis for time was represented as time spent in the outer 50 % of the pool over total swim time. Thigmotaxis for distance was represented as distance swam in the outer 50 % of the pool over total distance swam.

PATH CIRCUITY. Path circuity was calculated as the direct distance to the platform over the total distance traveled to the platform.

HEADING DIRECTION. Heading direction angle represents the actual trajectory of the rat in relation to a direct trajectory toward the hidden platform (Wallace et al., 2002). A heading direction angle of 0º indicates that the rat's trajectory is in a direct path toward the hidden platform. Heading direction angles at 1.2-1.5 seconds after the start of the trial were obtained from Ethovision 3.1 software for each rat on each of the four trials per day during the place task.

Golgi-Cox Staining

Thirteen weeks post-stroke and two weeks after completion of Morris water maze testing, rats were overdosed with pentobarbital (100 mg/kg, i.p.) and transcardially perfused with 0.9% saline and 10,000 U heparin/liter. The brains were removed and immersed whole in Golgi-Cox solution (Glaser et al., 1981) for two weeks. The brains were coronally sectioned at 200 μm on a vibratome, mounted on 2% gelatinized slide and reacted as described by Gibb and Kolb (Gibb et al., 1998). Slides were coded to blind the experimenters to the antibody treatment group.

Stroke Size and Hippocampal Area Analysis

Golgi-Cox stained coronal brain sections were traced, and bilaterally the hippocampus was traced, using Neurolucida software (mbf Bioscience, Williston, VT, USA) and with

the aid of an atlas (Paxinos, 2005). Stroke size was represented as percent of the intact contralateral hemispheric area (total area of the intact contralateral hemisphere minus total area of the intact ipsilesional hemisphere over total area of the intact contralateral hemisphere). Hippocampal areas were represented as a ratio of the right hippocampal area/ left hippocampal area.

Neuroanatomical Analysis

Golgi-Cox stained hippocampal CA3 and CA1 pyramidal cells and dentate gyrus granule cells were analyzed in the dorsal hippocampus as described below.

For illustration purposes, images of representative CA3 and CA1 pyramidal cells and dentate gyrus granule cells were taken. Image stacks were acquired every 5 μm for 130 μm using Neurolucida software, and then a minimum intensity z projection was generated using ImageJ software.

DENDRITIC BRANCHING AND LENGTH. An average of four apical and basilar dendritic trees of CA3 and CA1 pyramidal cells, and dendritic trees of dentate gyrus granule cells were traced for each side of the hippocampus using Neurolucida software and Leica DM 4000 B with a 63x objective. For inclusion neurons had to be well impregnated, unobstructed by other neurons or glial cells, and intact. Dendritic trees were analyzed for dendritic length and number of branch segments using the branched structure analysis tool of Neurolucida. For CA3 and CA1 pyramidal cells, branches originating from the cell body (basilar) or the apical shaft were considered first order, and

the next bifurcating branches were considered second order and so on. For dentate gyrus granule cells, branches originating from the cell body were considered first order, and the next bifurcating branches were considered second order and so on. For CA3 analysis 9 brains from each group were analyzed, and for CA1 and dentate gyrus analysis all brains from each group were analyzed.

SPINE DENSITY AND MORPHOLOGY. Four CA3 and CA1 pyramidal cell apical dendritic terminal branches of second or higher order were analyzed for each side of the hippocampus using a 100x oil immersion lens. For a 50 µm length segment of the branch dendritic protrusions were counted and assigned to a morphology category of filopodium, 2-headed, stubby, thin, and mushroom shaped as described by Bourne and Harris (Bourne and Harris, 2008). The first 10 µm of the dendrite after the branch point and the terminal 10 µm were excluded from analysis. For CA3 analysis 9 brains from each group were analyzed, and for CA1 analysis 9 brains from the normal aged group were analyzed, 9 from the stroke/control antibody group, and 8 from the stroke/anti-Nogo-A antibody group.

Statistical Analysis

P values of less than 0.05 were considered significant.

BEHAVIORAL DATA. Behavioral data analysis was performed with SAS software (SAS Institute, Cary, NC, USA) except where noted.

For comparison of place task time and distance to the platform we started with a general linear model repeated measures ANOVA (SPSS, Chicago, IL, USA). The results from this analysis are presented in Fig 10. When we examined plots of time and distance to the platform over the seven days of the place task for each of the rats, we saw a trend for normal aged rats and stroke/anti-Nogo-A rats to have steeper slopes than stroke/control antibody rats. To determine if there were statistically significant differences in the slopes we used a non-linear mixed model in which a y intercept and slope parameter were determined for each individual rat. Specifically for this analysis we used a likelihood based $\chi 2$ test of random-effects simple exponential two-parameter model, $\eta(x) = \theta_1 e^{-\theta_2 x}$, where x = day – 1 (Haines et al., 2004; Clementz et al., 2008). We did not need to correct for velocity because swim velocities during the place task did not differ between groups (p=0.2476; Fig 12). This model was able to identify more subtle differences in performance on the Morris water maze in aged rats, which have greater variability in Morris water maze testing.

For comparison of swim velocities we used a repeated measure ANOVA. For comparison of probe preference scores we used a one-way ANOVA SigmaStat (Systat, San Jose, CA, USA). For comparison of the matching-to-place task times to swim to the platform we used a two-way repeated measures ANOVA. For comparison of thigmotaxis we used a likelihood based $\chi 2$ test of random-effects simple exponential three-parameter model, $\eta(x) = \theta_1 e^{-\theta_2 x} + \theta_3$, where x = day – 1. For comparison of the path circuity, weight, activity score and coat score we used a repeated measures ANOVA followed by a Bonferroni post-hoc test using the SPSS software.

For comparison of heading direction angles we first generated angular variance, also known as the length of the mean vector (r), for each rat for each of the seven days of the place task using the Oriana circular statistics program (RockWare Inc., Golden, CO, USA). Angular variance ranges from 0 to 1, with 0 meaning that the rat's heading direction angles are random, and with a 1 meaning that the rat's heading direction angles are all in the same direction. We then compared angular variances across groups using a repeated measures ANOVA (SPSS). Secondly, we generated a mean heading direction angle, ranging from 0-360º, for each rat for each of the seven days of the place task using Oriana. We then compared mean heading direction angles across groups for each day of the place task using the Watson-Williams F test with Oriana (Wallace et al., 2002).

NEUROANATOMICAL DATA. Neuroanatomical data analysis was performed with SigmaStat as follows: a t-test for stroke size, a one-way ANOVA with Student-Newman-Keuls post-hoc for comparison of hippocampal areas, and dendritic arbor branching and length (in cases when the data was not normal and we used a Kruskal Wallis one-way ANOVA on ranks with Dunn's method post-hoc), and a one-way ANOVA for comparison of spine density and morphology.

Experimental Timeline

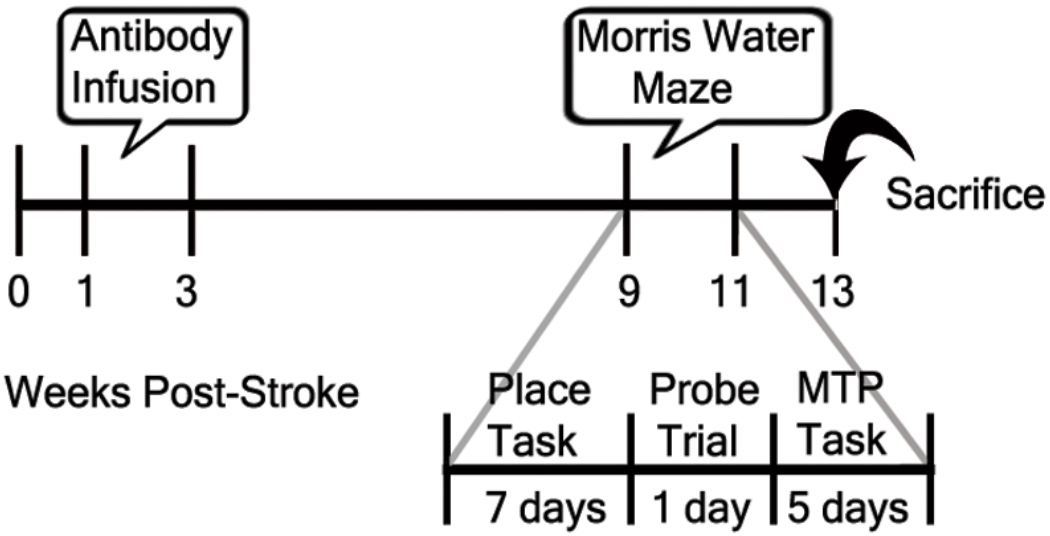

Figure 6. Experimental timeline. Aged rats underwent MCAO and one week later infusion of a anti-Nogo-A antibody or control antibody began. Nine weeks post-stroke, treated rats and normal aged rats began training on the Morris water maze to assess spatial memory. After completion of behavioral testing, rats were sacrificed and the brains processed for the Golgi-Cox stain. MTP=Matching-to-Place task

RESULTS

Health of aged rats post-stroke

After MCAO both stroke groups lost about 100 grams of weight as compared to unlesioned normal aged rats, and there was no difference between the weight lost by the two stroke groups (normal aged vs. stroke/control antibody p=0.002, normal aged vs. stroke/anti-Nogo-A antibody p=0.003, stroke control antibody vs. stroke/anti-Nogo-A antibody p=1.00; Fig 7A). To determine if general activity level, or grooming behavior is affected by stroke in aged rats we assessed rats each week for activity level and condition of the coat. We detected no differences between groups for activity level (p=0.051; Fig 7B) and coat condition (p=0.390; Fig 7C).

Some aging related health problems were observed and included 5 rats with subcutaneous tumors, 2 rats with cysts, and 1 rat with a small pituitary tumor. However, it was not necessary to drop any of these animals from behavioral testing or neuroanatomical analysis.

Stroke size did not differ between the two stroke groups

Analysis of the stroke lesions showed a mean size of approximately 22% of the intact contralateral hemisphere and included the sensorimotor cortex with minimal subcortical involvement (Fig 8). The size of the stroke lesion did not significantly differ between the stroke/control antibody group and the stroke/anti-Nogo-A antibody group (p=0.706; Fig 8B).

Ratio of right hippocampal areas to left hippocampal areas showed slight differences

Analysis of hippocampal areas was performed by taking a ratio of the right hippocampal areas to the left hippocampal areas. The right hippocampus is ipsilateral to the sensorimotor cortex stroke. A value of 1 means that the right and left hippocampus have equal areas. There was a significant effect for group ($p=0.024$), and post-hoc analysis showed a significant difference between the normal aged group and the stroke/control antibody group ($p=0.020$). The stroke/control antibody group mean was 1.149, while the normal aged group mean was 1.038, demonstrating that the stroke/control antibody group had slightly larger right hippocampus to left hippocampus ratios than the normal aged group. The normal aged group was no different from the stroke/anti-Nogo-A antibody group ($p=0.233$), and the stroke/control antibody group was no different from the stroke/anti-Nogo-A antibody group ($p=0.097$). The slight difference between the normal aged and stroke/control antibody groups may be due to the limitations of tracing structures on Golgi-Cox processed tissue and is probably not a meaningful difference.

Performance on the spatial reference memory task is improved in aged rats after stroke and treatment with anti-Nogo-A immunotherapy

Rats were tested over seven days in the place task, a spatial reference memory task. At the start of the place task animals in all groups found the hidden platform in a similar time frame ($p= 0.2122$; Fig 11A, A'). As testing continued the rate at which rats in the stroke/anti-Nogo-A antibody group acquired the hidden platform location was faster than the stroke/control antibody group ($p=0.00001$). In fact, the stroke/anti-Nogo-A antibody

group was indistinguishable from the normal aged group (p=0.1573), while the rate at which the stroke/control antibody group acquired the hidden platform location was slower than the normal aged group (p=0.00001). These findings were supported by analyzing the distance the rats took to locate the hidden platform. At the start of the place task animals in all groups swam similar distances to locate the platform (p= 0.2122; Fig 11B, B'). As testing continued the rate at which rats in the stroke/anti-Nogo-A antibody group acquired the hidden platform location was faster than the stroke/control antibody group (p=0.0003). However, both stroke groups had slower rates to acquire the hidden platform location than the normal aged group (p=0.0055 for stroke/anti-Nogo-A antibody, $p \approx 0$ for stroke/control antibody). Taken together, these results indicate that rats in the stroke/anti-Nogo-A antibody group acquired the hidden platform location faster than rats in the stroke/control antibody group.

At the completion of the place task, a probe trial was undertaken to assess if animals knew the former hidden platform location. All groups equally preferred the quadrant where the platform was previously located with no significant differences between groups (p=0.876; Fig 13). Therefore, at the end of the place task all groups had equally learned the hidden platform location.

Performance on a spatial working memory task is unaltered by stroke and antibody treatments

Following the probe trial, rats were tested on the matching-to-place task, a spatial working memory task. Rats in all groups found the platform faster on trial 2 than on trial 1 ($p<0.0001$), and there were no significant differences between groups (p=0.4387 for

trial 1, p=0.0550 for trial 2; Fig 14). Therefore, all groups performed equally well on the matching-to-place task, and there was no apparent effects of stroke on spatial working memory.

Effects of stroke on behavior observed during the place task

Thigmotaxis was defined as swimming in the outer 50% of the pool area. At the start of the place task all groups swam similar times in the periphery of the pool (p=0.1572; Fig 15A, A'). As testing continued both stroke groups significantly spent more time swimming in the periphery of the pool as compared to normal aged rats (p=0.0006), and the two stroke groups were not significantly different from each other (p=0.4028). At the end of the place task all groups swam similar times in the periphery of the pool (p=0.5220). Thigmotaxis for distance showed similar results with the two stroke groups swimming significantly more distance in the periphery of the pool as compared to normal aged (p=0.0003; Fig 15B, B'). Therefore, rats with stroke regardless of treatment spent more time than normal aged rats in the periphery of the pool.

Path circuity is defined as the ratio of the direct distance to the platform/ the actual swim distance to the platform during a trial. Both stroke groups swam significantly less direct paths to the platform than normal aged rats (p=0.015 for stroke/control antibody, p=0.023 for stroke/anti-Nogo-A antibody; Fig 16), and the two stroke groups were not significantly different from each other (p=1.00). Therefore, rats with stroke regardless of treatment took less direct paths to reach the platform, as compared to normal aged rats.

Swim paths taken during Morris water maze testing

Swim paths from one animal in each group for the place task, probe trial and matching-to-place task are shown in Figures 17-22.

To analyze what swim trajectory the rats took at the start of each trial we analyzed heading angles in relation to the platform for all place task trials at 1.2 to 1.5 seconds after the start of the trial for angular variance and mean angle. These are used as a measure of how accurate the swim path direction was for the platform at the beginning of each trial during the place task. Angular variance, or the spread of the heading direction angles for each rat, across the seven days of the place task did not significantly differ between groups ($p=0.345$; Fig 23). On day two of the place task the mean heading direction angle for the stroke/control antibody treated group significantly differed from the stroke/anti-Nogo-A treated group ($p=0.014$; Fig 24). Mean angles did not significantly differ between groups on the other six days of the place task (Fig 24).

Dendritic complexity was slightly reduced in the hippocampus on the same side as the stroke in both stroke groups

Following behavioral testing and 13 weeks post-stroke, we examined the dendritic arbors of Golgi-Cox stained hippocampal CA3 and CA1 pyramidal cells and dentate gyrus granule cells (Fig 25).

For CA3 pyramidal cells, first we compared the total number of branch segments and total dendritic length for the apical and basilar dendritic trees across groups. In CA3 pyramidal cell apical dendritic trees ipsilateral to the stroke both stroke groups had significant decreases as compared to normal aged rats in total number of branch segments

($p<0.001$), and total dendritic length ($p<0.05$; Fig 26A). In CA3 pyramidal cell basilar dendritic trees ipsilateral to the stroke both stroke groups had significant decreases as compared to normal aged rats in total number of branch segments ($p<0.05$), but there were no significant differences in total dendritic length ($p=0.100$; Fig 26B). Next we compared the number of branch segments and dendritic length of CA3 pyramidal cells by branch order across groups. In CA3 pyramidal cell apical dendritic trees ipsilateral to the stroke both stroke groups had significant decreases as compared to normal aged rats in number of branch segments (1^{st} , 2^{nd}, 4^{th}, 5^{th} orders, and 3^{rd} order only for stroke/control antibody), and dendritic length (0 order i.e. apical dendrite, and 1^{st} order; Fig 26A'). In CA3 pyramidal cell basilar dendritic trees ipsilateral to the stroke both stroke groups had significant decreases as compared to normal aged rats in number of branch segments (3^{rd}, 4^{th} orders, and 1^{st} order only for stroke/control antibody), and dendritic length (4^{th} order; Fig 26B').

For CA1 pyramidal cells, first we compared the total number of branch segments and total dendritic length for the apical and basilar dendritic trees across groups and there were no significant differences (Fig 27A, B). Next we compared the number of branch segments and dendritic length of CA1 pyramidal cells by branch order across groups. In CA1 pyramidal cell apical dendritic trees ipsilateral to the stroke the stroke/control antibody rats had significant decreases as compared to normal aged rats in number of branch segments (1^{st} order; Fig 27A'). In CA1 pyramidal cell basilar dendritic trees ipsilateral to the stroke the stroke/anti-Nogo-A antibody rats had significant decreases as compared to normal aged rats in dendritic length (2^{nd} order; Fig 27B').

For dentate gyrus granule cells, first we compared the total number of branch segments and total dendritic length for the dendritic trees across groups and there were no significant differences (Fig 28A). Next we compared the number of branch segments and dendritic length of dentate gyrus granule cells by branch order across groups. In dentate gyrus granule cell dendritic trees ipsilateral to the stroke the stroke/control antibody rats had significant decreases as compared to normal aged rats in number of branch segments (1^{st} order; Fig 28A').

Therefore, there was a decrease in dendritic complexity on the same side as the stroke in CA3, CA1 and dentate gyrus neurons in both stroke groups.

Hippocampal dendritic spine density and morphology showed no differences between groups

Dendritic spine density of CA3 and CA1 pyramidal cell apical dendrites of second order or higher did not significantly differ between groups (Fig 29A, C). When we analyzed number of dendritic spines by morphology there were no significant differences between groups for thin, stubby and mushroom spines (Fig 29B, D). Furthermore, there was no significant difference between groups for number of filopodia (Fig 29B, D).

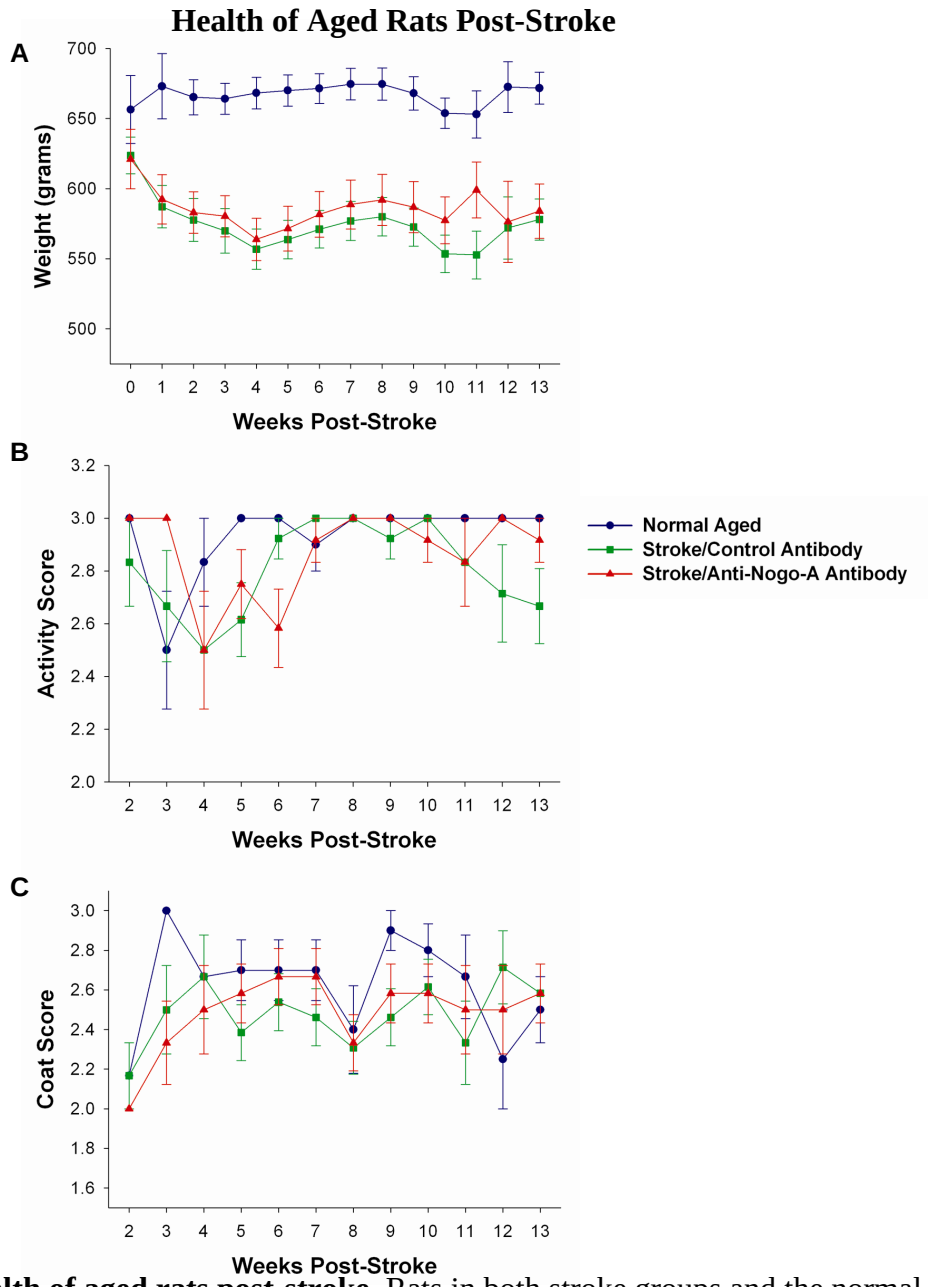

Figure 7. Health of aged rats post-stroke. Rats in both stroke groups and the normal aged rats were weighed, and evaluated on a 3 point score for activity level (1=sick, 2=low activity, 3=normal activity) and coat condition (1=dirty and rough, 2=moderate, 3= smooth and shiny) at least once per week. (A) Both stroke groups had lower weights than the normal aged group, but there was no difference between the two stroke groups ($p<0.005$, repeated measures ANOVA, Bonferroni test for post-hoc comparison). (B) There were no differences between groups for activity level. (C) There were no differences between groups for coat condition. Error bars denote ± standard error of the mean.

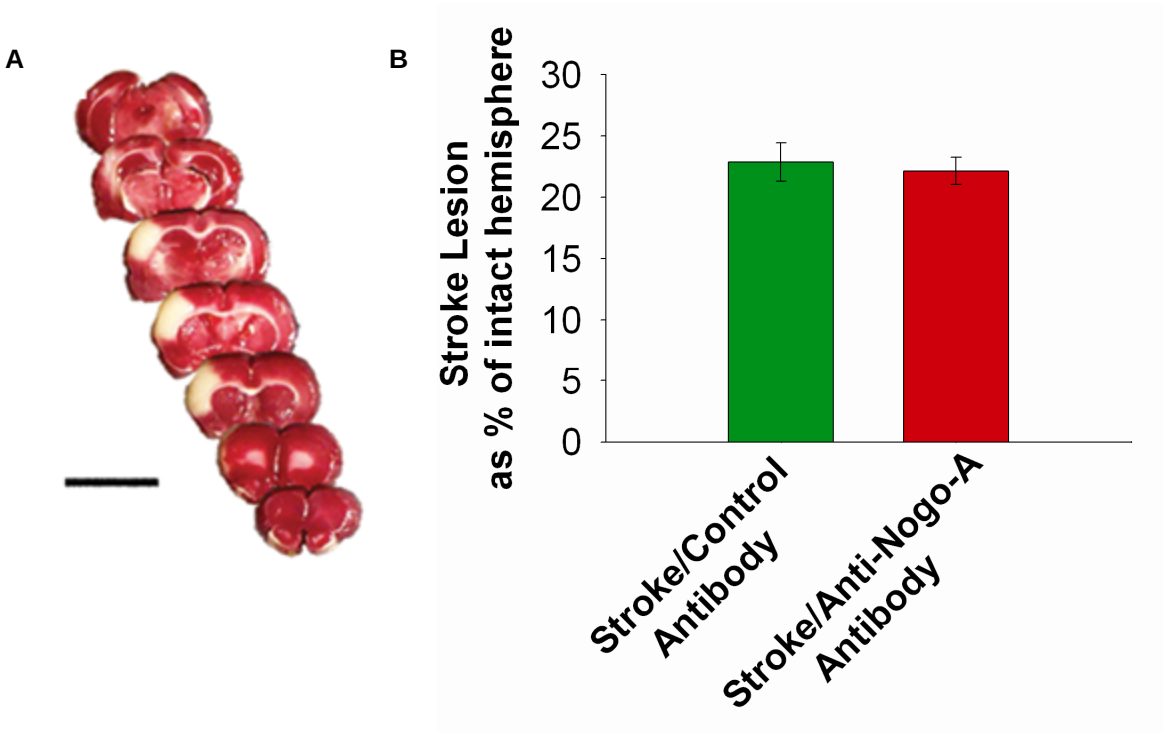

Figure 8. Stroke lesion size. (A) Representative right sided stroke lesion one day post-stroke in an aged rat (scale bar=1 cm). In the TTC (2,3,5-triphenyl-2H-tetrazolium chloride)-reacted coronal brain sections viable tissue appears red and the ischemic infarction appears white demonstrating sensorimotor cortex involvement and subcortical sparing. (B) The stroke lesion size, represented as percent of the intact hemisphere, did not differ between the two stroke groups ($p=0.706$, t-test). Error bars denote ± standard error of the mean.

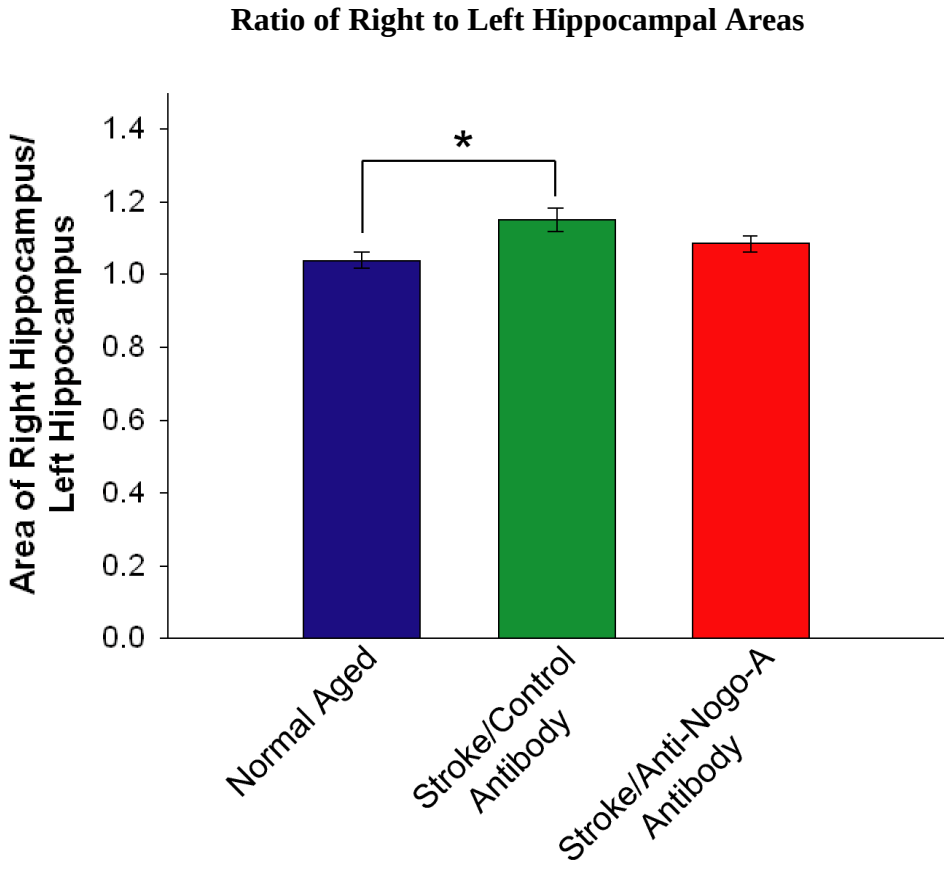

Figure 9. Ratio of Right to Left Hippocampal Areas. Analysis by a one-way ANOVA found a significant effect for group ($p<0.05$), and post-hoc analysis by the Student-Newman-Keuls test showed that the normal aged group and stroke/control antibody group were significantly different ($p<0.05$). Error bars denote ± standard error of the mean. *$p<0.05$.

Place Task Mean Time and Distance to Locate the Hidden Platform During the Place Task

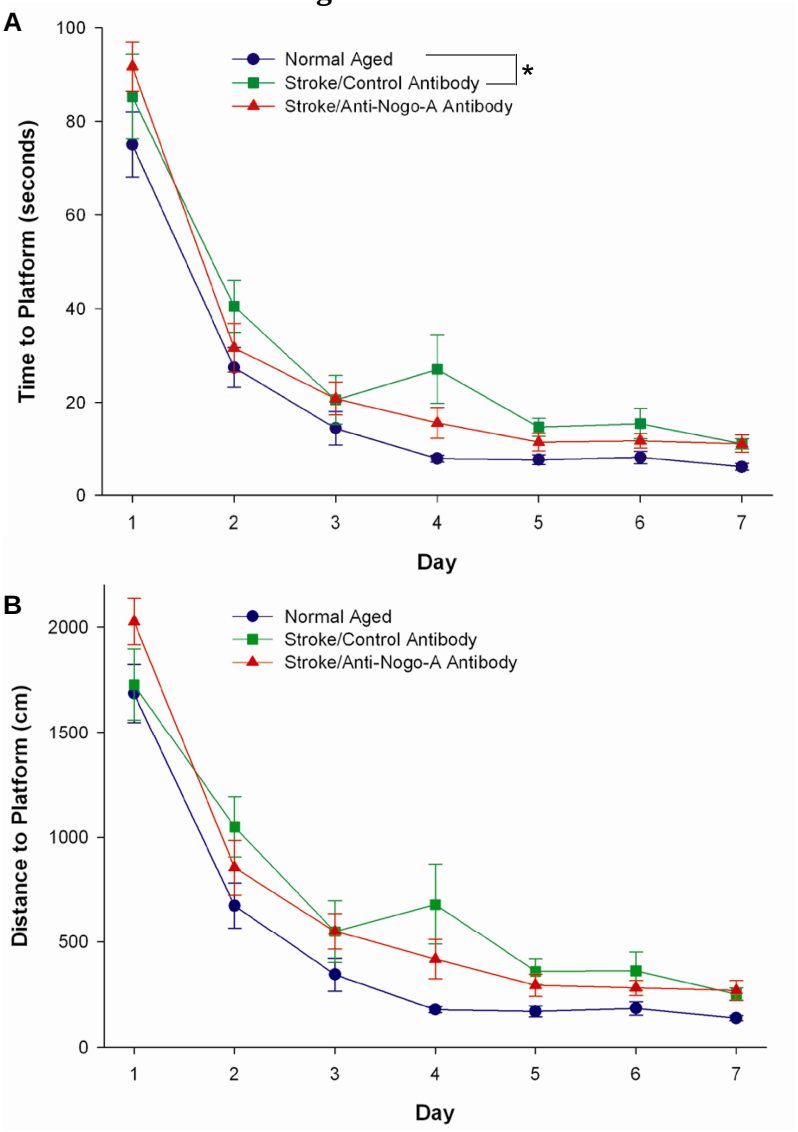

Figure 10. Place task mean time and distance to locate the hidden platform. (A) Analysis by a repeated measures ANOVA of time to locate the hidden platform found a significant effect for group ($p=0.044$) and post hoc analysis by the Bonferroni test showed that the stoke/control antibody group took significantly more time to locate the platform than normal aged rats ($p=0.043$). The stroke/anti-Nogo-A antibody group was not significantly different from the normal aged group ($p=0.258$) or the stroke/control antibody group ($p=1.000$). (B) Analysis by a repeated measures ANOVA of distance to locate the hidden platform did not find a significant effect for group ($p=0.064$), so there was not a significant difference between the three groups for distance to located the hidden platform. Error bars denote ± standard error of the mean. *$p<0.05$. (Figure discussed in methods statistical analysis section).

Rate to Acquire the Location of the Hidden Platform During the Place Task

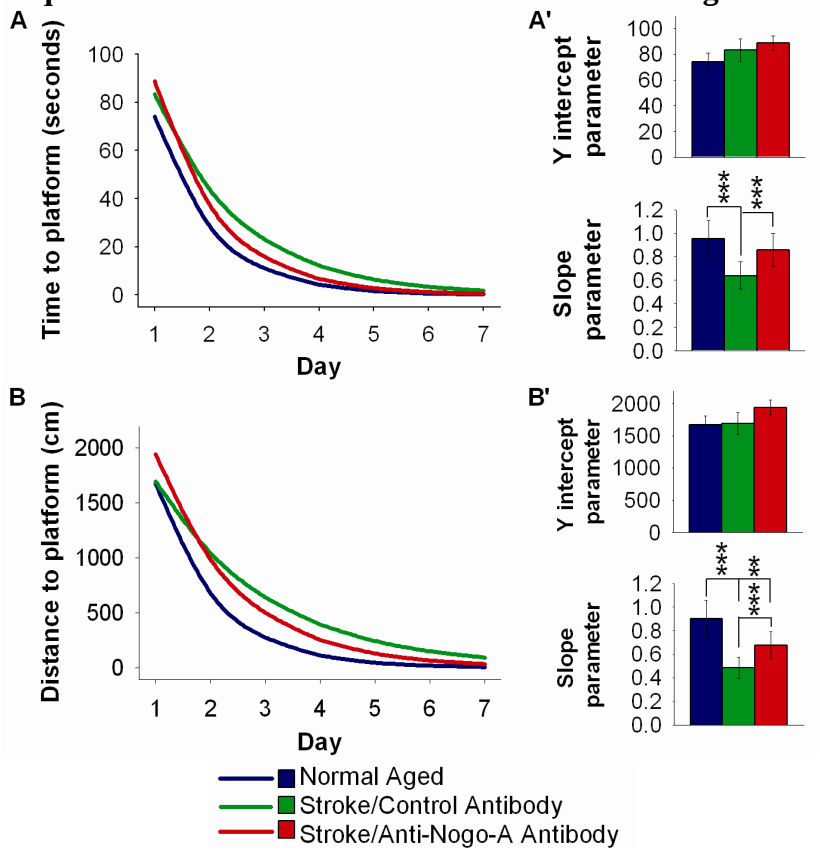

Figure 11. Improved performance on a spatial reference memory task after stroke and treatment with anti-Nogo-A immunotherapy. (A) Time to locate the hidden platform during the Morris water maze place task. Average curves of the fitted functions for each group. (A') Averages of the individual parameters of the functions. Time at the start of testing, or the y intercept, was the same for all groups. As testing continued normal aged and stroke/anti-Nogo-A antibody treated rats acquired the location of the platform faster than stroke/control antibody treated rats, as shown by the slope parameter ($p < 0.001$, likelihood based $\chi 2$ test of random-effects simple exponential two-parameter model, $\eta(x) = \theta_1 e^{-\theta_2 x}$, where x = day – 1). (B) Distance to locate the hidden platform during the Morris water maze place task. Average curves of the fitted functions for each group. (B') Averages of the individual parameters of the functions. Distance at the start of testing, or the y intercept, was the same for all groups. As testing continued all three groups acquired the location of the platform at significantly different rates, with the stroke/anti-Nogo-A antibody treated rats having faster rates to acquire the platform location than stroke/control antibody treated rats ($p<0.001$ for stroke/anti-Nogo-A antibody and stroke/control antibody, $p<0.01$ for normal aged and stroke/anti-Nogo-A antibody, $p<0.001$ for normal aged and stroke/control antibody, likelihood based $\chi 2$ test of random-effects simple exponential two-parameter model, $\eta(x) = \theta_1 e^{-\theta_2 x}$, where x = day –1). Error bars denote ± standard error of the mean. **p<0.01, ***p<0.001.

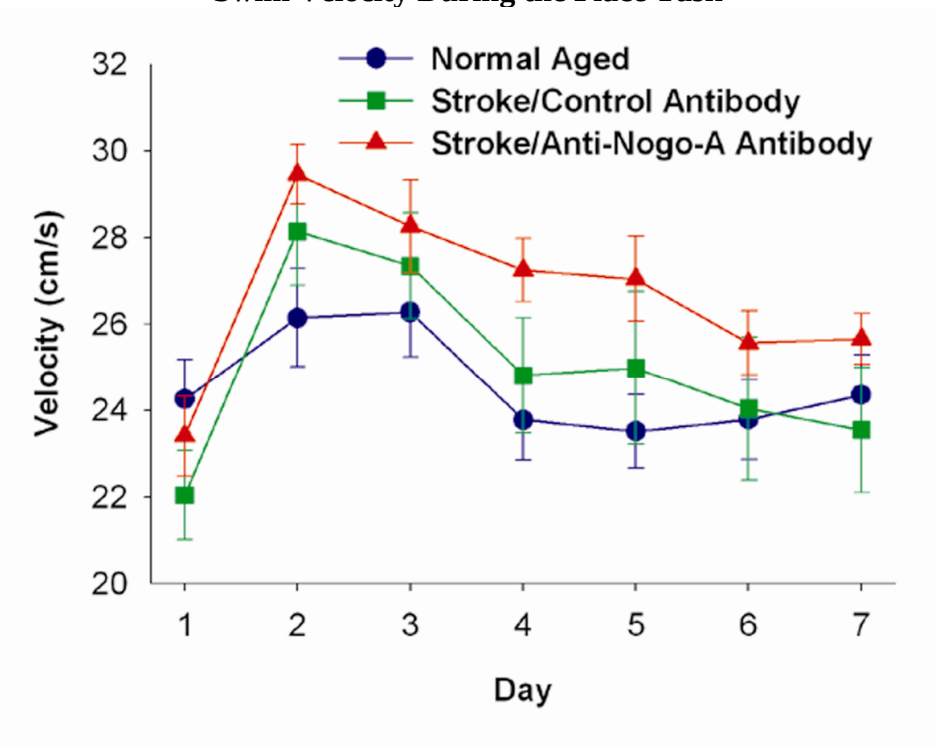

Figure 12. Swim velocity during the Morris water maze place task did not significantly differ across groups (p=0.2476, repeated measure ANOVA). Error bars denote ± standard error of the mean.

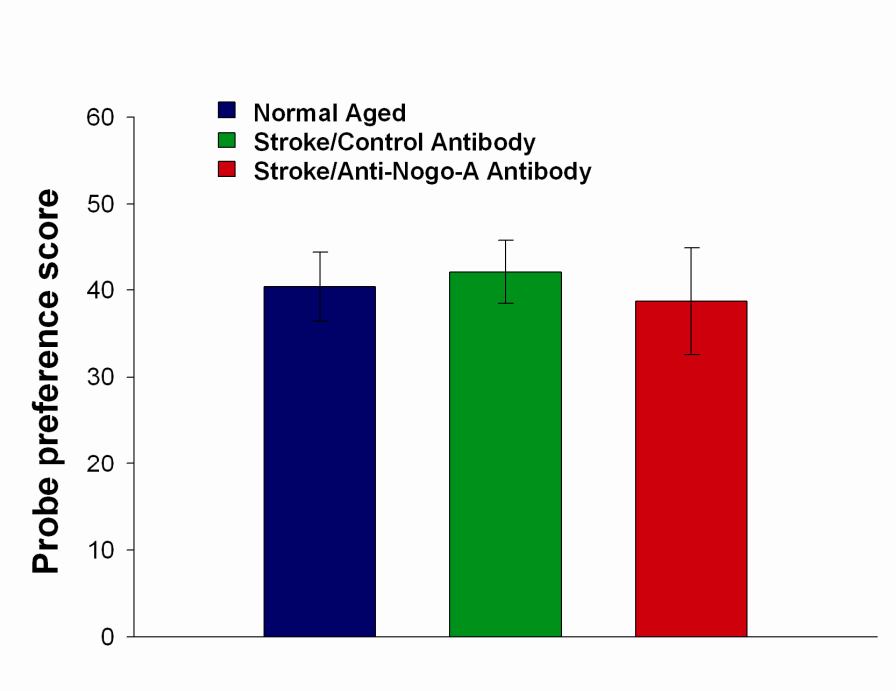

Figure 13. Probe Trial. During the probe trial all groups equally preferred the quadrant that contained the platform during the place task (p=0.876, one-way ANOVA). Error bars denote ± standard error of the mean.

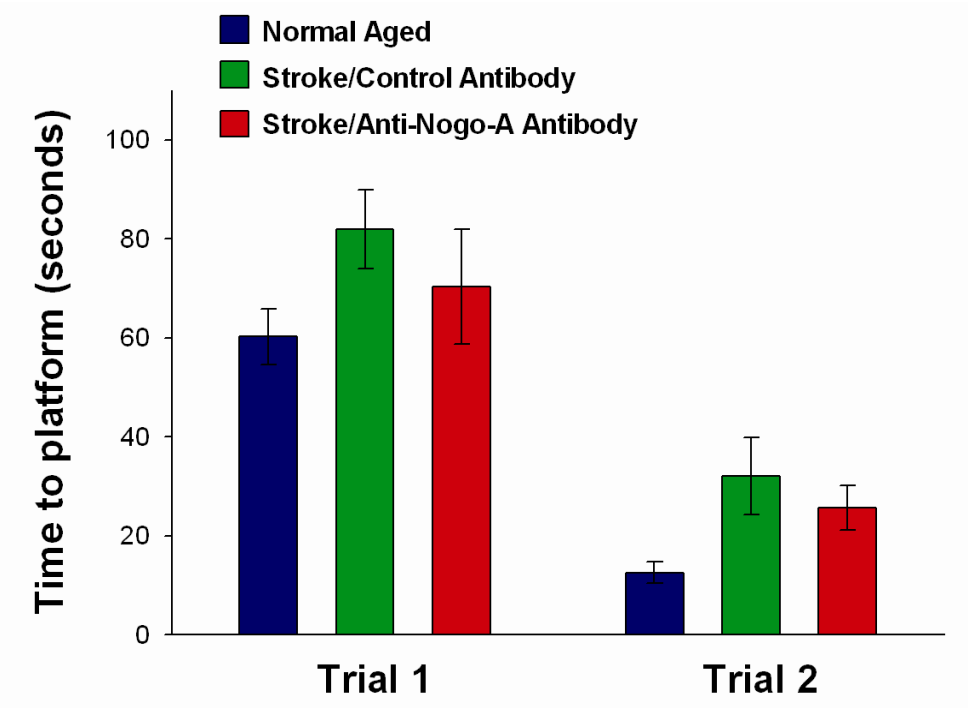

Figure 14. Matching-to-Place Task. During the matching-to-place task all groups found the platform faster on Trial 2 than on Trial 1 ($p<0.001$), and there were no significant differences between groups ($p=0.4387$ for trial 1, $p=0.0550$ for trial 2, two-way repeated measures ANOVA). Error bars denote ± standard error of the mean.

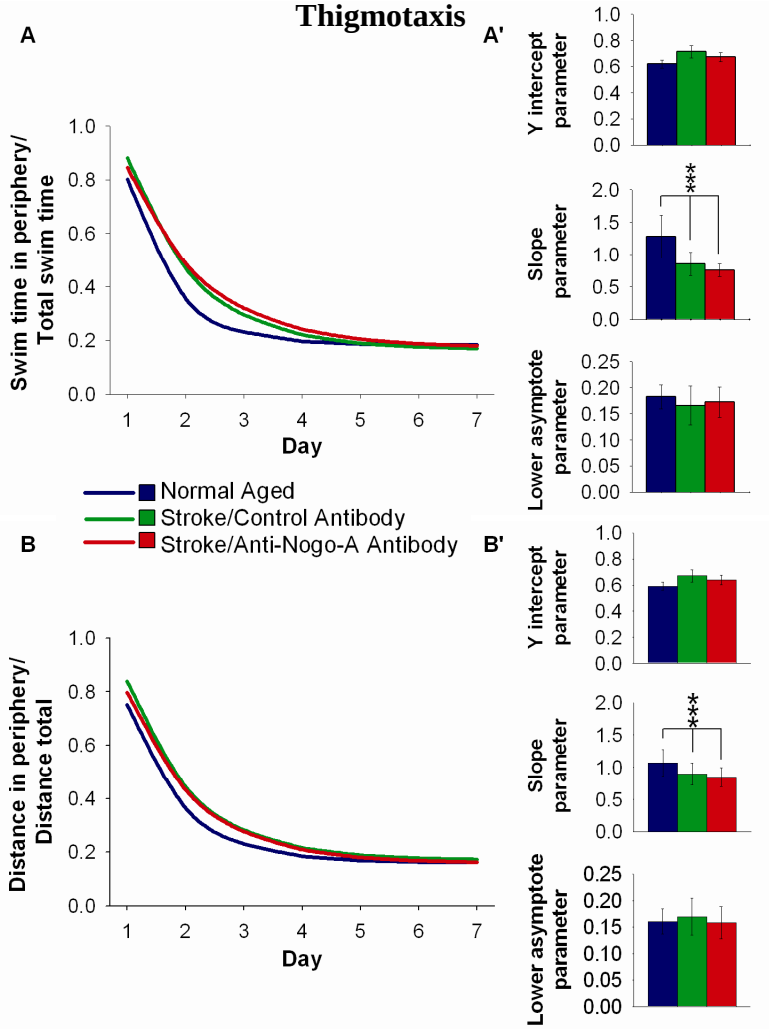

Figure 15. Thigmotaxis. (A) Thigmotaxis, time spent in the periphery, during the place task. Average curves of the fitted functions for each group. (A') Averages of the individual parameters of the functions. Thigmotaxis at the start of testing, or the y intercept, was the same for all groups. As testing continued both stroke groups showed more thigmotaxis behavior than normal aged rats ($p<0.001$, likelihood based $\chi 2$ test of random-effects simple exponential three-parameter model, $\eta(x) = \theta_1 e^{-\theta_2 x} + \theta_3$, where x = day – 1). Thigmotaxis at the end of testing, or the lower asymptote, was the same for all groups. (B) Thigmotaxis, distance swam in the periphery, during the place task. Average curves of the fitted functions for each group. (B') Averages of the individual parameters of the functions. Thigmotaxis at the start of testing, or the y intercept, was the same for all groups. As testing continued both stroke groups showed more thigmotaxis behavior than normal aged rats ($p<0.001$, likelihood based $\chi 2$ test of random-effects simple exponential three-parameter model, $\eta(x) = \theta_1 e^{-\theta_2 x} + \theta_3$, where x = day – 1). Thigmotaxis at the end of testing, or the lower asymptote, was the same for all groups. Error bars denote ± standard error of the mean. ***$p<0.001$.

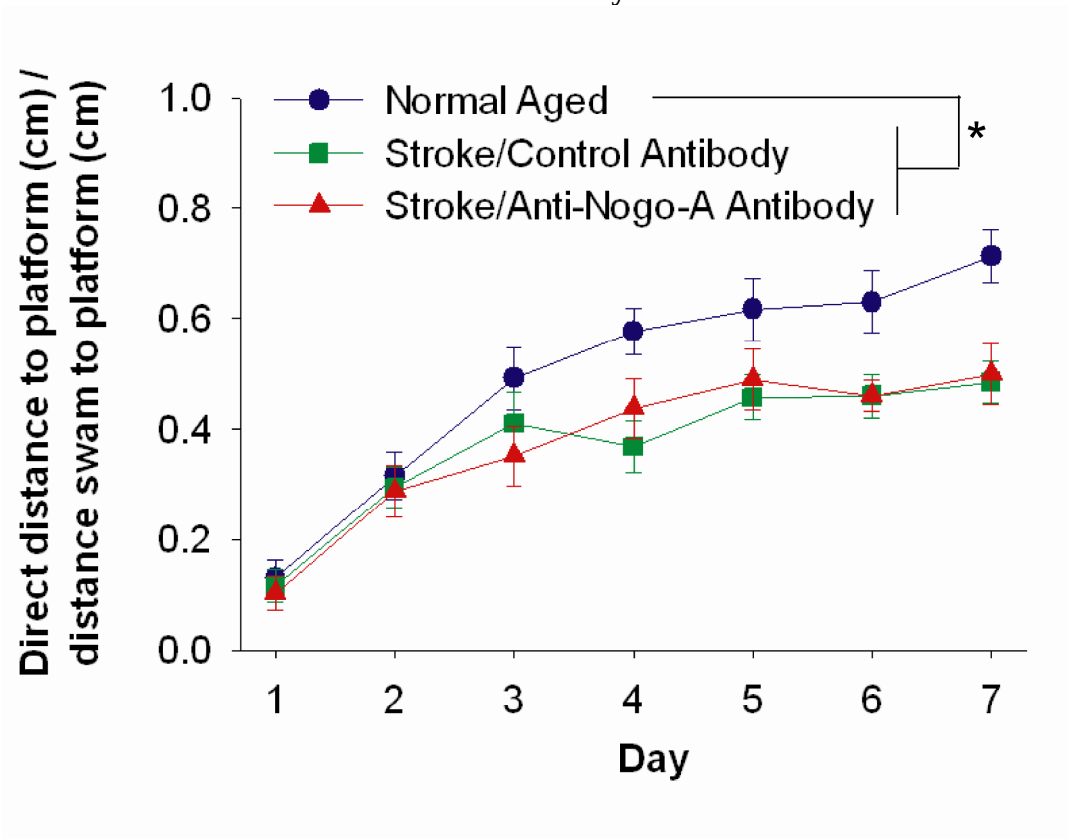

Figure 16. Path Circuity. The path circuity or direct distance to the platform/ the actual distance swam to the platform during a trial during the place task. Both stroke groups had significantly more circuitous paths than the normal aged group ($p<0.05$, repeated measures ANOVA, Bonferroni test for post-hoc comparison). Error bars denote ± standard error of the mean. *$p<0.05$.

Swim Paths for a Normal Aged Rat for the Place Task

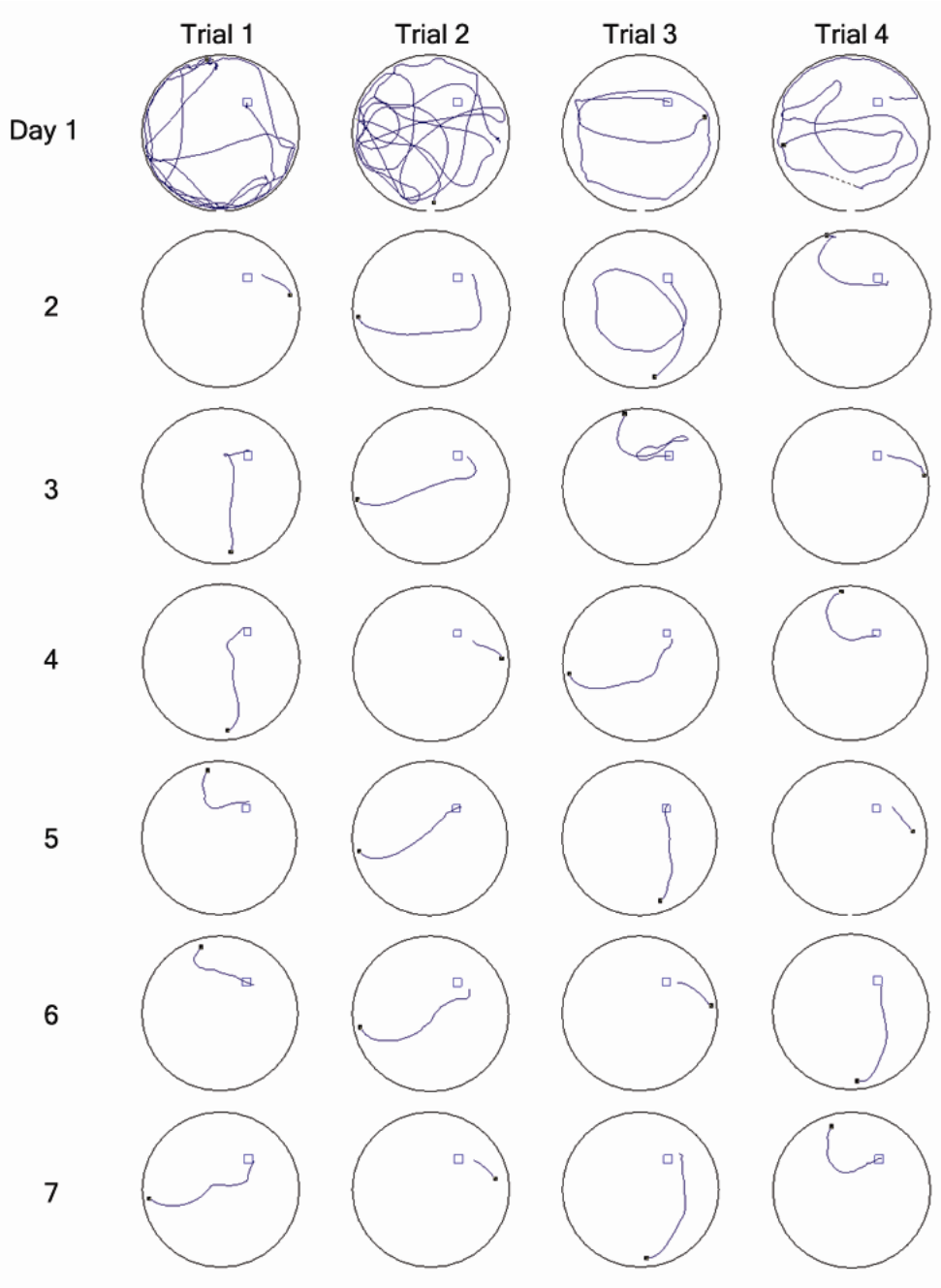

Figure 17. Swim Paths for a normal aged rat during seven days of place task testing. The start location is marked by a black dot, and the hidden platform is marked by a blue square.

Swim Paths for a Normal Aged Rat for the Probe Trial, and Matching-to-Place Task

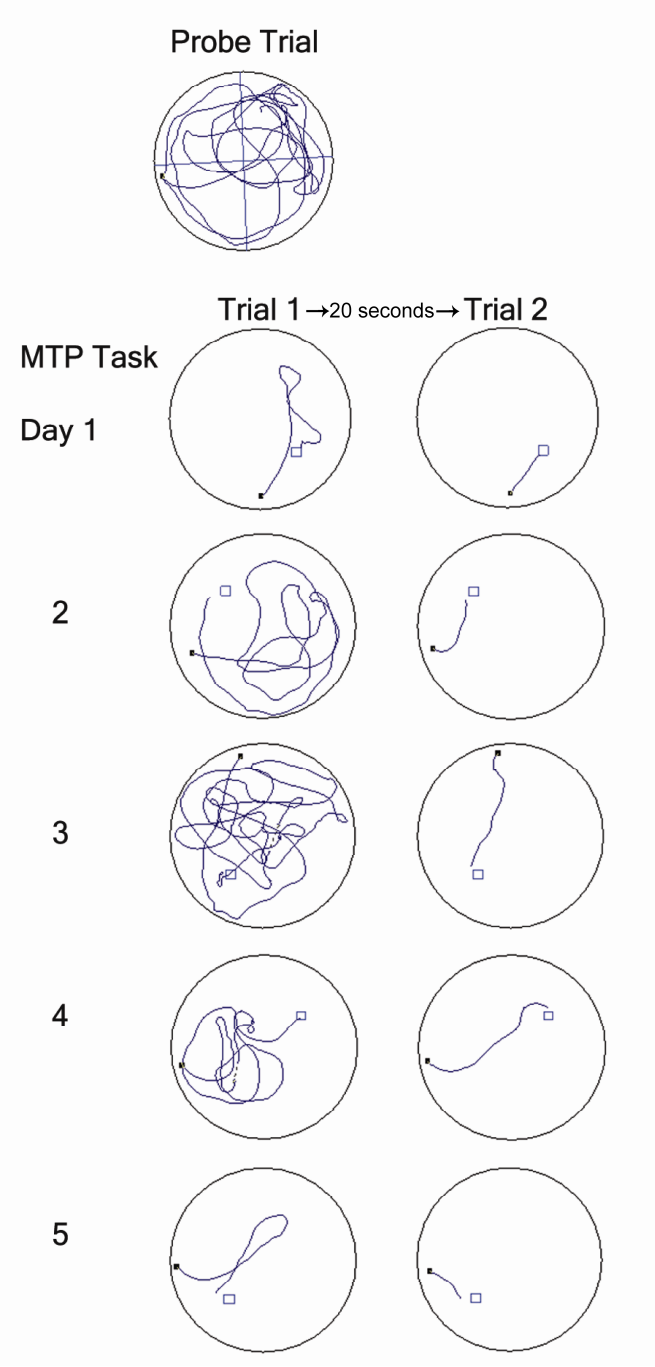

Figure 18. Swim Paths for a normal aged rat during the probe trial and five days of matching-to-place testing. The start location is marked by a black dot, and the hidden platform is marked by a blue square.

Swim Paths for a Stroke/Control Antibody Rat for the Place Task

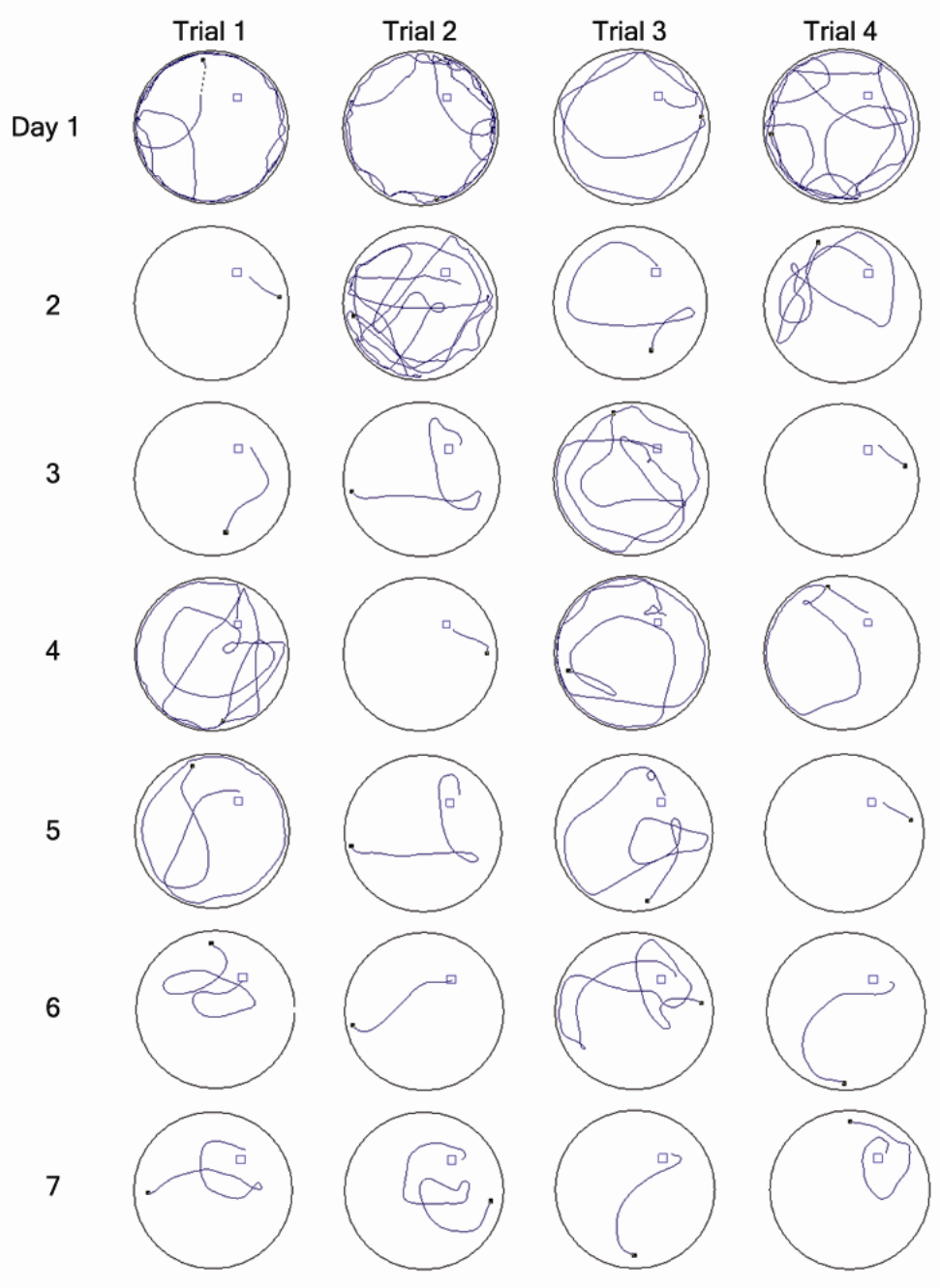

Figure 19. Swim Paths for a stroke/control antibody rat during seven days of place task testing. The start location is marked by a black dot, and the hidden platform is marked by a blue square.

Swim Paths for a Stroke/Control Antibody Rat for the Probe Trial, and Matching-to-Place Task

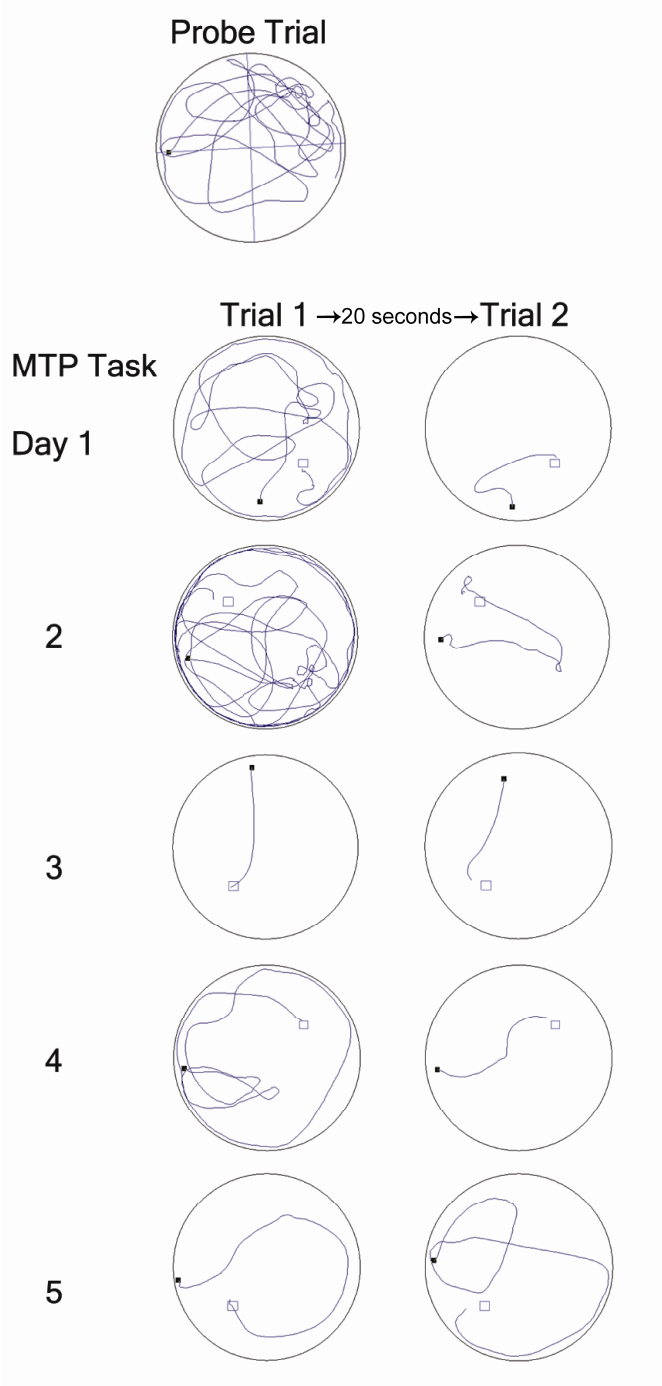

Figure 20. Swim Paths for a stroke/control rat during the probe trial and five days of matching-to-place testing. The start location is marked by a black dot, and the hidden platform is marked by a blue square.

Swim Paths for a Stroke/Anti-Nogo-A Antibody Rat for the Place Task

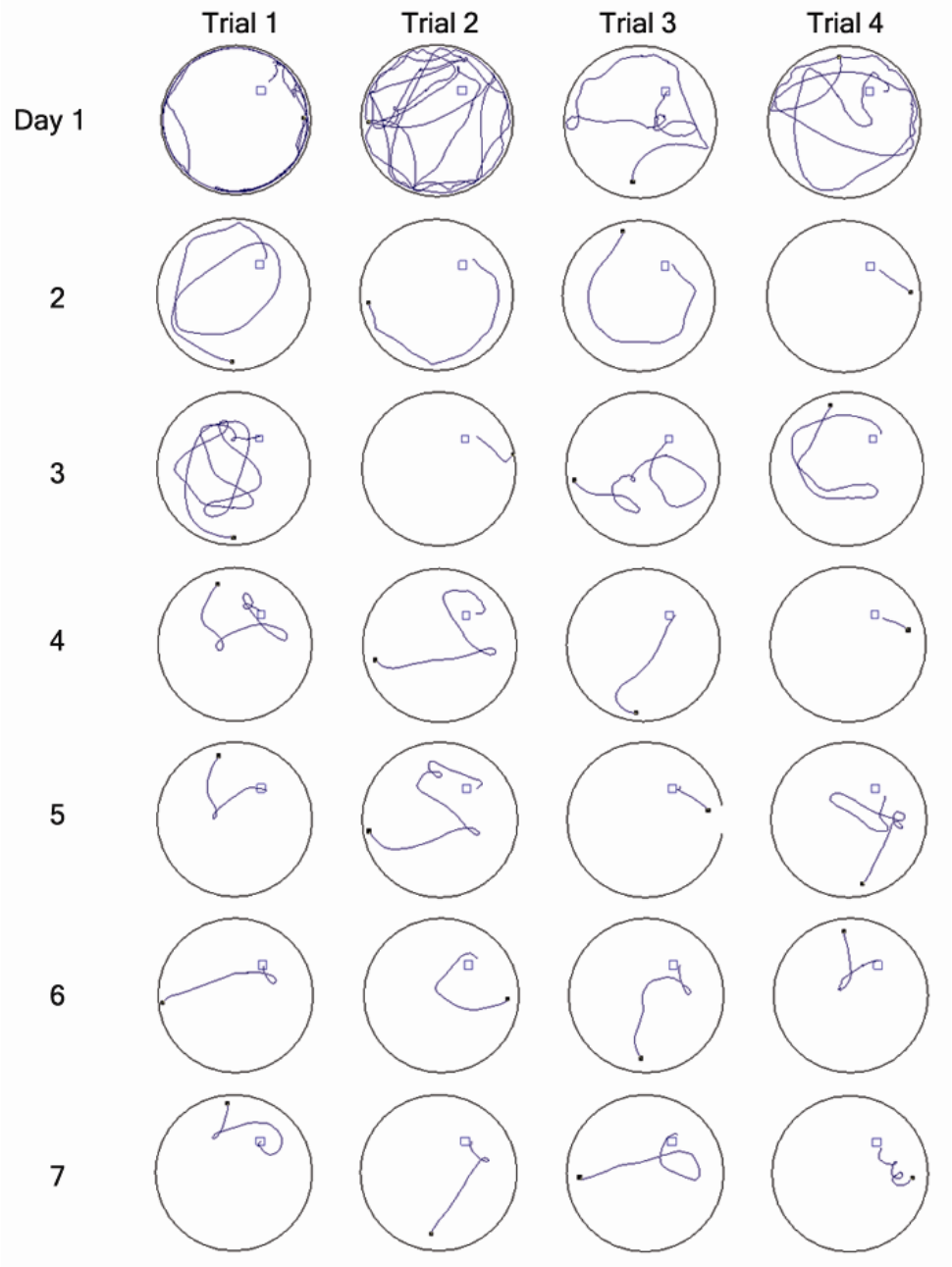

Figure 21. Swim Paths for a stroke/anti-Nogo-A antibody rat during seven days of place task testing. The start location is marked by a black dot, and the hidden platform is marked by a blue square.

Swim Paths for a Stroke/Anti-Nogo-A Antibody Rat for the Probe Trial, and Matching-to-Place Task

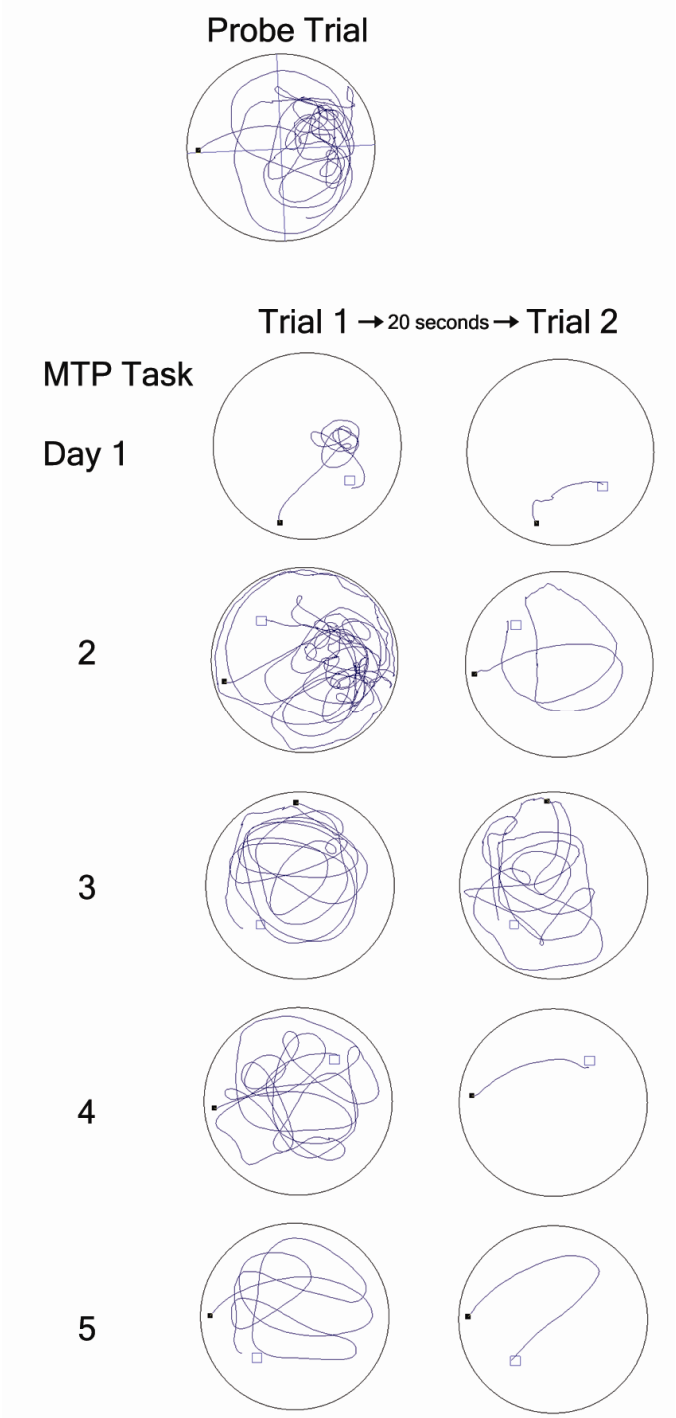

Figure 22. Swim Paths for a stroke/anti-Nogo-A antibody rat during the probe trial and five days of matching-to-place testing. The start location is marked by a black dot, and the hidden platform is marked by a blue square.

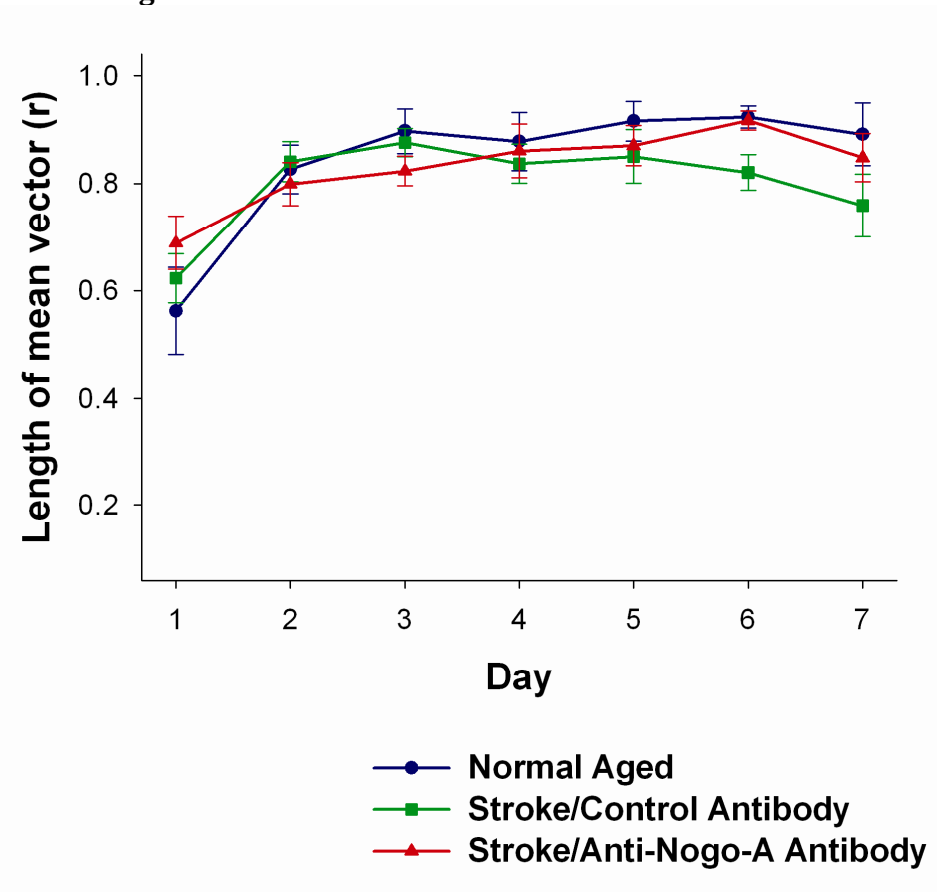

Figure 23. Angular variance at the start of place task trials. Heading direction angle represents the actual trajectory of the rat in relation to a direct trajectory to the platform. Angular variance or the length of the mean vector (r) represents the spread of the angles. There were no significant differences between the three groups when comparing the angular variances for individual rats across the seven days of the place task ($p=0.345$, repeated measures ANOVA). Error bars denote ± standard error of the mean.

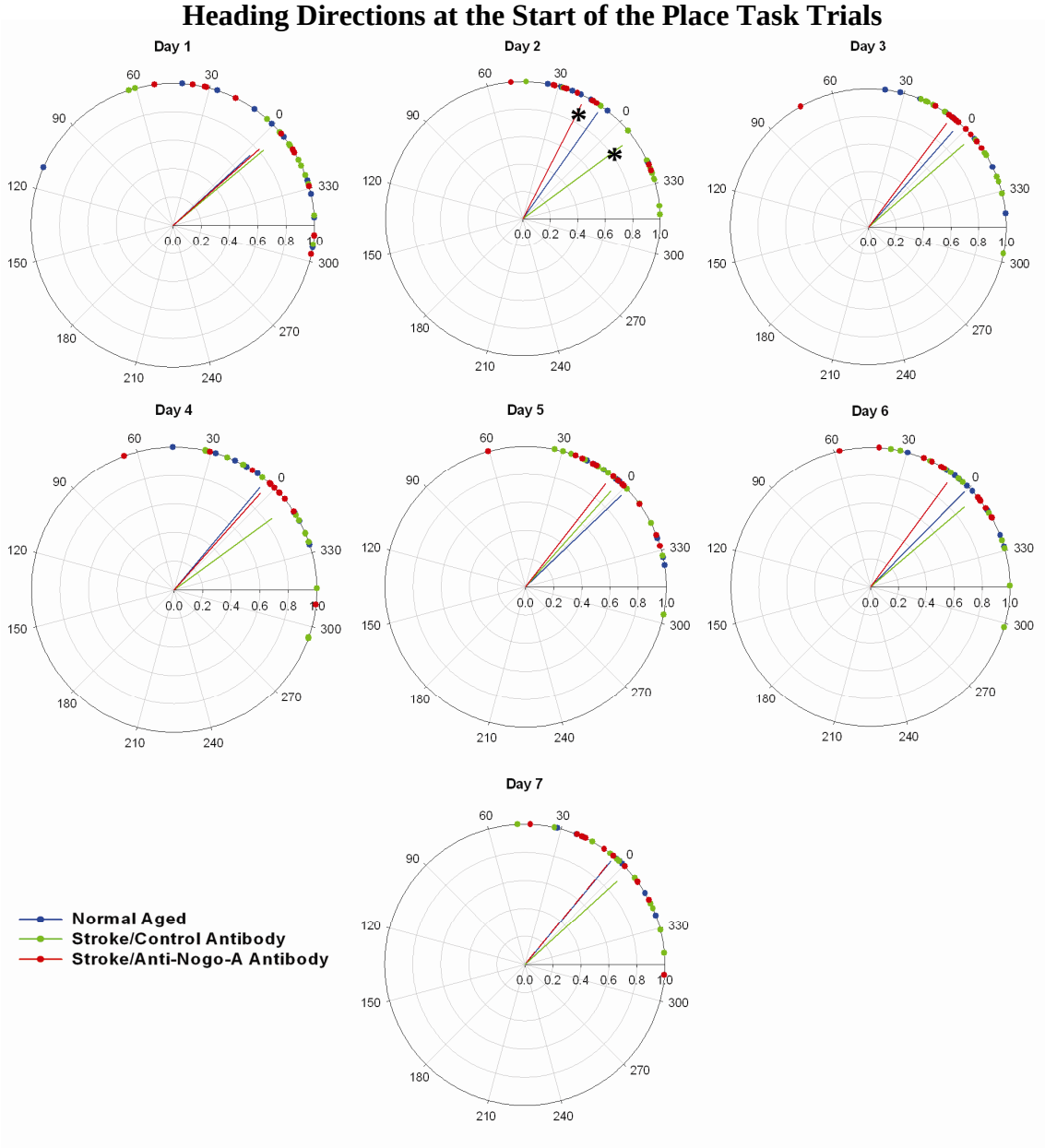

Figure 24. Heading directions at the start of the place task trials. The mean heading direction angles from the four daily trials for each rat are represented above as dots. The group mean heading direction angles for each day are represented as colored lines. The length of the line represents the angular variance, with longer lines having less variance. On day two the mean angle from the stroke/control antibody treated rats significantly differed from the stroke/anti-Nogo-A antibody treated rats ($p<0.05$, Watson-Williams F test). *$p<0.05$.

Representative Golgi-Cox Stained Hippocampal Neurons

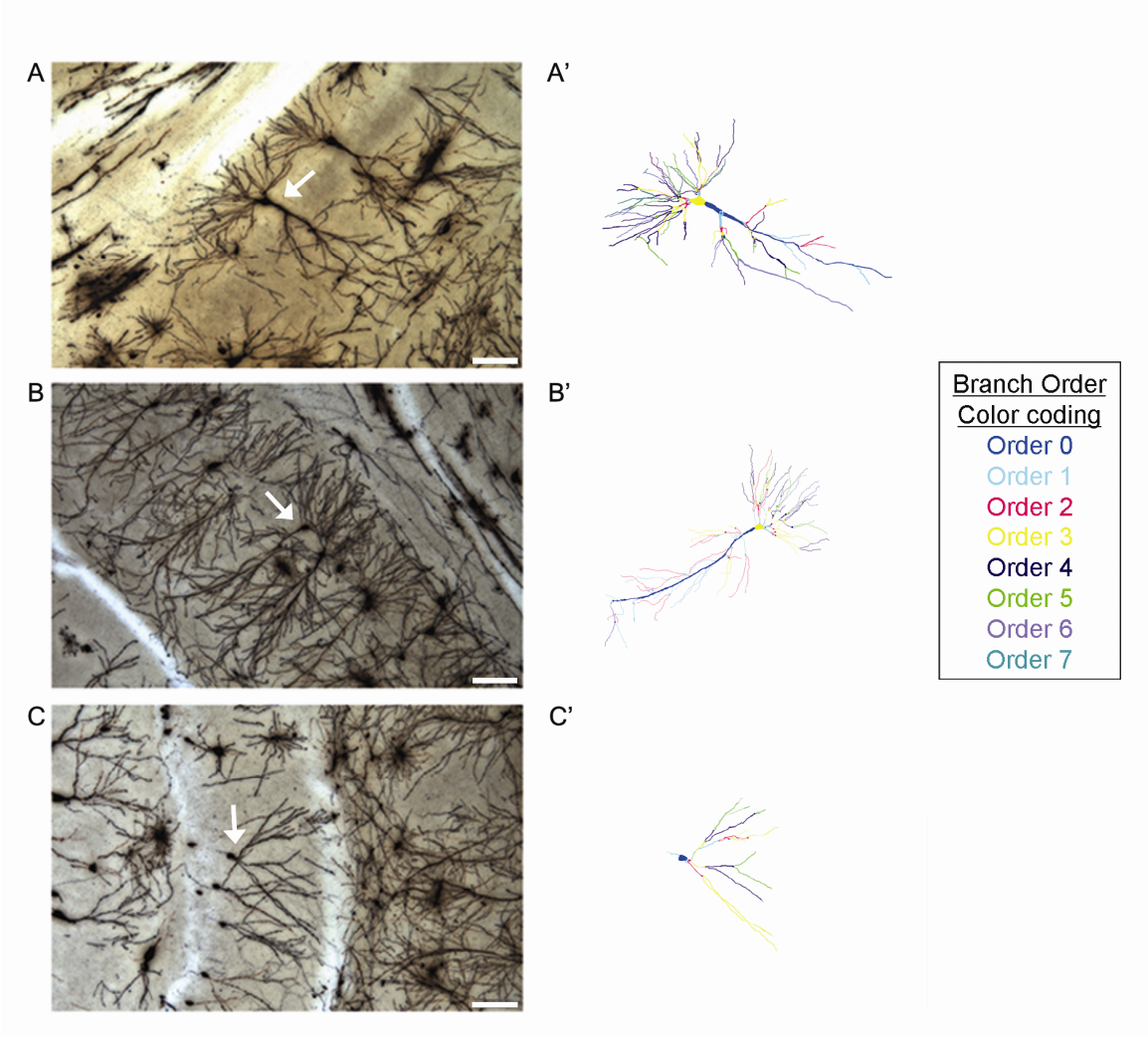

Figure 25. Representative Golgi-Cox stained hippocampal CA3 (A) and CA1 pyramidal cells (B) and dentate gyrus granule cell (C, white arrows), and the corresponding Neurolucida tracings (A', B', C'). Images were acquired from the hippocampus of a normal aged rat. Scale bar=100 μm.

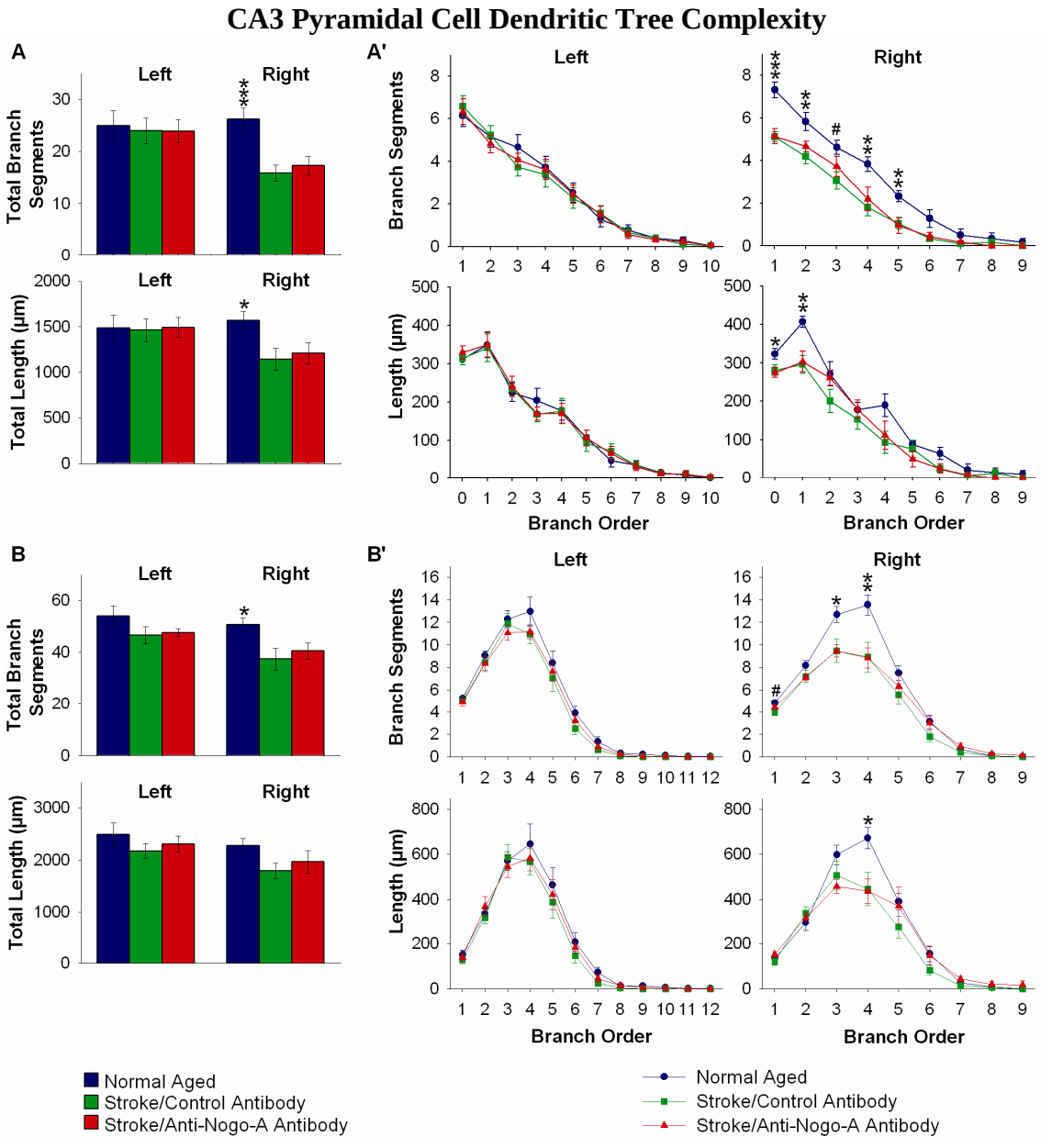

Figure 26. Decreased dendritic arbor complexity of CA3 pyramidal cells in both stroke groups ipsilateral to the stroke. (A) Quantification of apical total number of branch segments and total dendritic length, and (A') apical branch segments and dendritic length in each branch order. (B) Quantification of basilar total number of branch segments and total dendritic length, and (B') basilar branch segments and dendritic length in each branch order. Error bars denote ± standard error of the mean. *p<0.05, ** p<0.01, ***p<0.001 for normal aged vs. both stroke groups, and #p<0.05 for normal aged vs. stroke/control antibody (one-way ANOVA p values reported, Student-Newman-Keuls test for post-hoc comparison).

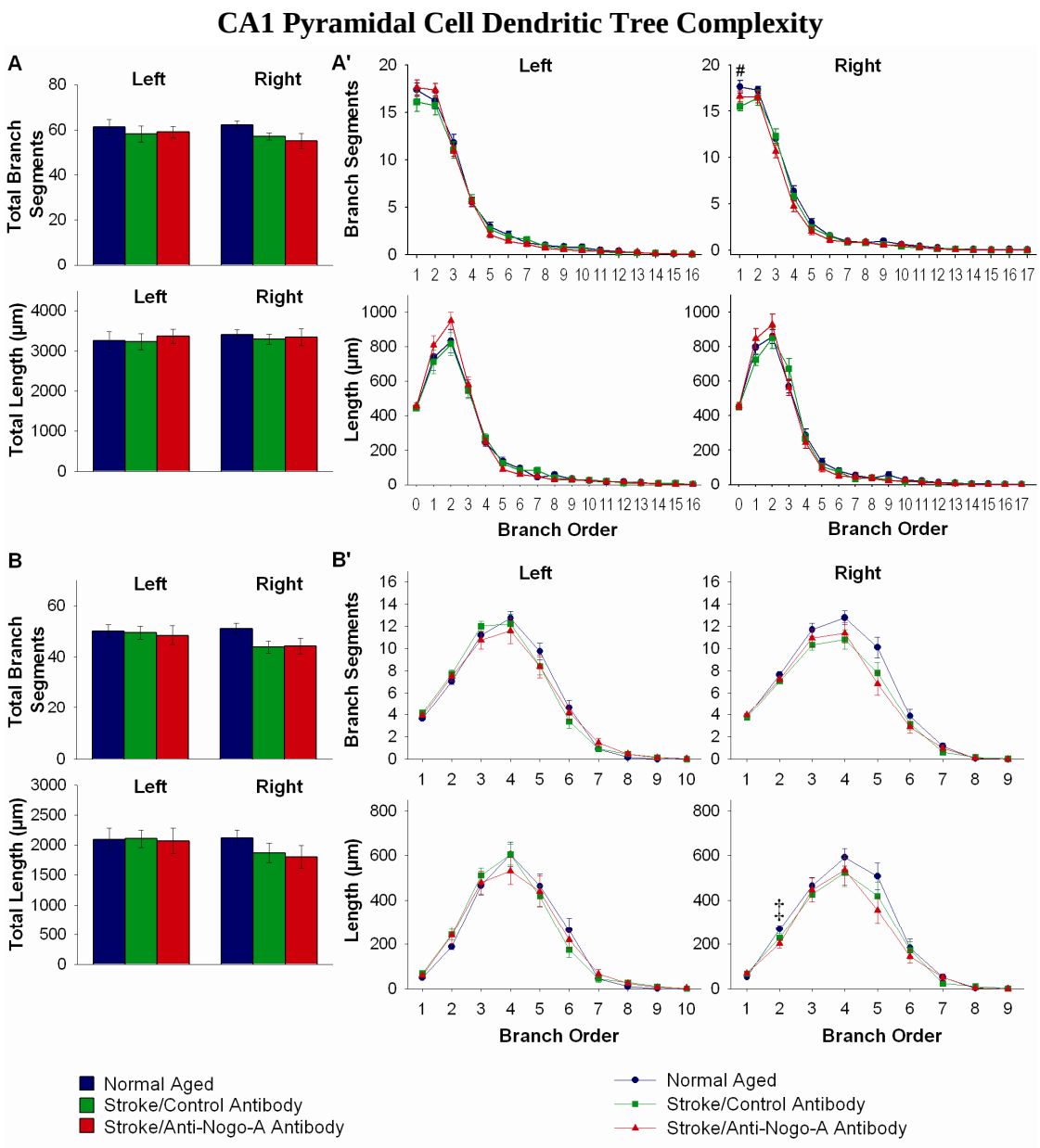

Figure 27. Decreased dendritic arbor complexity of CA1 pyramidal cells in both stroke groups ipsilateral to the stroke. (A) Quantification of apical total number of branch segments and total dendritic length, and (A') apical branch segments and dendritic length in each branch order. (B) Quantification of basilar total number of branch segments and total dendritic length, and (B') basilar branch segments and dendritic length in each branch order. Error bars denote ± standard error of the mean. #$p<0.05$ for normal aged vs. stroke/control antibody (one-way ANOVA p value reported, Student-Newman-Keuls test for post-hoc comparison). ‡$p<0.05$ for normal aged vs. stroke/anti-Nogo-A antibody (Kruskal Wallis one-way ANOVA on ranks p value reported, Dunn's method for post-hoc comparison).

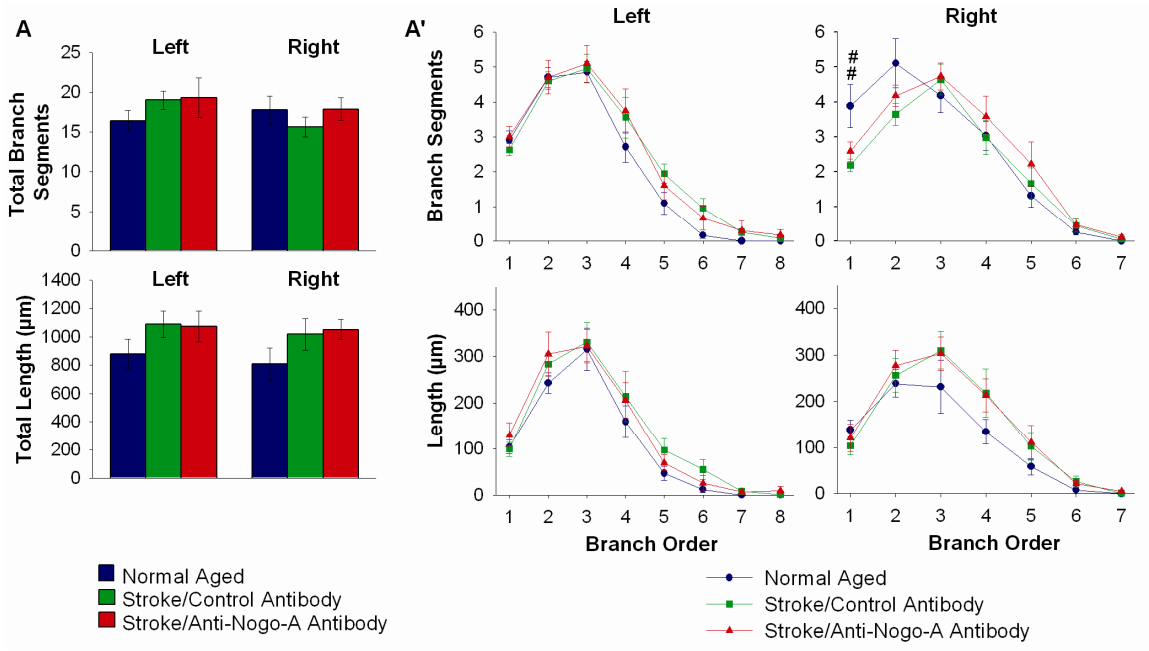

Figure 28. Decreased dendritic arbor complexity of dentate gyrus granule cells in the stroke/control antibody group ipsilateral to the stroke. (A) Quantification of total number of branch segments and total dendritic length, and (A') branch segments and dendritic length in each branch order. Error bars denote ± standard error of the mean. ##p<0.01 for normal aged vs. stroke/control antibody (Kruskal Wallis one-way ANOVA on ranks p value reported, Dunn's method for post-hoc comparison).

CA3 and CA1 Pyramidal Cell Apical Dendritic Spine Density and Morphology

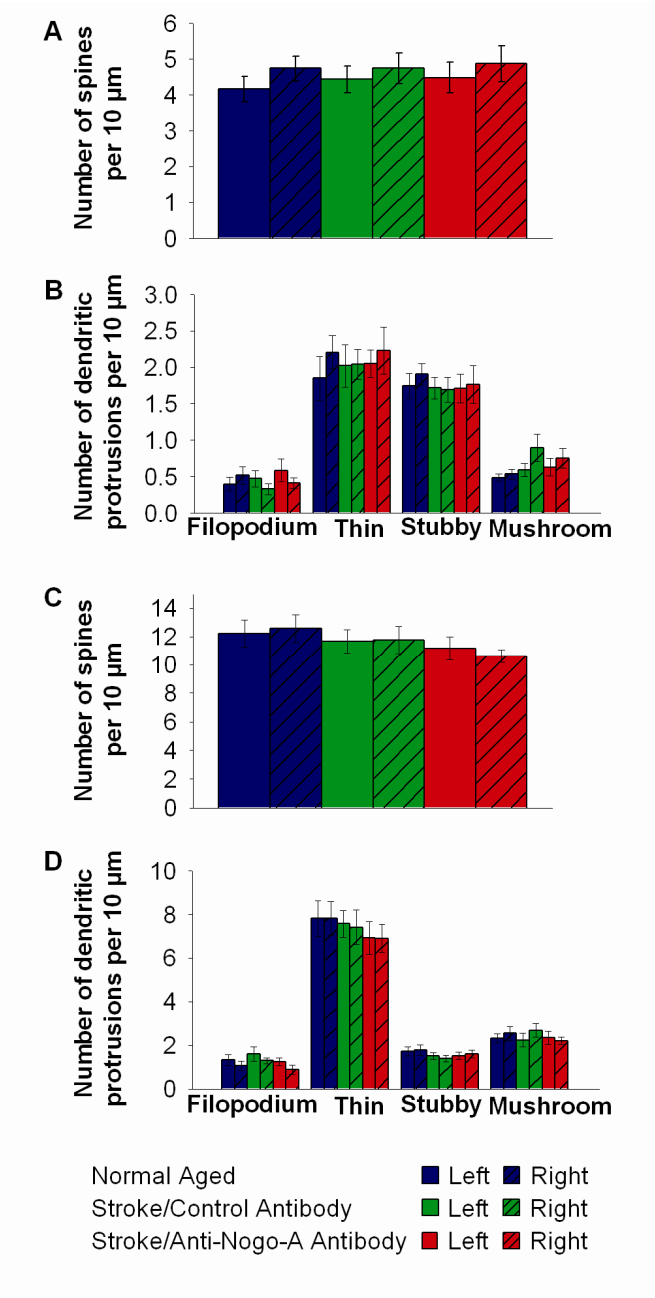

Figure 29. Apical dendritic spine density and morphology in CA3 and CA1 pyramidal cells did not significantly differ across groups. (A) Quantification of CA3 pyramidal cell dendritic spine density, and (B) CA3 pyramidal cell dendritic protrusion morphology. (C) Quantification of CA1 pyramidal cell dendritic spine density, and (D) CA1 pyramidal cell dendritic protrusion morphology. Error bars denote ± standard error of the mean.

DISCUSSION

The results from the present study show that anti-Nogo-A immunotherapy given one week following stroke in aged rats improved performance on the Morris water maze place task. However, improvement was not correlated with anatomical changes in dendritic arbors of hippocampal CA3 and CA1 pyramidal, dentate gyrus granule cells or dendritic spines of CA3 and CA1 pyramidal cells.

Previous studies have shown that anti-Nogo-A immunotherapy and the NgR(310)Ecto-Fc protein, which binds to the ligands of the Nogo-66 receptor (NgR1) and thereby blocks receptor activation, are effective up to one week after stroke in rats in inducing recovery of sensorimotor function in the stroke-impaired forelimb (Papadopoulos et al., 2002a; Wiessner et al., 2003a; Lee et al., 2004; Seymour et al., 2005a; Tsai et al., 2007). Furthermore, improvement on a sensorimotor task has been shown in aged rats after stroke given anti-Nogo-A immunotherapy, although the recovery took longer to occur as compared to adult rats (Markus et al., 2005a). The sensorimotor recovery was correlated in adult rats with axonal sprouting from intact pathways across the midline into subcortical denervated areas (Papadopoulos et al., 2002a; Wiessner et al., 2003a; Lee et al., 2004; Seymour et al., 2005a), and dendritic sprouting and increased dendritic spine density in the contralesional sensorimotor cortex (Papadopoulos et al., 2006). Further support for the role of Nogo-A in recovery from stroke is provided from genetic studies using knock-out models. Mice that lack the NgR1 or that lack Nogo-A and Nogo-B have improved sensorimotor recovery after a photothrombotic lesion to the sensorimotor cortex as compared to heterozygous littermates, and this correlates with

axonal sprouting from intact pathways across the midline into the denervated red nucleus and spinal cord (Lee et al., 2004).

In the present study we show improved performance on a spatial memory task after stroke in aged rats given anti-Nogo-A immunotherapy one week post-stroke. Several studies examining the therapeutic use of anti-Nogo-A immunotherapy to improve cognitive impairment in rodent brain injury models support our findings. In an experimental model of traumatic brain injury, adult rats that sustained a lateral fluid percussion injury and treatment with anti-Nogo-A immunotherapy starting 24 hours post-injury showed improved performance on the Morris water maze place task (Lenzlinger et al., 2005a; Marklund et al., 2007b). In that study, rats with traumatic brain injury given anti-Nogo-A immunotherapy had a higher expression of GAP-43 in CA1 of the hippocampus as compared to rats with traumatic brain injury and treated with control antibody (Marklund et al., 2007b). The higher levels of GAP-43 suggest that anti-Nogo-A immunotherapy may enhance the axonal growth potential of the hippocampus after traumatic brain injury. Additionally, after aspiration of the medial agranular cortex in a model of severe neglect adult rats treated with anti-Nogo-A immunotherapy immediately post-injury showed improvement from neglect. These behavioral improvements could be abolished by severing the corpus callosum causing the rats to once again exhibit severe neglect, and demonstrating the importance of the contralateral hemisphere in the behavioral recovery (Brenneman et al., 2008a). Interestingly, genetically modified unlesioned mice that lack Nogo-A have normal spatial memory on the Morris water maze but have enhanced motor coordination and balance as compared to heterozygous

littermates (Willi et al., 2008a). Our study adds to the growing body of literature of cognitive recovery with anti-Nogo-A immunotherapy by using the clinically relevant age group and time of treatment.

Due to the importance of the hippocampus for performance of spatial memory tasks (D'Hooge et al., 2001a), and the correlation of anti-Nogo-A immunotherapy with dendritic sprouting (Papadopoulos et al., 2006), we investigated whether the improved performance we found in the spatial reference memory task with anti-Nogo-A immunotherapy post-stroke would correlate with structural changes in the hippocampus. However, we found no differences in dendritic branching of CA3 and CA1 pyramidal and dentate gyrus granule cells, and no differences in spine density and morphology in CA3 and CA1 pyramidal cells between rats with stroke given anti-Nogo-A immunotherapy or given control antibody. This could be explained in several ways. First, morphological axonal or dendritic changes in brain areas other than the hippocampus may underlie the improved performance in the spatial memory task after anti-Nogo-A immunotherapy. Performance on the Morris water maze depends upon a distributed network of brain areas (D'Hooge and De Deyn, 2001a) that have neural activity in response to place, including the medial entorhinal cortex, striatum, subiculum and lateral septum (Knierim, 2006), areas which were not examined in this study. Interestingly, when rats received non-spatial pre-training to become familiar with the Morris water maze, blocking NMDA receptor-dependent LTP in the dentate gyrus did not result in impairment (Saucier et al., 1995). These studies suggest that, although the hippocampus is important for Morris water maze performance, other brain regions also contribute to performance on the Morris water

maze. Secondly, although dendritic growth was examined quite extensively in CA3, CA1 and the dentate gyrus, we did not investigate axonal growth in the hippocampus, raising the possibility that axonal growth may underlie the improved performance on the spatial memory task after anti-Nogo-A immunotherapy. Axonal growth in the hippocampus has been shown after treatment with anti-Nogo-A antibodies in cholinergic axons after damage to the septo-hippocampal pathway (Cadelli et al., 1991a) and in hippocampal slice cultures either intact or after cutting the Schaffer collaterals (Craveiro et al., 2008a), or perforant pathway (Mingorance et al., 2004b). Finally, we cannot rule out that non-morphological changes affecting factors such as electrophysiological characteristics or biochemical composition of hippocampal cells**,** or cells in other areas of the brain important for spatial memory may underlie the improved performance on the spatial memory task after anti-Nogo-A immunotherapy.

Previous studies have shown that unilateral MCAO impairs performance on the Morris water maze place task in adult (Yonemori et al., 1999; Dahlqvist et al., 2004) and aged rats (Andersen et al., 1999), as we also show in our study. Aging alone also causes impaired performance on the Morris water maze place task (Lindner, 1997; Andersen et al., 1999). Despite the consistent demonstration of impaired performance on the Morris water maze after unilateral MCAO by us and others and the importance of the hippocampus for performance on the Morris water maze, the MCAO does not cause gross histological damage to the hippocampus (Yonemori et al., 1999). Here we show a subtle decrease in dendritic complexity in CA3, CA1 and dentate gyrus neurons of the ipsilesional hippocampus. This is in contrast to a study of dendritic complexity after

transient global cerebral ischemia in rats, a model which causes neurodegeneration in CA1. In this study, 22 days post transient global cerebral ischemia, CA2/CA3 neurons were found to have increased dendritic volume, surface density of dendritic membrane, and number of synapses per neuron (Briones et al., 2006). Therefore, unilateral MCAO can cause decreased dendritic complexity in the ipsilesional hippocampus, while transient global cerebral ischemia can cause increased dendritic complexity in the hippocampus in non-degenerative cells.

Additional studies have examined the hippocampus after unilateral MCAO. One study reported an increase in the NMDA receptor subunit NR2B mRNA in the ipsilesional dentate gyrus, an increase in synapsin II bilaterally in the dentate gyrus, and a decrease in NGFI-A mRNA bilaterally in CA3 as compared to naive animals (Dahlqvist et al., 2004), suggesting that unilateral MCAO can effect gene expression in the hippocampus. On the other hand, another study of unilateral MCAO found no significant differences in the CA1 subregion of the hippocampus in LTP, microtubule-associated 2 positive fibers, and glial fibrillary acidic protein (GFAP) positive cells between the contralesional and ipsilesional sides (Okada et al., 1995). Furthermore, this study found no changes in acetylcholine levels in the dorsal and ventral hippocampus in rats after MCAO as compared to sham operated rats and intact rats. Therefore, unilateral MCAO appears to cause gene expression changes in the hippocampus.

In this study we found that rats with stroke, regardless of antibody treatment, spent more time swimming near the wall of the pool, i.e. thigmotaxis, and took less direct routes to the platform during the place task than normal aged rats. When we analyzed the

trajectory rats took at the start of place task trials, there were no differences in angular variance, and only slight differences in mean angle between groups. This suggests rats with stroke are using different navigational strategies during the Morris water maze task, but that their starting trajectory is similar to normal aged rats. Thigmotaxis is considered a maladaptive behavior because the hidden platform is never located near the wall. Increases in thigmotaxis behavior have previously been reported after permanent MCAO (Yonemori et al., 1999; Dahlqvist et al., 2004), and in aged animals as compared to adult animals (Andersen et al., 1999). Yonemori et al. (1999) reported that thigmotaxis behavior was correlated with shrinkage of the caudate-putamen, suggesting that damage to the caudate-putamen plays a role in thigmotaxis. It is possible that our model of MCAO could have caused ischemia and damage to the caudate-putamen. Thigmotaxis behavior has also been described in human subjects in a virtual maze task and in a real maze task. In these studies thigmotaxis behavior was correlated with lower performance on the spatial learning task, underperformance on working memory and spatial construction tests, and higher levels of fear (Kallai et al., 2005; Kallai et al., 2007). These results suggest that, although aged rats treated with anti-Nogo-A immunotherapy post-stroke are performing better on the Morris water maze than control antibody treated rats, they are not performing the task in the same manner as a non-stroke aged rat.

Neglect may have played a role in the Morris water maze performance of the aged rats from this study. As mentioned previously, damage to the medial agranular cortex causes neglect in rats (Brenneman et al., 2008b). Additionally, damage to the posterior parietal cortex can also cause neglect in rats (Reep et al., 2009) and this latter cortical

region is often perturbed in our model of MCAO. However, as rats in this study were not behaviorally evaluated for neglect, we are unable to say whether the MCAO caused neglect, or if the anti-Nogo-A immunotherapy had any affects on any potential neglect.

In conclusion, in the present study we found improved performance on the Morris water maze reference memory task after stroke and anti-Nogo-A immunotherapy in the aged, thereby providing evidence that anti-Nogo-A immunotherapy may have potential as a treatment for cognitive impairment after stroke in the aged.

CHAPTER FOUR

RECOMBINANT ADENO-ASSOCIATED VIRUS 2/8 MEDIATED NOGO-A KNOCKDOWN IN AGED RATS DOES NOT ALTER DENDRITIC SPINES

ABSTRACT

Nogo-A is most widely known as a myelin axonal growth inhibitor, but Nogo-A is also found in many populations of neurons where it may have distinct functions different from growth inhibition. We have previously shown that AAV2/8 mediated Nogo-A knockdown in neonatal rat cortical neurons led to decreased dendritic spine density and an increased percentage of dendritic spines with an immature morphology. Aged rats underwent injection of the AAV2/8 vector bilaterally into the dorsal hippocampus to deliver an shRNA to knockdown Nogo-A. Four weeks later the rats were sacrificed and brains processed for confocal imaging and dendritic spine analysis. We found that AAV2/8 mediated knockdown of Nogo-A in the aged rat hippocampus does not alter dendritic spine density or morphology in CA1 pyramidal cell apical dendritic trees. Taken together, these data suggest that neuronal Nogo-A may play disparate roles in synaptic structural plasticity in different neuronal populations.

INTRODUCTION

The Nogo-A protein, well described as a myelin growth inhibitor (Gonzenbach and Schwab, 2008), is found in oligodendrocyte myelin sheaths (Wang et al., 2002c) and in many CNS neurons (Wang et al., 2002c; Hunt et al., 2003; Buss et al., 2005) and has emerged as an important therapeutic target in several neurological disorders such as stroke and spinal cord injury. When anti-Nogo-A immunotherapy is given to rats one week after stroke, performance on a skilled sensorimotor test (Papadopoulos et al., 2002a; Markus et al., 2005a; Seymour et al., 2005a; Tsai et al., 2007) is improved, and in adult rats this improvement is correlated with axonal compensatory growth (Papadopoulos et al., 2002a; Markus et al., 2005a; Seymour et al., 2005a) and dendritic plasticity in the contralesional sensorimotor cortex (Papadopoulos et al., 2006). Anti-Nogo-A immunotherapy also leads to cognitive recovery after experimental brain injury models such as traumatic brain injury (Lenzlinger et al., 2005a; Marklund et al., 2007b) and severe neglect (Brenneman et al., 2008a) in rats. After unilateral cervical spinal cord injury in adult Macaque monkeys anti-Nogo-A immunotherapy improved recovery of hand dexterity, and this recovery was correlated with axonal compensatory growth (Freund et al., 2006; Freund et al., 2007b; Freund et al., 2009). Evidence also suggests that Nogo-A may be important in Alzheimer ’s Disease and temporal lobe epilepsy. The Nogo-A protein has altered expression in the hippocampal neurons of patients who had Alzheimer’s Disease (Gil et al., 2006b) and temporal lobe epilepsy (Bandtlow et al., 2004; Gil et al., 2006b), and is associated with beta-amyloid deposits in patients who had Alzheimer ’s Disease (Gil et al., 2006b). For all of these reasons, understanding the role

of Nogo-A in growth inhibition and the exact role that it plays in neuronal function may lead to new therapeutic avenues for treating various neurological disorders.

Current evidence suggests that neuronal Nogo-A has additional functions in addition to axonal growth inhibition (Montani et al., 2009). For example, immunogold labeling of Nogo-A demonstrated particles near to the post-synaptic density (Liu et al., 2003), and knocking down Nogo-A in neonatal cortical neurons led to reduced dendritic spine density and an increased percentage of immature spine morphologies (Pradhan, 2007). Because of the altered expression of Nogo-A in hippocampal neurons in several neurological diseases and because of these potential additional roles for neuronal Nogo-A in synaptic structural plasticity, we sought to knockdown Nogo-A in the hippocampus of aged rats and assess changes in dendritic spines morphology. We injected an AAV2/8 vector bilaterally into the dorsal hippocampus to deliver a shRNA to knockdown Nogo-A. The AAV2/8 vector was chosen to deliver the shRNA sequence because it can support persistent transgene expression for chronic experiments, and the host immune response to AAV is minimal (Daya and Berns, 2008). Reduction of Nogo-A levels is obtained by utilizing the endogenous RNAi machinery of the cell by which short double stranded RNA is incorporated into the RNA-induced silencing complex (RISC) and leads to sequence specific downregulation of homologous mRNA translation (Castanotto et al., 2009a). This method of gene silencing is advantageous over knock-out models for studying the function of a gene in adult or aged animals, because it avoids the possible confounding effects of silencing the gene during development, when it may have

different functions. Additionally, knock-out models are more likely to have compensatory mechanisms such as upregulation of another gene.

We found that knocking down Nogo-A in CA1 pyramidal cells of aged rats did not alter dendritic spine density or morphology.

METHODS

AAV Constructs

Plasmids were constructed as previously described by (Pradhan, 2007). Expression cassettes flanked by AAV2 inverted terminal repeats were packaged into AAV8 capsids. Briefly, the control EGFP plasmid was generated by inserting the EGFP cDNA into the Xhol and BgIll restriction sites in pAAV-MCS (Stratagene, La Jolla, CA, USA). The Nogo-A knockdown plasmid was generated by annealing the oligonucleotides corresponding to 856-874 of the rat Nogo-A cDNA into the Bbs1 and Xba1 site of the mU6pro plasmid, and then inserting the resulting fragment into the pAAV-EGFP plasmid at the MIuI site upstream of the CMV promoter.

Plasmids were packaged as previously described by (Pradhan, 2007) using a Virapack transfection kit (Stratagene). The AAV2 inverted terminal repeat constructs were co-transfected in AAV-293 cells with p5E-VD282, and pHelper plasmids (Stratagene). Purification by iodixanol step gradient was followed by centrifugation to concentrate and desalt (Biomax 100K concentrator, Millipore, Bedford, MA, USA). For titer estimation EGFP positive cells were counted 72 hours after serial dilutions and

infection of HT1080 cells. Titers for both the AAV-EGFP, and AAV-shNogo856 were 2 $\times 10^9$ infectious particles (iu)/ml.

Animal Subjects

Experiments were approved by the Institutional Animal Care and Use Committee of Hines Veterans Affairs Hospital. Aged male Fischer 344 rats (21-22 months of age at start of study) were divided into two groups: (1) control AAV-EGFP (n=10, 6 used for dendritic spine analysis), and (2) AAV-shNogo856 (n=9, 8 used for dendritic spine analysis). In the AAV-EGFP 4 animals were dropped from dendritic spine analysis. Two died due to aged related complications, and two had misplaced injection locations. In the AAV-shNogo856 group one animal was dropped from dendritic spine analysis due to misplaced injection locations. Animals were single housed and were maintained in a 12 hour light/dark cycle, with free access to food and water.

Intracranial Injection Surgery

The experimental design is depicted in Fig 30. Rats were anesthetized with isoflurane inhalant anesthesia (3% in oxygen) and secured in a rat stereotaxic frame. The skull was exposed through a midline incision in the scalp, and the head was aligned and leveled using a rat alignment tool (David Kopf Instruments, Tujunga, CA, USA). The appropriate virus was injected bilaterally into the dorsal hippocampus using a 32 gauge needle, a 5 µl or 10 µl syringe (Hamilton, Reno, NV, USA), and a microsyringe pump (UtraMicroPump with SYS-Micro4 controller, World Precision Instruments, Sarasota, FL, USA) at a rate

of 0.2 µl/minute. Six rats from the AAV-EGFP group and 7 rats from the AAV-shNogo856 group were injected with 3 µl of virus on each side of the hippocampus at coordinates 2.35 mm lateral, 5.3 mm posterior, and 2.5 and 2.3 mm ventral (1.5 µl for each depth), relative to bregma. Due to small lesions at the injection sites the final 4 rats in the AAV-EGFP group (2 used for dendritic spine analysis), and 2 rats from the AAV-shNogo856 group (2 used for dendritic spine analysis) were injected with less virus, 1 µl of virus, on each side of the hippocampus at the same coordinates except at only one depth (2.3 mm). Body temperature was maintained at 37.5º C with a heating pad and an autotuning temperature controller connected to a rectal probe (TCAT-2, Physitemp Instruments, Inc., Clifton, NJ, USA).

Dendritic Spine Analysis

Four weeks post-intracranial injection rats were overdosed with pentobarbital (100 mg/kg, intraperitoneal) and transcardially perfused with 0.9% saline and 10,000 U heparin/liter followed by 4% paraformaldehyde. The brains were removed and immersed whole in 4% paraformaldehyde for 1 hour, and then transferred to 30% sucrose for three days. Brains were frozen in isopentane on dry ice at -25º C and then stored at -80º C until there were sectioned coronally on a cryostat at 50 µm. Our experiments with AAV transduction in neonatal rats used 200 µm sections taken on the vibratome, but we found that we were unable to image dendritic spines when we processed the aged tissue in this way. Alternate free floating sections were reacted with cupric sulfate 2.5 mM in ammonium acetate 50 mM buffer for 15 minutes to reduce lipofuscin autofluorescence as

described by Schnell et al.(1999). Sections were then mounted to slides and coverslipped with Dako fluorescence mounting media (Dako North America, Inc., Carpinteria, CA, USA).

Dorsal hippocampal CA1 pyramidal cell apical dendrites in the stratum radiatum layer were analyzed for dendritic spine density and morphology. For selection the dendritic tree of a cell had to be well filled with EGFP. Thin optical sections (.9 μm) of first order or higher dendrites were acquired with a Zeiss 510 laser scanning microscope (488 nm laser, pinhole 112) and a 60x objective (1.2 N.A. water corrected), and 4x zoom. For each dendrite, 10 μm segments were identified using NIH ImajeJ software and for inclusion the segment had to be at least 10 μm from the branch point. For each segment dendritic protrusions were counted and assigned to a morphology of filopodia, thin, stubby, mushroom or 2-headed as described by Bourne and Harris (2008). Additionally, the length and head diameters of each protrusion were measured. Five dendritic segments were analyzed per brain.

Immunostaining

Alternate free floating sections were selected for immunostaining of Nogo-A (Cheatwood et al., 2008) and glial fibrillary acidic protein (GFAP). Sections were blocked for 1 hour at room temperature with 10% normal goat serum (NGS), and 0.25% Triton-X 100 (TX100) in 0.01 M phosphate buffered saline (PBS). Next the sections were incubated overnight at 4º C with either purified mouse monoclonal anti-Nogo-A antibody (11C7) or the rabbit polyclonal anti-GFAP (Sigma, St. Louis, MO, USA) at 1:500 with 5% NGS

and 0.25% TX100 in PBS. After washing, sections were incubated for 1 hour at room temperature with the appropriate secondary antibody, either Alexa Fluor 594 goat anti-mouse or tetramethylrhodamine goat anti-rabbit (Invitrogen, Carlsbad, CA, USA), at 1:1000 with 5% NGS and 0.25% TX100 in PBS. Next, sections were washed and reacted with cupric sulfate as described above to reduce lipofuscin autofluorescence. Sections were then mounted to slides and coverslipped with Dako fluorescence mounting media. Thin optical sections (1 μm) were acquired with a Zeiss 510 laser scanning microscope (561 and 488 nm lasers, pinhole 80 and 84) and a 40x objective (1.2 N.A. water corrected), and 1x zoom. Using the same settings sections (13.1 μm) were also acquired with a 10x objective. For comparison of Nogo-A expression levels optical sections were acquired at the same detector gain and amplifier offset.

Statistical Analysis

For analysis of dendritic spine data t-tests were used, and when the data were not normal the Mann-Whitney Rank Sum Test was used (SigmaStat, Systat, San Jose, CA, USA).

Experimental Timeline

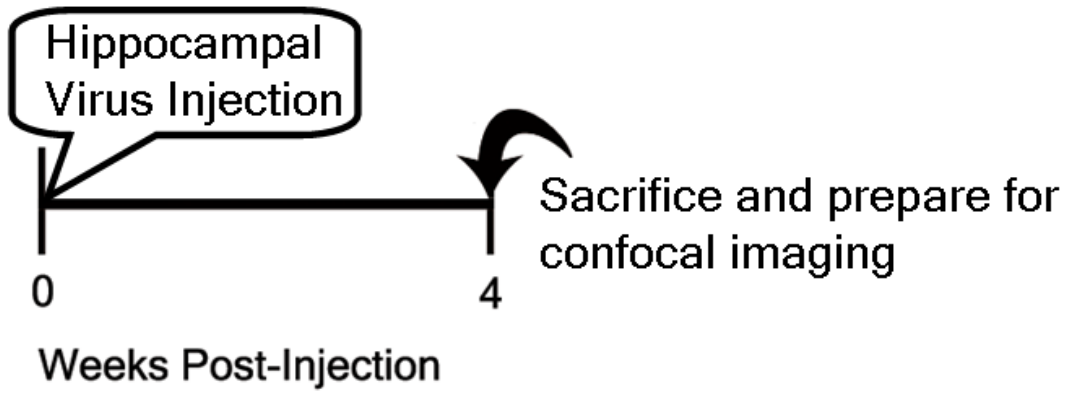

Figure 30. Experimental timeline. Aged rats underwent bilateral intra-hippocampal injections of AAV-EGFP or AAV-shNogo856. Four weeks post-injection rats were sacrificed and the brains processed for confocal imaging.

RESULTS

Nogo-A knockdown reduced the levels of the Nogo-A protein in CA1 pyramidal cells

To confirm knockdown of the Nogo-A gene in aged rats by AAV mediated delivery of shNogo856, we immunostained alternate sections for Nogo-A expression. Nogo-A immunoreactivity in transduced CA1 pyramidal cells was markedly reduced in the AAV-shNogo856 rats (Fig 35D-F, 36D-F) when compared to control AAV-EGFP rats (Fig 35A-C, 36A-C). Therefore, AAV mediated delivery of shNogo-856 effectively reduced the expression of Nogo-A in CA1 pyramidal cells of aged rats. Furthermore, the shRNA used in these experiments has been shown previously to effectively reduce the levels of Nogo-A gene expression both *in vitro* and *in vivo* in neonatal rats (Pradhan, 2007).

Nogo-A knockdown did not alter dendritic spine density and morphology in CA1 pyramidal cells

EGFP filled apical dendrites of hippocampal CA1 pyramidal cells were analyzed for dendritic spine density and morphology. Mean dendritic spine density in the AAV-shNogo856 group was 9.8 spines per 10 μm and in the control AAV-EGFP group was 11.47 spines per 10 μm, and dendritic spine density did not significantly differ between the groups ($p = 0.230$; Fig 32A). In order to examine dendritic protrusion morphology we subjectively assigned each dendritic protrusion analyzed to a morphology of thin, stubby, mushroom, two-headed or filopodial (Fig 31A, Bourne and Harris, 2008). In both groups the most common morphology was stubby, followed by thin, mushroom and filopodial (Fig 32B). The number of protrusions for each of the morphologies did not significantly differ between the AAV-shNogo856 group and the control AAV-EGFP group ($p = 0.176$

for filopodium, p=0.426 for thin, p=0.531 for stubby, p=0.459 for mushroom; Fig 32B). In addition, we quantified the length and head diameter of each dendritic protrusion analyzed (Fig 31B). Mean dendritic spine length in the AAV-shNogo856 group was 0.57 μm and in the control AAV-EGFP group was 0.61μm (Fig 33A). Mean dendritic spine head diameter in the AAV-shNogo856 group was 0.38 μm and in the control AAV-EGFP group was 0.39 μm (Fig 34A). Spine length and head diameter did not significantly differ between the AAV-shNogo856 group and the control AAV-EGFP group (p=0.214 for spine length, p=0.475 for head diameter; Fig 33A, 34A). Furthermore, when we analyzed length and head diameter by morphology and included filopodial forms, we found no significant differences between the AAV-shNogo856 group and the control AAV-EGFP group (p=0.358 for filopodial length, p=0.122 for thin length, p=0.626 for stubby length, p=0.308 for mushroom length, p=0.382 for filopodial head diameter, p=0.491 for thin head diameter, p=0.466 for stubby head diameter, p=0.764 for mushroom head diameter; Fig 33B, 34B). Therefore, Nogo-A knockdown in aged rats does not affect morphology or density of dendritic protrusions in CA1 pyramidal cells.

AAV intra-hippocampal injection in aged rats caused EGFP positive astrocytes and dose-dependent tissue disruption at the injection site

To start we injected 3 μl of either AAV-EGFP or AAV-shNogo856 bilaterally into the dorsal hippocampus at a titer of 2×10^9 infectious units (iu)/ml. Four weeks later when the animals were sacrificed, we found robust expression of the EGFP reporter transgene in CA1 pyramidal cells, dentate gyrus granule cells and CA3 pyramidal cells (Fig 37A). We also saw cells of a non-neuronal morphology containing EGFP dispersed throughout

the hippocampus. Immunostaining for GFAP showed that many of these cells containing EGFP of non-neuronal morphology were astrocytes (Fig 37). Additionally, we saw microlesions at many of the injections sites (present in 50% of AAV-EGFP brains, and 100% of AAV-shNogo856 brains), which were focused in the area of the dentate gyrus and were found in both rats with AAV-EGFP injections and AAV-shNogo856 injections (Fig 37A-C). The cells containing EGFP of non-neuronal morphology, many of which were astrocytes, were concentrated around the microlesions. To determine if the microlesions were dose-dependent we injected an additional 6 animals with 1 μl of either AAV-EGFP (4 rats) or AAV-shNogo856 (2 animals) bilaterally into the dorsal hippocampus at a titer of 2×10^9 iu/ml. Four weeks later when the animals were sacrificed, we found robust expression of the EGFP reporter transgene in hippocampal neurons, and by rough visual examination there appeared to be fewer transduced cells than in animals with the higher dose, though we did not quantify this. Four of the six animals had well filled CA1 pyramidal neurons so these animals were included in dendritic spine analysis. None of the animals with the lower dose had microlesions at the injection site. In the animals with the lower dose cells containing EGFP of a non-neuronal morphology were still present. Therefore, AAV-EGFP and AAV-shNogo856 intra-hippocampal injections in aged rats caused dose-dependent microlesions at the injection sites, and cells to contain EGFP-positive cells of non-neuronal morphology, many of which were astrocytes.

Representative EGFP Filled Dendrite Segment

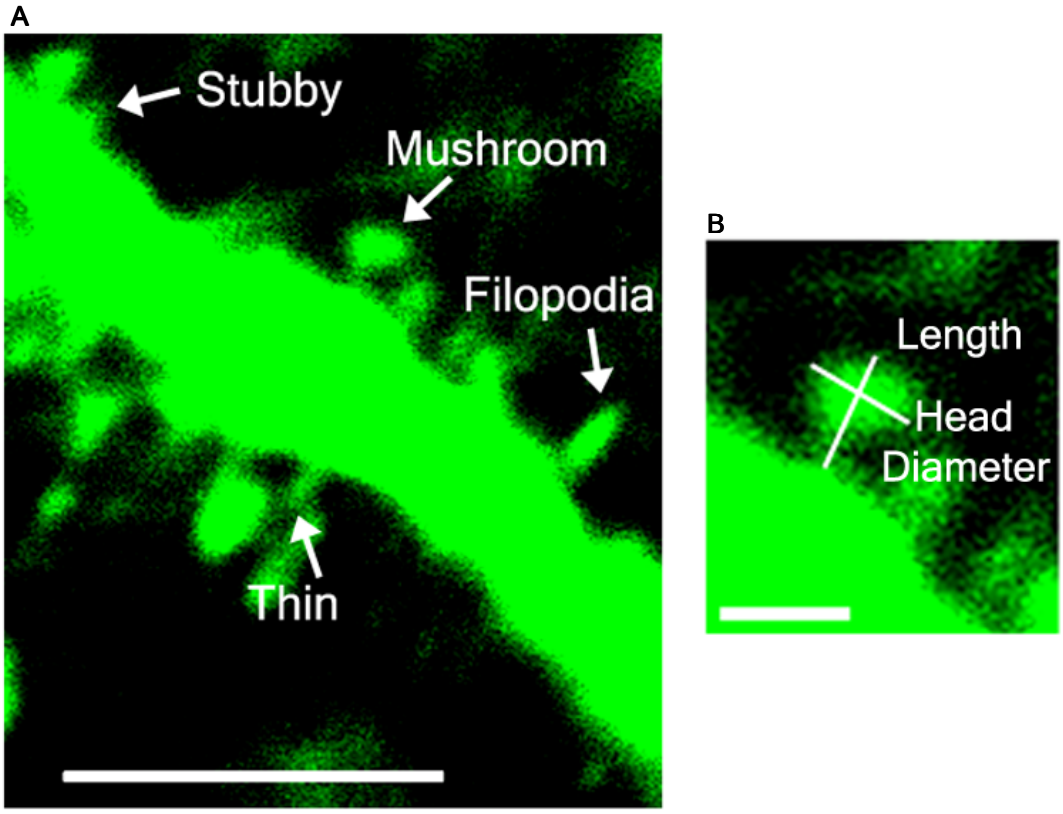

Figure 31. CA1 pyramidal cell apical dendrite segment. (A) Example of a first order apical dendrite segment. Scale Bar =5 μm. (B) Enlargement of a mushroom spine to show how spine length and spine head diameter were delineated. Scale Bar= 1 μm.

CA1 Pyramidal Cell Apical Dendritic Protrusion Density

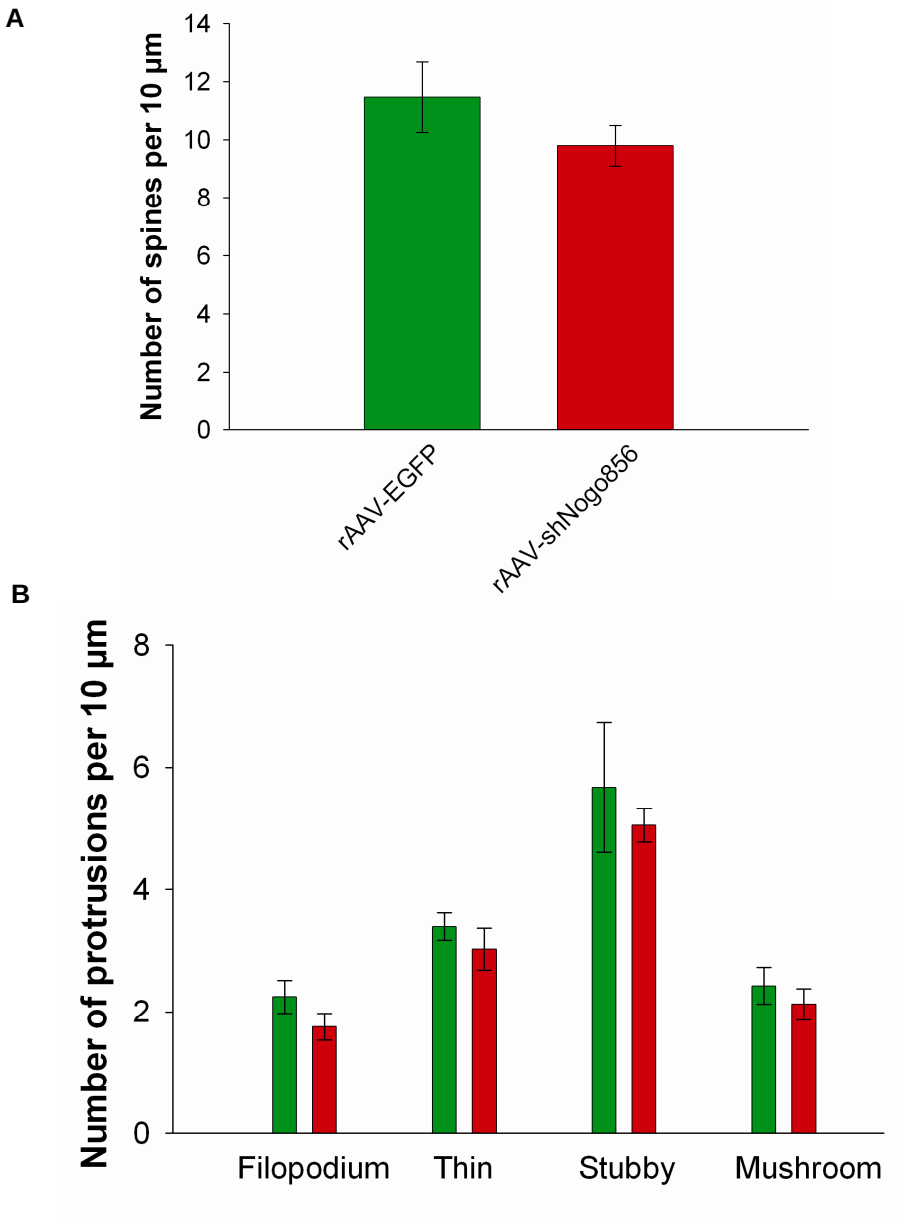

Figure 32. CA1 pyramidal cell dendritic protrusion density is unaltered after Nogo-A knockdown. (A) Quantification of dendritic spine density (excluding filopodia), and (B) dendritic protrusion density by morphology. Error bars denote ± standard error of the mean.

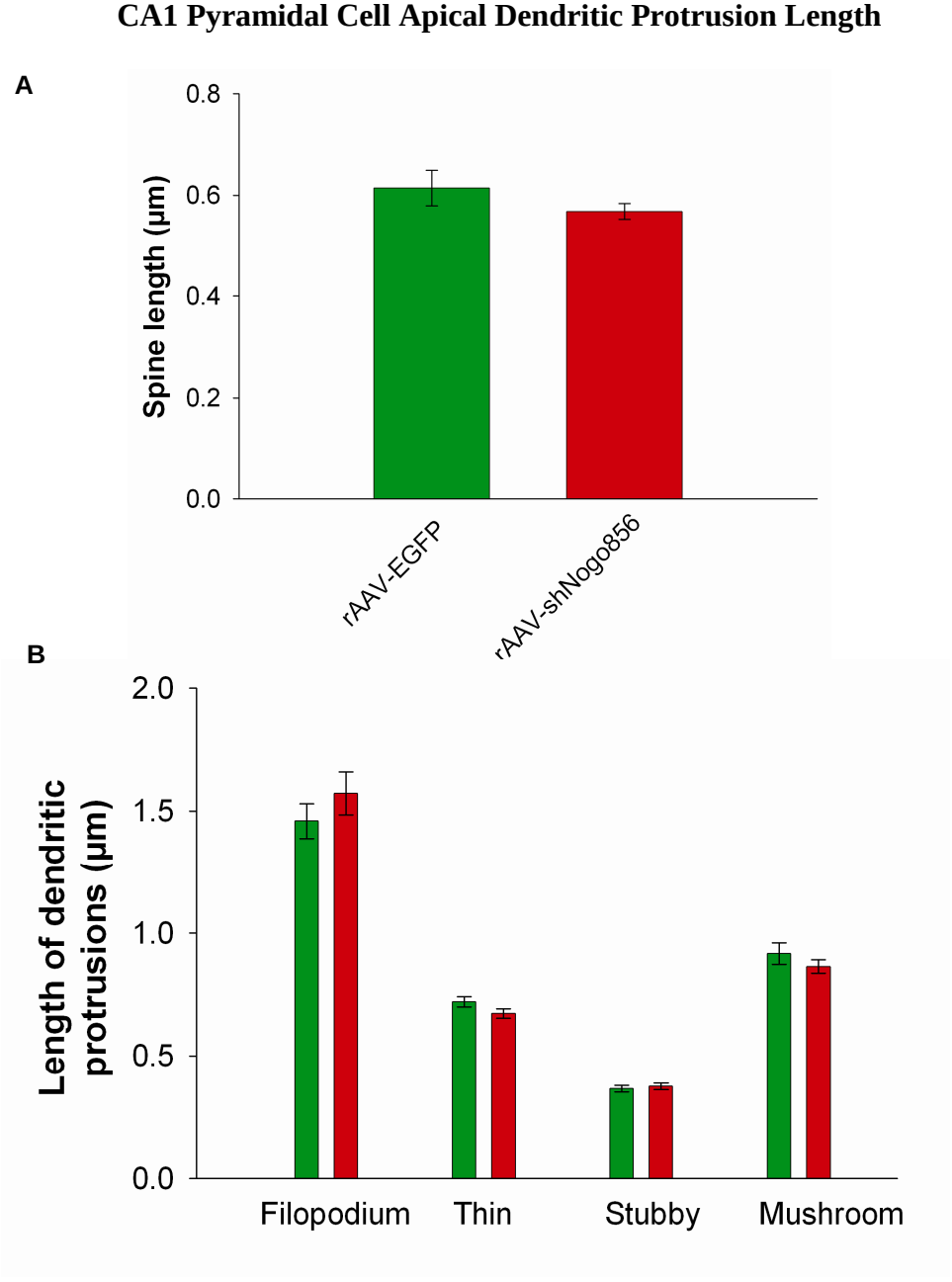

Figure 33. CA1 pyramidal cell dendritic protrusion length is unaltered after Nogo-A knockdown. (A) Quantification of dendritic spine length (excluding filopodia), and (B) dendritic protrusion length by morphology. Error bars denote ± standard error of the mean.

CA1 Pyramidal Cell Apical Dendritic Protrusion Head Diameter

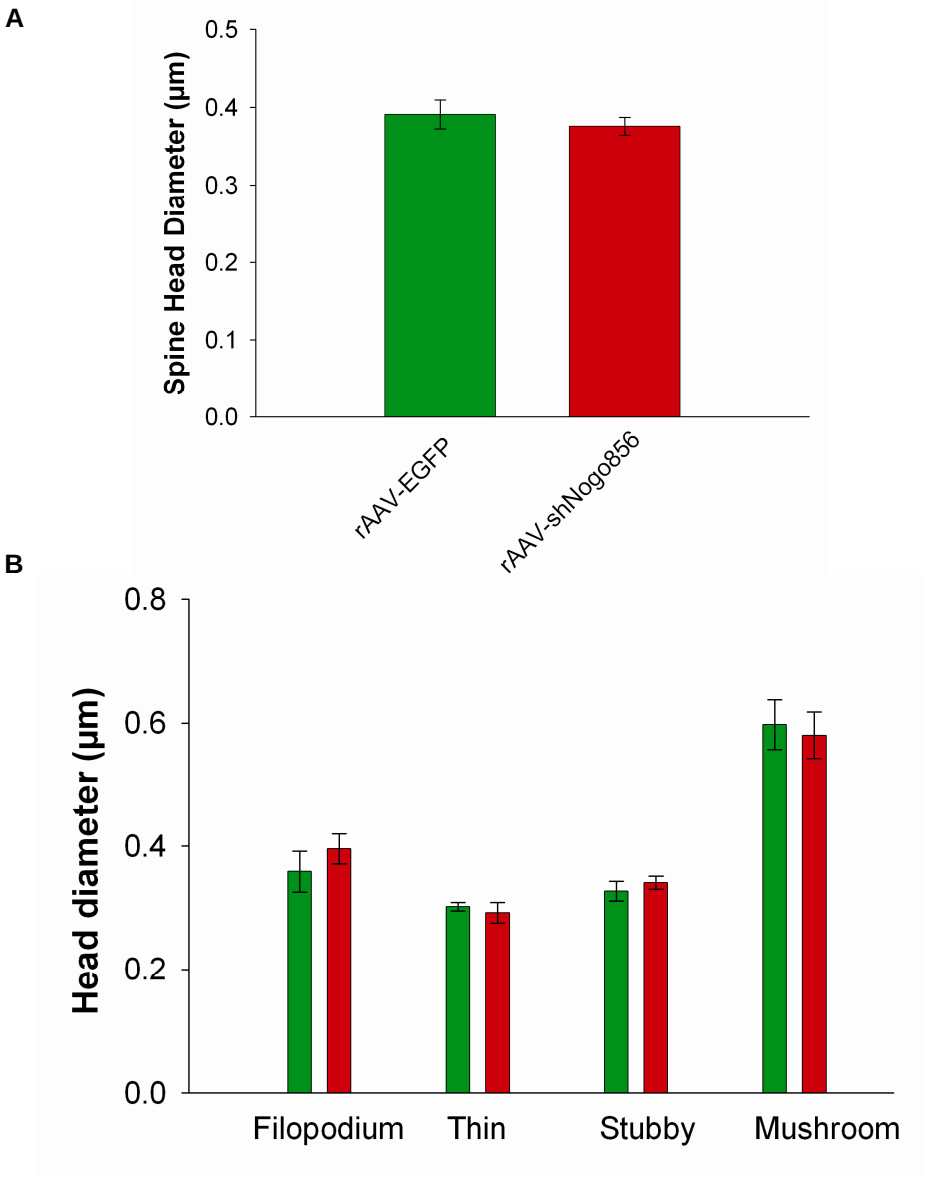

Figure 34. CA1 pyramidal cell dendritic protrusion head diameter is unaltered after Nogo-A knockdown. (A) Quantification of dendritic spine head diameter (excluding filopodia and 2-headed), and (B) dendritic protrusion head diameter by morphology. Error bars denote ± standard error of the mean.

Decreased Nogo-A Protein Expression after Nogo-A Knockdown

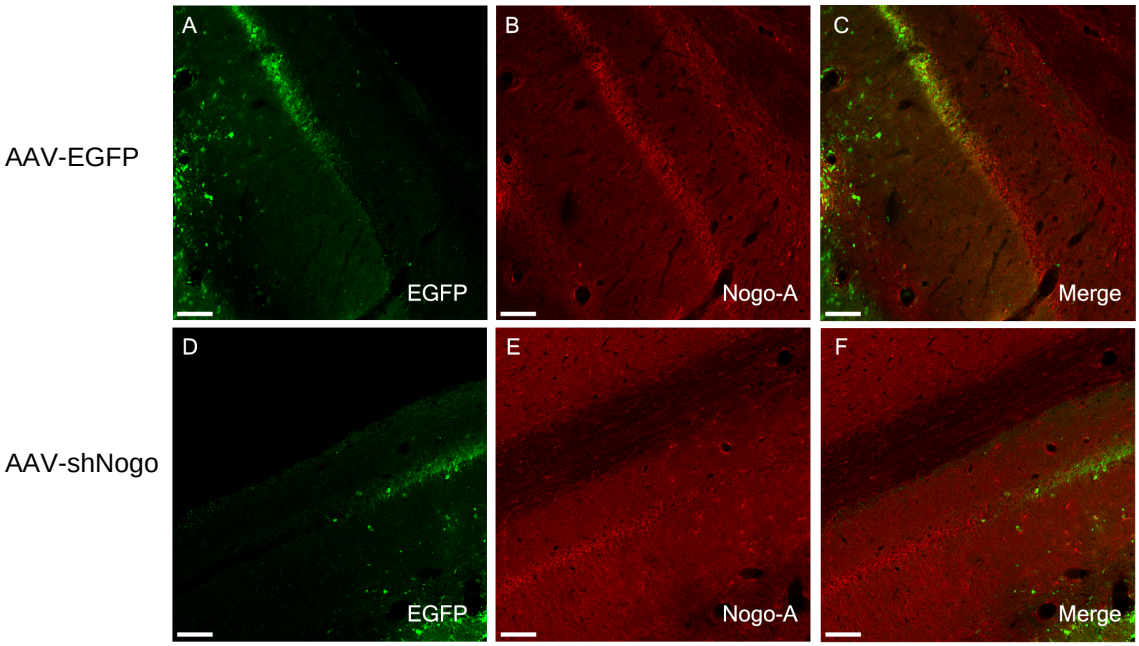

Figure 35. Knockdown of Nogo-A gene expression in CA1 pyramidal cells. In animals injected with control AAV-EGFP transduced CA1 pyramidal cells expressing EGFP show robust expression of Nogo-A, as shown by the colocalization of EGFP and Nogo-A (C). In animals injected with AAV-shNogo856 transduced CA1 pyramidal cells expressing EGFP show markedly reduced expression of Nogo-A, as shown by reduced colocalization of EGFP and Nogo-A (F). Scale Bars=100 μm.

Decreased Nogo-A Protein Expression after Nogo-A Knockdown (High Magnification)

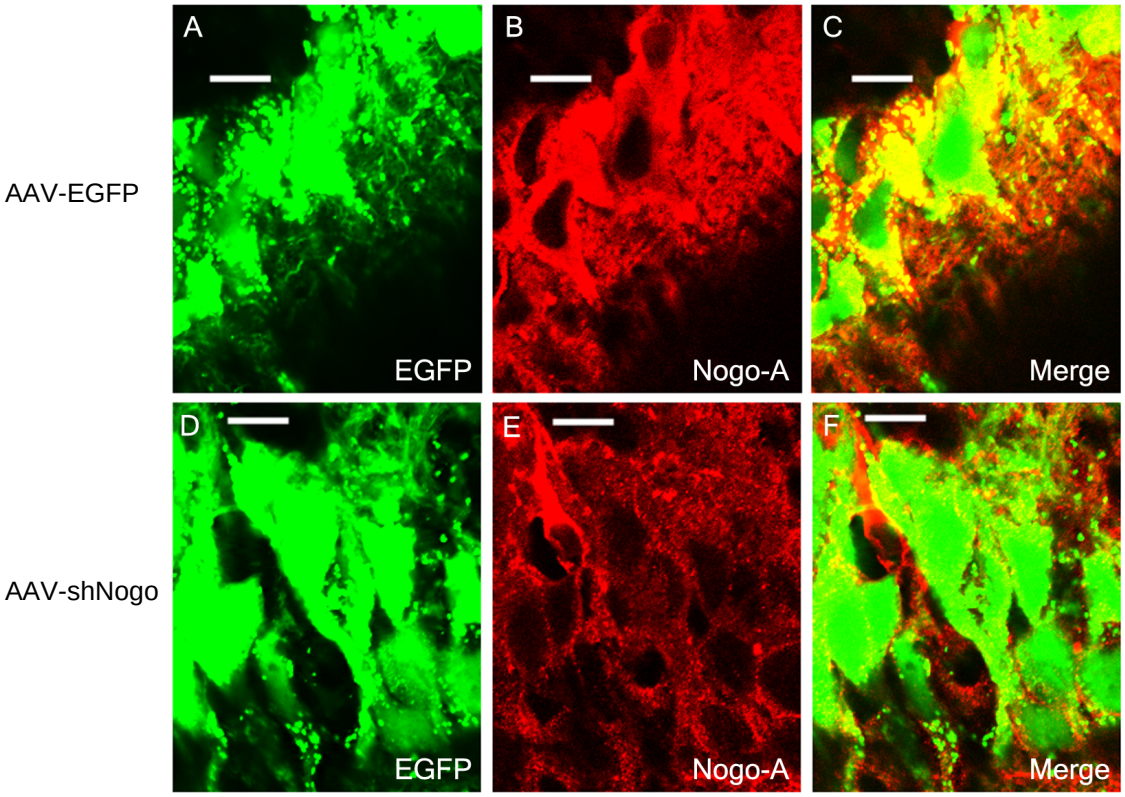

Figure 36. Knockdown of Nogo-A gene expression in CA1 pyramidal cells. In animals injected with control AAV-EGFP transduced CA1 pyramidal cells expressing EGFP show robust expression of Nogo-A, as shown by the colocalization of EGFP and Nogo-A (C). In animals injected with AAV-shNogo856 transduced CA1 pyramidal cells expressing EGFP show markedly reduced expression of Nogo-A, as shown by reduced colocalization of EGFP and Nogo-A (F). Scale Bars=10 μm.

Transduction of Astrocytes by AAV2/8

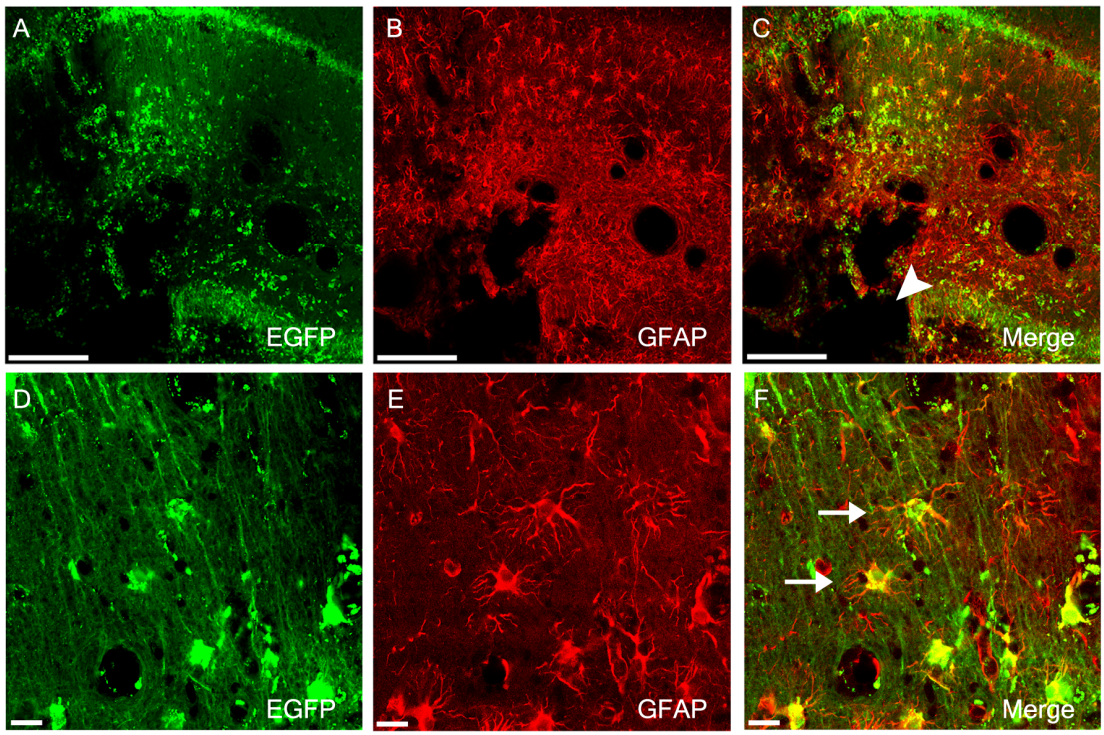

Figure 37. Injection of AAV-EGFP or AAV-shNogo856 at a volume of 3 µl and a titer of 2×10^9 iu/ml often caused microlesions at the injection site in the location of the dentate gyrus (arrow head). In addition to neurons, cells of non-neuronal morphology were found to contain EGFP (arrows) and immunostaining of GFAP showed that many of these cells were astrocytes (arrows). Scale Bar for A-C=200 µm, Scale Bar for D-F=20 µm .

DISCUSSION

In the present study we successfully demonstrated neuronal transgene transfer by AAV2/8 and RNAi mediated knockdown of Nogo-A in the hippocampus of aged rats. However, decreasing the expression of the Nogo-A protein in the hippocampus of normal aged rats did not affect apical dendritic spine density or morphology in CA1 pyramidal cells.

The Nogo-A protein is most often thought of as a myelin-associated inhibitor of axonal plasticity in the CNS. Work in our laboratory has also shown that Nogo-A can inhibit dendritic plasticity (Papadopoulos et al., 2006). However, the Nogo-A protein is also expressed by many neurons in the CNS by rodents (Wang et al., 2002c; Hunt et al., 2003) and humans (Buss et al., 2005), and recent evidence suggests that neuronal Nogo-A may have additional functions in addition to inhibiting axonal plasticity (Montani et al., 2009). During development the expression of Nogo-A in the brain precedes that of the NgR (Wang et al., 2002c), a receptor that in part mediates the growth inhibitory effects of Nogo-A. During development large projection neurons of the chick optic tectum express Nogo-A during the process of neuritogenesis (Caltharp et al., 2007). We have previously reported that knocking down Nogo-A during development in neocortical pyramidal neurons led to decreased dendritic spine density and an increased percentage of immature dendritic spine morphologies (Pradhan, 2007). This has important consequences for synaptic transmission because dendritic spines are the main site of excitatory synapses, and the morphology of dendritic spines relates to their function (Bourne and Harris, 2008). Taken together, these studies of Nogo-A during development

support the idea that neuronal Nogo-A has a role in CNS development, circuit formation, and structural synaptic plasticity.

Further evidence points to a role in the adult for neuronal Nogo-A in synaptic plasticity. Nogo-A is located at the post-synaptic density of spinal cord motor neurons (Liu et al., 2003), and is located presynaptically at the neuromuscular junction (Dodd et al., 2005). Genetic manipulation to specifically overexpress Nogo-A in adult Purkinje cells led to the retraction and loss of inhibitory Purkinje cell terminals, suggesting a role for neuronal Nogo-A in the maintenance of inhibitory synapses (Aloy et al., 2006). Nogo-A has also been shown to inhibit integrin signaling (Hu and Strittmatter, 2008), and integrins have been implicated in regulating dendritic spine morphology (Webb et al., 2007). The NgR1 has also been shown to be involved in synaptic plasticity. In the cortex the NgR1 is located both pre and post-synaptically (Wang et al., 2002c), and mutant mice without NgR1 have a shift of dendritic spine morphologies in the apical CA1 pyramidal cell dendritic tree so there are more stubby spines and fewer mushroom and thin spines as compared to heterozygous controls (Lee et al., 2008). This represents a shift towards more immature dendritic spine morphologies. In this study, mice lacking NgR1 had enhanced FGF2-dependent LTP, and attenuated LTD at hippocampal Schaffer collateral-CA1 synapses. Taken together, these studies suggest that neuronal Nogo-A and its receptor NgR1 play a role in synaptic plasticity.

Evidence suggests that neuronal Nogo-A may be important in other cellular functions. In addition to being located on myelin sheaths (Wang et al., 2002c), and in neurons at the synapse (Liu et al., 2003) and on the cell membrane (Dodd et al., 2005),

Nogo-A is also found at polyribosomes, in the rough endoplasmic reticulum (Jin et al., 2003a), throughout the dendritic trees of some neurons (Mingorance et al., 2004b), and in axons (Wang et al., 2002c). One study showed that Nogo-A may be involved in the shaping and stabilization of tubular endoplasmic reticulum (Voeltz et al., 2006). Another study found that Nogo-A interacts with Nogo-B and Nogo-C, and hypothesized that they may complex to form a channel or transporter (Dodd et al., 2005). These findings suggest that Nogo-A has additional as of yet unidentified functions.

We chose to study the effects of knocking down Nogo-A on dendritic spines in hippocampal CA1 pyramidal cells for several reason. Firstly, hippocampal CA1 pyramidal cells express Nogo-A both in rodents (Huber et al., 2002; Hunt et al., 2003; Mingorance et al., 2004b) and in humans (Buss et al., 2005; Gil et al., 2006b). A study in adult rats showed Nogo-A expression throughout the dendritic tree of CA1 pyramidal cells (Mingorance et al., 2004b). Secondly, mice lacking the NgR1 had altered dendritic spine morphology in the CA1 pyramidal cell dendritic tree, suggesting that Nogo-A-NgR1 signaling may affect dendritic spines in CA1 pyramidal cells. Finally, neuronal Nogo-A protein expression has been shown to be altered in the hippocampus in several neurological diseases. Nogo-A protein is increased in hippocampal neurons of Alzheimer's Disease (Gil et al., 2006b), and temporal lobe epilepsy patients (Bandtlow et al., 2004; Gil et al., 2006b). Nogo-A is also found in association with neuritic plaques in the brains of Alzheimer 's Disease patients (Gil et al., 2006b). We studied aged rats to make our results more applicable to neurological diseases of aging such as Alzheimer 's Disease.

The lack of observed dendritic spine structural changes in hippocampal CA1 pyramidal cells after knocking down Nogo-A can be explained several ways. First, another protein could compensate for the reduction in Nogo-A levels. We have previously shown *in vitro* knockdown of Nogo-A using the shNogo856 in the Neuroblastoma B104 cell line does not affect the expression of Nogo-B or Nogo-C (Pradhan, 2007). This makes it unlikely that Nogo-B or Nogo-C are compensating for the loss of Nogo-A, but another protein that modulates synaptic structural plasticity could compensate for the loss of Nogo-A. Secondly, the function of neuronal Nogo-A in dendritic spine structural plasticity could differ between different neuronal types and ages. We showed that knockdown of Nogo-A in neonatal rat cortical neurons altered dendritic spine density and morphology (Pradhan, 2007), but neuronal Nogo-A may not have the same affect on dendritic spines in CA1 pyramidal cells as in cortical neurons. Finally, neuronal Nogo-A may not function in senescent neurons the same as in developing neurons. This would explain why knocking down neuronal Nogo-A in neonatal cortical neurons had an affect on dendritic spine structure (Pradhan, 2007), while knocking down neuronal Nogo-A in aged CA1 pyramidal neurons did not affect dendritic spine structure. To help elucidate the function of neuronal Nogo-A in the aged hippocampus, further studies in aged rats with hippocampal knockdown of Nogo-A are need to investigate hippocampal LTP and LTD, synaptic density, and the structure of the endoplasmic reticulum.

The present study successfully used AAV2/8 for neuronal transgene transfer. AAV serotype 8 is a promising viral vector for gene delivery to neurons in the CNS,

because it has previously been shown to predominantly transduce neurons (Broekman et al., 2006; Klein et al., 2006a), and has more efficient gene transfer in the rodent CNS that some of the other AAV serotypes (Broekman et al., 2006; Harding et al., 2006; Klein et al., 2006a). Though one study found that viral vector purification by the CsCl-gradient method of AAV8, but not AAV9, AAV10, or AAV43, caused astrocyte transduction and astrogliosis in the rat hippocampus, in addition to neuronal transduction (Klein et al., 2008). However, when AAV8 was purified by iodixanol there was the expected predominately neuronal transduction in the rats hippocampus. Therefore, Klein et al. concluded that the CsCl purification caused AAV8 to transduce astrocytes in addition to neurons, and they hypothesized that this was due to the higher protein and residual GFP they found in preps purified by the CsCl-gradient method. Indeed, another study using the CsCl purification method saw astrocyte transduction with AAV8 and AAV5 (Harding et al., 2006). Similarly, we also found astrocytes containing EGFP, and in rats with a higher injection dose we found microlesions at the injection sites surrounded by cells containing EGFP of non-neuronal morphology, many of which were astrocytes. It is likely these astrocytes were transduced by the AAV2/8, but it is also possible that the astrocytes phagocytized the EGFP from dying transduced neurons. Though the AAV8 we used was purified by iodixanol, this batch of vector may have had a higher protein and residual EGFP content that usual. This would explain why we observed transduction of both neurons and astrocytes, and astrogliosis, which may have caused microlesions at the injection site. This illustrates that small differences in the preparation and purification of viral vectors can alter their transduction pattern.

In conclusion, viral mediated RNAi is a valid approach to alter the protein expression of neurons in aged rats. However knocking down Nogo-A in the hippocampus of aged rats did not alter the dendritic spine density or morphology of CA1 pyramidal cells, indicating a minimal role for Nogo-A in spine density and morphology in this population of neurons in this age group.

CHAPTER FIVE

GENERAL DISCUSSION

SUMMATION OF RESULTS

This project demonstrates that anti-Nogo-A immunotherapy improves performance on a spatial reference memory task after sensorimotor cortical stroke in aged rats. Aged rats with stroke and treated with anti-Nogo-A immunotherapy acquired the location of the hidden platform in the Morris water maze place task more rapidly than aged rats with stroke and treated with a control antibody. At the end of the place task all groups performed equally on the probe trial, demonstrating that rats in all groups were able to eventually learn the location of the hidden platform.

The same animals from behavioral testing were used to assess dendritic arbor complexity and dendritic spine density and morphology of hippocampal neurons. The results demonstrate that sensorimotor cortical stroke causes decreased dendritic arbor complexity in the ipsilesional hippocampus, but that anti-Nogo-A immunotherapy does not protect hippocampal neurons from these structural changes. Differences in dendritic spine density or morphology in hippocampal neurons after stroke or anti-Nogo-A immunotherapy were not detected.

Anti-Nogo-A immunotherapy is directed against Nogo-A on the surface of any type of cell, including oligodendrocytes and neurons, so further studies in this dissertation continued to investigate what role specifically neuronal Nogo-A plays in dendritic

structural plasticity in hippocampal neurons. Reduction of Nogo-A expression levels in CA1 hippocampal neurons by RNAi did not cause detectable changes in dendritic spine density or morphology.

THERAPEUTIC POTENTIAL OF ANTI-NOGO-A IMMUNOTHERAPY

The Nogo-A protein is well known as a myelin associated inhibitor of axonal plasticity (Gonzenbach and Schwab, 2008), and has also been found to be expressed in many CNS neurons (Wang et al., 2002c; Hunt et al., 2003; Buss et al., 2005). Mounting evidence suggests that the Nogo-A protein may be a therapeutic target in several different neurological diseases such as stroke and SCI. The overall idea is that by neutralizing Nogo-A there will be enhanced axonal and dendritic plasticity, and this will allow the CNS to modify its neural circuits in response to injury or disease and lead to recovery of function.

For example, in a non-human primate model of SCI, adult Macaque monkeys given a unilateral cervical spinal cord injury and treated with anti-Nogo-A immunotherapy had improved recovery of hand dexterity and axonal compensatory growth (Freund et al., 2006; Freund et al., 2007b; Freund et al., 2009). In rodent models of stroke, adult and aged rats given a unilateral sensorimotor cortical stroke and treated with anti-Nogo-A immunotherapy had improved skilled forelimb sensorimotor function (Papadopoulos et al., 2002a; Markus et al., 2005a; Seymour et al., 2005a; Tsai et al., 2007), and in adult rats the improvement correlated with axonal compensatory growth

(Papadopoulos et al., 2002a; Seymour et al., 2005a) and dendritic plasticity in the contralesional sensorimotor cortex (Papadopoulos et al., 2006).

Further experiments, including the studies described in this dissertation, show that anti-Nogo-A immunotherapy may also be effective in treating cognitive impairments. After lateral fluid percussion injury, rats treated with anti-Nogo-A immunotherapy had improved performance on a spatial memory task (Lenzlinger et al., 2005a; Marklund et al., 2007b). Another study showed recovery from a cortical injury causing severe neglect after anti-Nogo-A immunotherapy. When the corpus callosum was then cut, the severe neglect was again manifested, demonstrating that the contralateral cortex was involved in the recovery induced by anti-Nogo-A immunotherapy (Brenneman et al., 2008b). The work described in this dissertation provides further evidence that anti-Nogo-A immunotherapy is an effective treatment for cognitive impairments after various types of brain injury. This opens the possibility that anti-Nogo-A immunotherapy could be effective in treating cognitive impairments caused by other etiologies such as Alzheimer's disease. Furthermore, the studies in this dissertation give support to an earlier study that anti-Nogo-A immunotherapy is effective in aged subjects (Markus et al., 2005b), which is important because stroke is much more prevalent in the aged human population.

The studies in this dissertation also demonstrate that viral vector mediated RNA interference is an effective way to decrease Nogo-A expression in neurons. Vector mediated gene therapy against Nogo-A is a promising approach, but it has limitations to be addressed including cell specificity of transduction, possible tissue damage at the

injection site and possible host immune response. This approach may have more utility for injection at the location of prior damage such as in SCI.

Anti-Nogo-A immunotherapy also has limitations to be addressed. Currently, anti-Nogo-A immunotherapy has only been proven to be effective when delivered into the cerebroventricular system, including the intrathecal route (Tsai et al., 2007). However, intrathecal delivery could be a limiting factor for delivery to the very aged population with multiple co-morbidities who are most likely to experience a stroke. Therefore, development of an intravenous anti-Nogo-A immunotherapy is of great importance.

Anti-Nogo-A immunotherapy is in phase I clinical trials for acute spinal cord injury and clinical trials for stroke are currently in development. If the promise shown by rodent and non-human primate pre-clinical studies is also realized in human trials then anti-Nogo-A immunotherapy has the potential to make remarkable advances in the treatment of neurological disease.

FUTURE DIRECTIONS

These experiments show that anti-Nogo-A immunotherapy improves performance on a spatial memory task in aged rats after stroke. However, anti-Nogo-A immunotherapy did not affect dendritic plasticity in the hippocampus, a brain area particularly important for spatial memory. Further studies are needed to identify neuroanatomical correlates of the improved performance in spatial memory after stroke and treatment with anti-Nogo-A immunotherapy.

One promising avenue to explore is axonal plasticity in the hippocampus. In hippocampal slice cultures treatment with anti-Nogo-A antibodies increased axonal regeneration/sprouting either in intact preparations or after cutting the Schaffer collaterals (Craveiro et al., 2008a) or perforant pathway (Mingorance et al., 2004b). Therefore, future studies should investigate axonal plasticity within the circuitry of the hippocampus and in its efferents and afferents after stroke and treatment with anti-Nogo-A immunotherapy.

Another promising avenue to explore is neuroanatomical plasticity within the cholinergic system. Cholinergic axons have been shown to regenerate/sprout after treatment with anti-Nogo-A antibodies in fibers innervating the sensorimotor cortex after aspiration lesion and neocortical graft (Schulz et al., 1998), and in fibers innervating the hippocampus after fimbria-fornix lesions (Cadelli and Schwab, 1991b). Furthermore, disruption of the cholinergic system can cause impaired performance on the Morris water maze (D'Hooge and De Deyn, 2001b). Therefore, future studies should investigate axonal plasticity within the cholinergic system after stroke and treatment with anti-Nogo-A immunotherapy.

APPENDIX A:

IACUC APPROVAL LETTERS

VA RESEARCH & DEVELOPMENT

DEPARTMENT OF VETERANS AFFAIRS
VA CHICAGO HEALTH CARE SYSTEM

INSTITUTIONAL ANIMAL CARE AND USE COMMITTEE

MEMORANDUM

Date: April 25, 2006

From: Hines NCVA IACUC Chair

Subject: Approval of IACUC Submission

To: Dr. Kartje

1. Title/Promise #: Nogo-A Blockade and Functional Recovery after Stroke in the Aged

2. Funding Source: Dept. of VA

3. On ***March 22, 2006*** your protocol submission was brought before the IACUC and required further clarifications and modifications. On April 25, 2006 your response submission for the above was received, reviewed and **Chair Approved**. This will be reflected in the minutes of the ***May 2006*** IACUC meeting.

4. Please note that, if you have not done so already, you must secure approval of the Hines/NCVA Research and Development (R & D) Committee prior to initiating work in the above-mentioned ACORP. Thus no IACUC number will be assigned and animal orders can not be processed until R & D approval is obtained.

5. Should it become necessary to make any changes in this protocol, you must submit a modification request for approval prior to initiating changes. Failure to comply with these provisions can result in suspension of the research.

6. Please verify the information below; if corrections are required, notify the Hines/NCVA IACUC coordinator immediately. Animal purchases are processed via the VMU office.

   a. Category: E
   b. Species: Rats
   c. #Animals approved: 192
   d. Approval Date: April 25, 2006
   e. Approval Termination: April 1, 2009
   f. IACUC #: H06-011

William A. Wolf, PhD
IACUC Chair

VA RESEARCH & DEVELOPMENT

DEPARTMENT OF VETERANS AFFAIRS
VA CHICAGO HEALTH CARE SYSTEM

INSTITUTIONAL ANIMAL CARE AND USE COMMITTEE

MEMORANDUM

Date: July 26, 2007

From: Hines NCVA IACUC Chair

Subject: Approval of IACUC Submission

To: Dr. Kartje

1. Title/Promise #: Neuronal Nogo-A knockdown in the postnatal rat hippocampus

2. Funding Source: Dept of VA

3. On ***June 19, 2007*** your protocol submission was brought before the IACUC and required further clarifications and modifications. On ***July 26, 2007*** your response submission for the above was received, reviewed and **Chair Approved**. This will be reflected in the minutes of the ***August*** IACUC meeting.

4. Please note that, if you have not done so already, you must secure approval of the Hines/NCVA Research and Development (R & D) Committee prior to initiating work in the above-mentioned ACORP.

5. Should it become necessary to make any changes in this protocol, you must submit a modification request for approval prior to initiating changes. Failure to comply with these provisions can result in suspension of the research.

6. Please verify the information below: if corrections are required, notify the Hines/NCVA IACUC coordinator immediately. Animal purchases are processed via the VMU office.

   a. Category: B(~~28~~ 33) E(~~200~~ 2640)
   b. Species: Rats
   c. #Animals approved: see above
   d. Original Approval Date: 07/26/07
   e. Approval Termination: 07/01/10
   f. IACUC #: H07-020

Stuart Johnson, MD
IACUC Chair

APPENDIX B:

PILOT EXPERIMENTS

APPENDIX B: PILOT EXPERIMENTS

OPTIMIZATION OF MCAO IN FISCHER 344 RATS

Rationale

Stroke lesion size and location after MCAO in rats can vary depending upon the strain of rat used due to differences in vasculature. For our stroke experiments we usually use Long Evans black-hooded rats because reproducible stroke lesions to the sensorimotor cortex with subcortical sparing result from MCAO with permanent ipsilateral carotid occlusion and 60 minute contralateral carotid occlusion. However, aged rodent colonies of Long Evans black-hooded rats are not maintained by the vendors, so it is very expensive and time consuming to acquire aged Long Evans black-hooded rats. Our goal for this experiment was to determine if reproducible stroke lesions to the sensorimotor cortex could be accomplished in another rat strain. We chose the Fischer 344 strain because the National Institute on Aging maintains an aged Fischer 344 rodent colony, and these rats are readily available at a reasonable cost to researchers funded by the National Institutes of Health, or the Department of Veterans Affairs.

Methods

Animal Subjects

Experiments were approved by the Institutional Animal Care and Use Committee of Hines Veterans Affairs Hospital. Subjects were aged male Fischer 344 rats (20-22 months of age at time of sacrifice).

Stroke Surgery

MCAO was performed as described in chapter 3, except that ipsilateral and contralateral carotid occlusions were varied.

TTC (2,3,5-triphenyl-2H-tetrazolium chloride) reaction

Rats were overdosed with pentobarbital (100 mg/kg, i.p.) and the brain was removed, and cut into 2 mm coronal sections using a rat brain matrix on ice. The sections were then incubated for 25 minutes at room temperature in 2% TTC (Sigma, St. Louis, MO, USA) in phosphate buffered 0.9% saline, and then fixed in 4% paraformaldehyde.

Results

In Fischer 344 rats, MCAO without ipsi or contralateral carotid occlusion did not cause a stroke lesion (App B Fig 1A,B). MCAO with permanent ipsilateral carotid occlusion and 30 or 60 minute contralateral carotid occlusion caused a stroke lesion to the sensorimotor cortex with some minimal subcortical involvement (App B Fig 1C,D). MCAO with permanent ipsilateral carotid occlusion and no contralateral carotid occlusion caused a stroke lesion to the sensorimotor cortex and spared subcortical structures (App B Fig 1E). However, when we repeated this procedure in another aged Fisher 344 rat, no stroke lesion resulted (described in the next section of Appendix B).

Middle Cerebral Artery Occlusion in Fischer 344 Aged Rats.

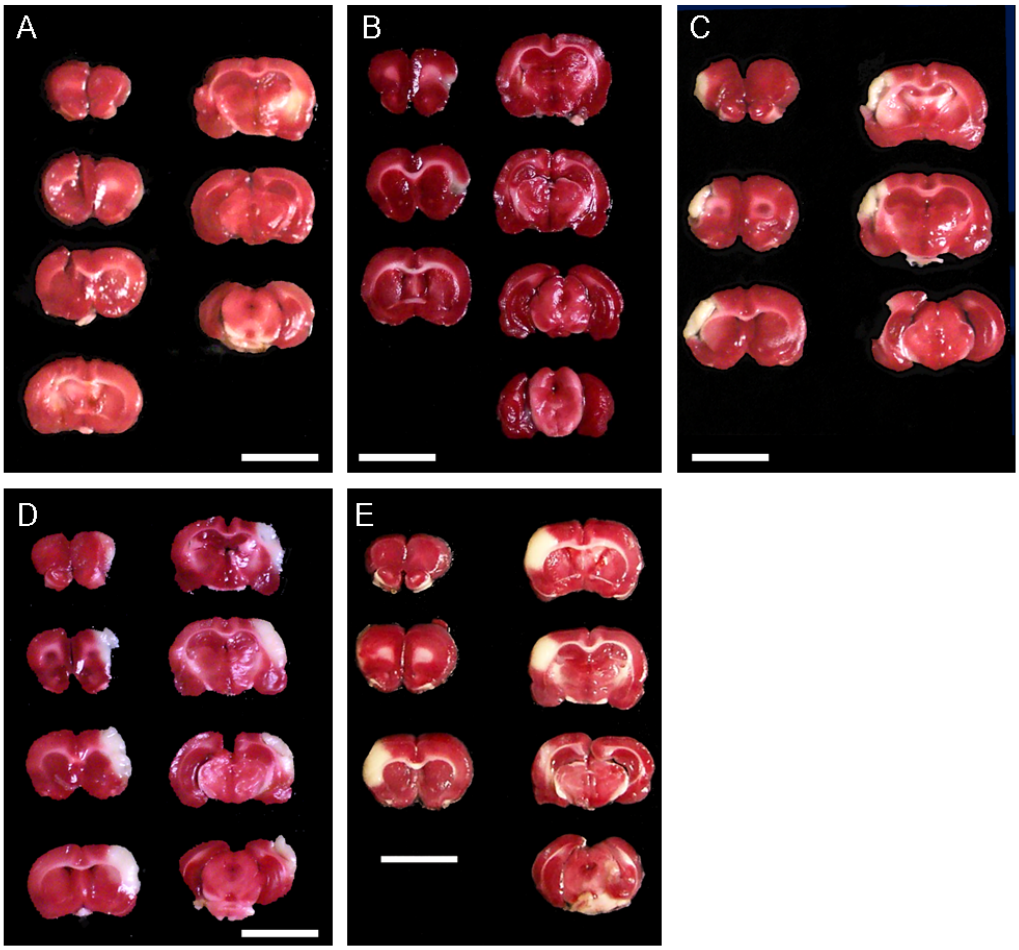

App. B Figure 1. Middle Cerebral Artery Occlusion in Fischer 344 Aged Rats. Thirty minutes post-stroke, left MCAO and no carotid occlusion (A). One day post-stroke, right MCAO and no carotid occlusion (B). Three days post-stroke, right sided stroke after MCAO, permanent ipsilateral carotid occlusion and 30 minute contralateral carotid occlusion, note minimal subcortical damage (C). One day post-stroke, left sided stroke after MCAO, permanent ipsilateral carotid occlusion and 60 minute contralateral carotid occlusion, note minimal subcortical damage (D). One day post-stroke, right sided stroke after MCAO and permanent ipsilateral carotid occlusion and no contralateral carotid occlusion (E). Scale Bar = 1 cm.

Conclusion

This experiment demonstrates that in Fischer 344 aged rats induction of reproducible sensorimotor cortical strokes requires MCAO with permanent ipsilateral carotid occlusion and at least 30 minute contralateral carotid occlusion.

APPENDIX B: PILOT EXPERIMENTS

ANTIBODY SPREAD AFTER INTRACEREBROVENTRICULAR INJECTION

Rationale

It has been demonstrated that after infusion of the 11C7 anti-Nogo-A antibody into the lateral ventricle of adult rats after stroke the antibody spreads throughout the entire neuroaxis (Weinmann et al., 2006). We sought to repeat this experiment in aged rats with a MCAO.

Methods

Animal Subject

Experiments were approved by the Institutional Animal Care and Use Committee of Hines Veterans Affairs Hospital. Subject was one male Fischer 344 (21 months of age).

Stroke Surgery

MCAO on the right was performed as described in chapter 3 with permanent ipsilateral carotid occlusion and no contralateral carotid occlusion.

Antibody Intracerebroventricular Infusion

Infusion of the 11C7 antibody was performed as described in chapter 3, except the cannula was placed at coordinates 1.3 mm lateral (right), 3 mm posterior, and 3.8 mm ventral (relative to bregma).

Immunostaining

Three weeks post-stroke the rat was overdosed with pentobarbital (100 mg/kg, intraperitoneal) and transcardially perfused with 0.9% saline and 10,000 U heparin/liter followed by 4% paraformaldehyde. The brain and spinal cord was removed and immersed whole in 4% paraformaldehyde for 1 hour, and then transferred to 30% sucrose for four days. The brain and spinal cord was stored at -80º C until they were sectioned coronally on a cryostat at 40 μm. Alternate free floating sections were selected for immunostaining. Sections were blocked for 1 hour at room temperature with 10% normal goat serum (NGS), and 0.25% Triton-X 100 (TX100) in 1x Tris buffered saline (TBS). Next the sections were incubated overnight at 4º C with rabbit anti-mouse IgG1 (Invitrogen, Carlsbad, CA, USA) at 1:500 with 5% NGS and 0.25% TX100 in TBS. After washing, sections were incubated for 1 hour at room temperature with biotin-XX goat anti-rabbit IgG (Invitrogen), at 1:500 with 5% NGS and 0.25% TX100 in TBS. After washing, sections were incubated for 1 hour at room temperature with streptavidin alexa fluor 488 conjugate (Invitrogen), at 1:1000 with 5% NGS and 0.25% TX100 in TBS. Next sections were washed and reacted with cupric sulfate for 15 minutes as described in chapter 4 to reduce lipofuscin autofluorescence. Sections were then mounted to slides and coverslipped with Fluoromount-G (Southern Biotech, Birmingham, AL, USA). Images were acquired at 5x using a Leica fluorescent microscope.

Results

Two occurrences made the results difficult to interpret. First, the cannula was placed too far rostrally and ended up in the fimbria of the hippocampus instead of the right lateral ventricle. Therefore, the antibody was being delivered to the parenchyma, rather than into the cerebral spinal fluid. Second, the rat did not have a detectable stroke lesion resulting from MCAO and permanent occlusion of the ipsilateral carotid artery. The 11C7 antibody was concentrated around the injection location in the fimbria and dorsal hippocampus, but spread to other areas of the brain including the cortex (App B Fig 2).

Spread of the 11C7 Antibody after Infusion into the Fimbria of the Hippocampus

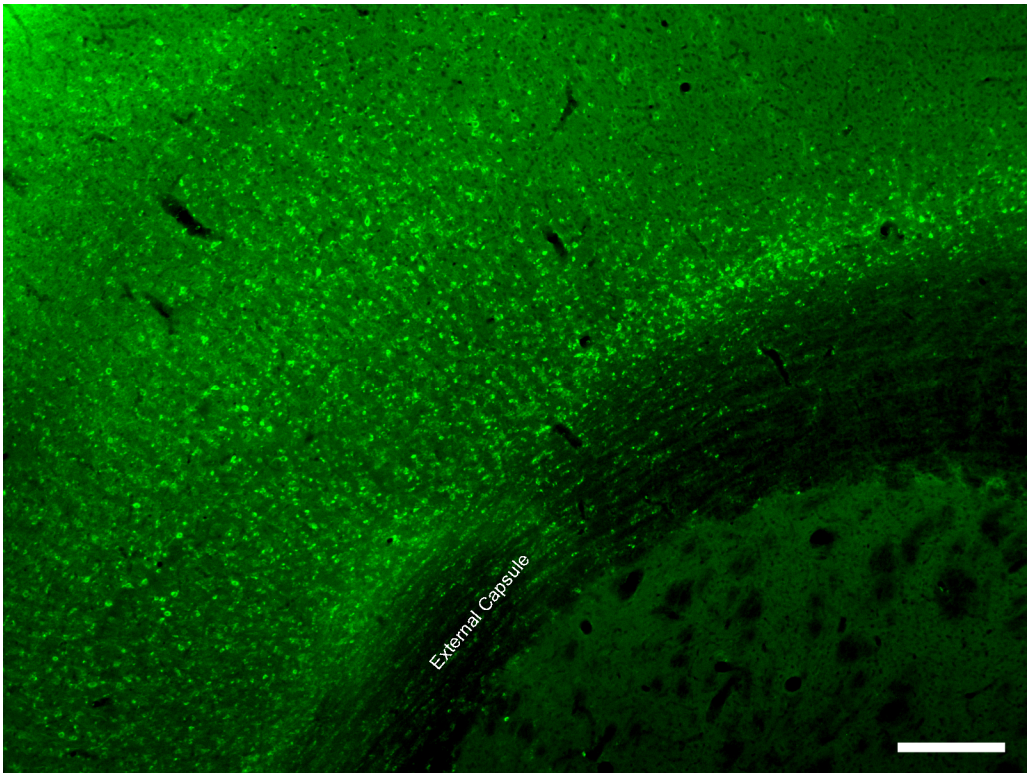

App. B Figure 2. Spread of the 11C7 antibody to the right cortex after infusion. 11C7 is immunostained in the cortex and the external capsule. 5x objective, Scale Bar=250 μm.

Conclusion

Due to the incorrect cannula placement the results of this experiment cannot show the extent to which 11C7 can spread after infusion into the lateral ventricle. However, the results do show that even with misplacement of the cannula, the antibody was able to spread considerable distances, even bilaterally in the dorsal hippocampus. This experiment also shows that stroke lesions in Fischer 344 rats are not consistent after

MCAO with permanent ipsilateral carotid occlusion and no contralateral carotid occlusion, when taken together with the experiments described above in Appendix B.

APPENDIX B: PILOT EXPERIMENTS

OPTIMIZE AAV2/8 HIPPOCAMPAL INJECTIONS IN AGED RATS

Rationale

We have previously injected AAV2/8 vectors carrying the EGFP transgene into the cortex of neonatal rats (Pradhan, 2007), but we have not done so with aged animals. This experiment was undertaken to optimize injection location and amount of AAV2/8 for transduction of the aged rodent hippocampus.

Methods

Animal Subjects

Experiments were approved by the Institutional Animal Care and Use Committee of Hines Veterans Affairs Hospital. Subjects were 13 male Fischer 344 rats (20-23 months of age at time of sacrifice).

Intracranial Injection Surgery

Intracranial injection surgeries were performed as described in chapter 4, except with various injection locations and amounts. For pilot rats 1-8 we used vectors that had been stored in the refrigerator for over a year and likely their titers had decreased from the titer measured when they were prepared. The initial titers of these vectors were as follows: AAV-EGFP 8×10^{5} iu/ml, AAV-shLuciferase (Luc) 1.8×10^{8} iu/ml, and AAV-shNogo856 3×10^{7} iu/ml. For pilot rats 9-13 we used a freshly prepared batch of vectors with the following titers: AAV-EGFP 2×10^{9} iu/ml, and AAV-shNogo856 2×10^{9} iu/ml Also the

early surgeries were performed without the microinjection pump. Injection location, amounts and any unique features for each rat are described in the results sections. On a technical note, all injections before pilot rat 13 were done with metal hub (N) Hamilton needles and luer tip (LT) syringes. We discovered that these needles can leak at the junction between the needle and the syringe, and we feel that this explains some of the variability in transduction in pilot rats 1-12. After discovering this, we began to use removable needles (RN) and the RN syringes and had more consistent results as described in the main experiment in chapter four.

Tissue Processing

Rats were overdosed with pentobarbital (100 mg/kg, intraperitoneal) and transcardially perfused with 0.9% saline and 10,000 U heparin/liter followed by 4% paraformaldehyde. The brains were removed and immersed whole in 4% paraformaldehyde for 1 hour, and then transferred to 30% sucrose for three days. The brains were stored at -80º C until they were sectioned coronally on a cryostat. Sections were washed and reacted with cupric sulfate as described in chapter 4 to reduce lipofuscin autofluorescence. Sections were then mounted to slides and coverslipped with Fluoromount-G (Southern Biotech, Birmingham, AL, USA). Images were acquired using a Leica fluorescent microscope.

Results

Rat 1

Rat 1 was injected with 6 µl of AAV-EGFP on each side of the hippocampus at coordinates 2 mm lateral, 3.6 mm posterior, and 3.5 and 2.8 mm ventral (3 µl for each depth), relative to bregma (Klein et al., 2006b). Two weeks later the rat was sacrificed. The brain sections from this rat had a 45 minute cupric sulfate treatment to reduce lipofuscin autofluorescence. We found that the injections were too far rostral and ventral and transduced cells were located in the fimbria of the hippocampus.

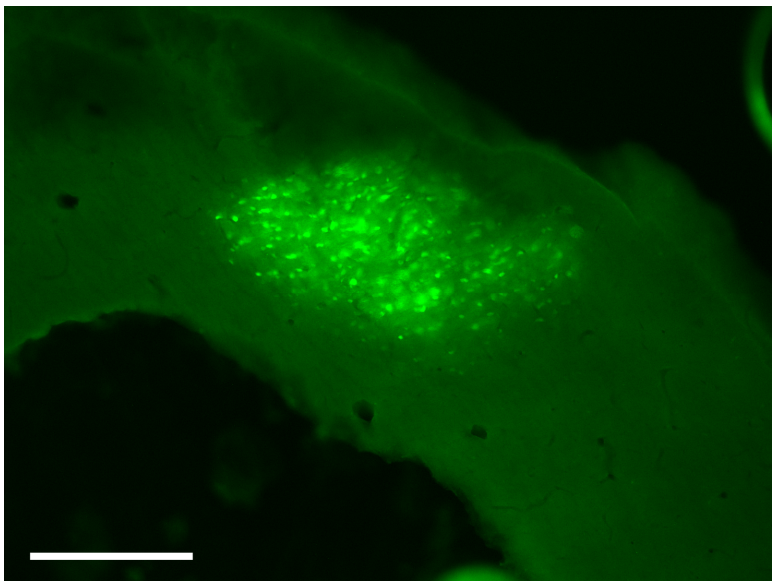

App. B Figure 3. AAV-EGFP transduction in the fimbria of pilot rat 1. 10x objective, Scale Bar=250 µm.

Rat 2

Rat 2 was injected with 6 µl in the left hippocampus and 2 µl in the right hippocampus with AAV-shLuc also containing the EGFP transgene. On the left the coordinates were 1.5 mm lateral, 4.54, 5.34 and 6.55 mm posterior (2 µl for each location), and 2.5 mm

ventral, relative to bregma. On the right the coordinates were 1.5 mm lateral, 4.54 and 5.34 posterior (1 μl for each location), and 2.5 mm ventral, relative to bregma. Two weeks later the rat was sacrificed. We found that 15 minutes of Cupric Sulfate treatment sufficient to significantly reduce the lipofuscin autofluorescence, and all further rat brains were treated for 15 minutes. On the left injections were a bit too ventral, but there was good transduction of hippocampal cells. On the right there was minimal transduction of the hippocampus. Additionally, a planned third injection location on the right was not completed because of rupture of a cerebral sinus, demonstrating that 1.5 mm lateral is too close to the midline.

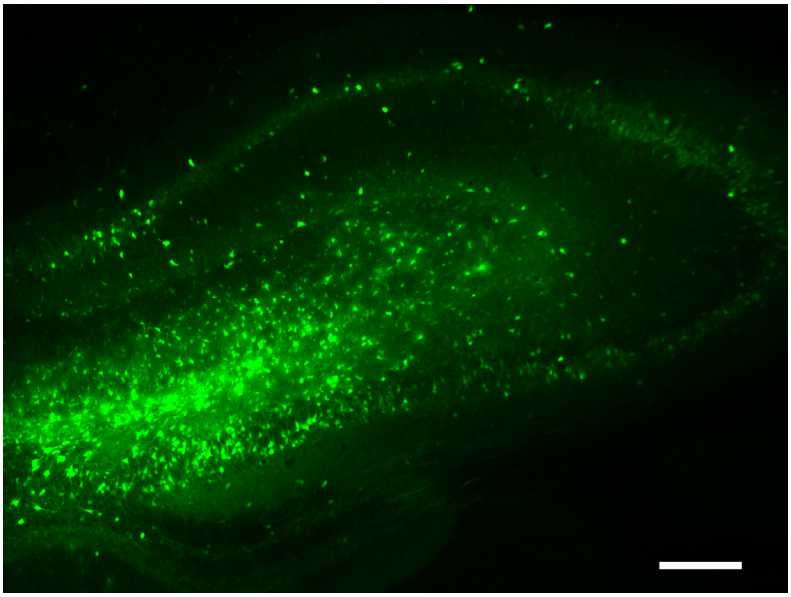

App. B Figure 4. AAV-shLuc transduction in the left dorsal hippocampus of pilot rat 2. 5x objective, Scale Bar=250 μm.

Rat 3

Rat 3 was injected with 4 µl in the left hippocampus and 2 µl in the right hippocampus with AAV-shLuc. On the left the coordinates were 2.0 mm lateral, 4.8 and 5.8 mm posterior (2 µl for each location), and 2.5 mm ventral, relative to bregma. On the right the coordinates were 2.0 mm lateral, 4.54 and 5.34 posterior (1 µl for each location), and 2.5 mm ventral, relative to bregma. Two weeks later the rat was sacrificed. Bilaterally in the hippocampus transduction was minimal, but the few transduced cells were in the middle of the dorsal hippocampus.

Rat 4

Rat 4 was injected with 6 µl of AAV-shNogo856 on each side of the hippocampus at coordinates 2 mm lateral, 4.5, 5.3 and 6.1 mm posterior, and 2.0 and 2.5 mm ventral (1 µl for each depth), relative to bregma. Two weeks later the rat was sacrificed. The injections appeared to be a bit too dorsal causing neocortical transduction, and did not spread far enough lateral in the dorsal hippocampus.

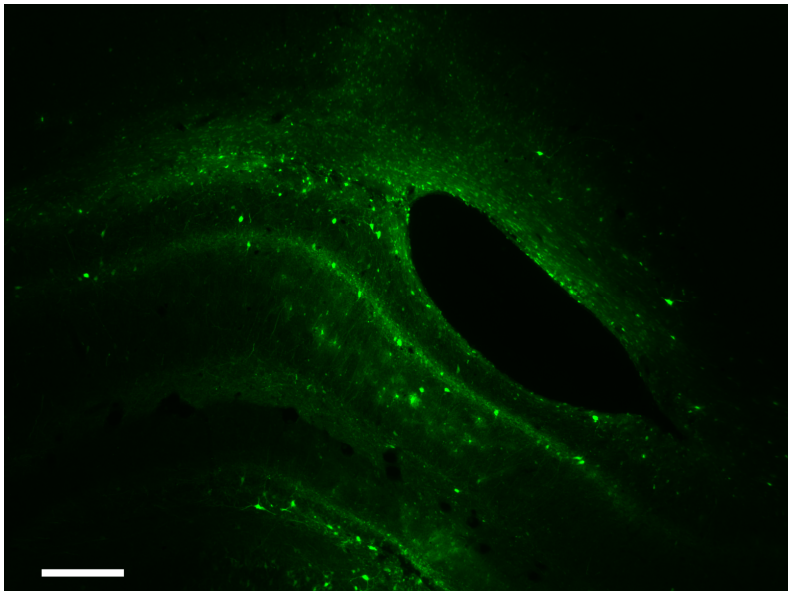

App. B Figure 5. AAV-shNogo856 transduction in the right dorsal hippocampus of pilot rat 4. 5x objective, Scale Bar=250 μm.

Rat 5

Rat 5 was injected with 6 μl of AAV-shNogo856 on the left side of the hippocampus at coordinates 2 mm lateral, 4.5, 5.3 and 6.1 mm posterior, and 2.0 and 2.5 mm ventral (1 μl for each depth), relative to bregma. Two weeks later the rat was sacrificed. Transduction was minimal, but the few transduced cells were located in the dorsal hippocampus.

Rat 6

Rat 6 was injected with 6 μl of AAV-shNogo856 on each side of the hippocampus at coordinates 2 and 2.75 mm lateral, 5 and 5.6 mm posterior (more posterior location is also the more lateral), and 2.5 and 2.3 mm ventral (1.5 μl for each depth), relative to bregma. Two weeks later the rat was sacrificed. Injections were too dorsal on the right and too ventral on the left.

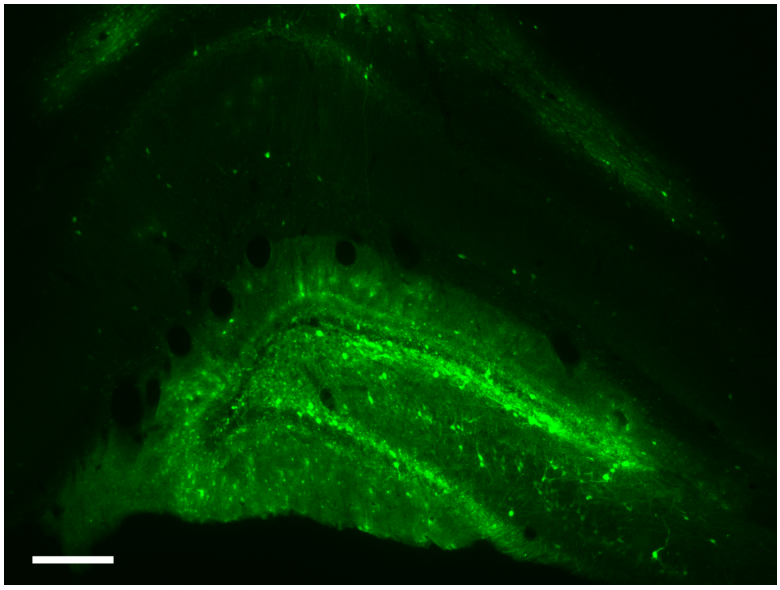

App. B Figure 6. AAV-shNogo856 transduction in the left dorsal hippocampus of pilot rat 6. Note that on this side the injections were too ventral causing transduction in the dentate gyrus, but not in CA1. 5x objective, Scale Bar=250 μm.

Rat 7

Rat 7 was injected with 6 μl of AAV-shNogo856 on the right side of the hippocampus at coordinates 2 mm lateral, 5.3 mm posterior, and 2.5 and 2.3 mm ventral (3 μl for each depth), relative to bregma. Two weeks later the rat was sacrificed. Transduction was not far enough ventral or lateral. We found bilateral transduction from this unilateral injection of vector.

Rat 8

Rat 8 was injected with 6 μl of AAV-Luc on each side of the hippocampus at coordinates 2 and 2.75 mm lateral, 5.3 mm posterior, and 2.5 and 2.3 mm ventral (1.5 μl for each depth), relative to bregma. Two weeks later the rat was sacrificed. The injection locations

were within the dorsal hippocampus and the injections caused transduction of many hippocampal cells.

Rats 9 and 10

Rats 9 and 10 were injected with 6 µl of AAV-EGFP on each side of the hippocampus at coordinates 2 and 2.75 mm lateral, 5.3 mm posterior, and 2.5 and 2.3 mm ventral (1.5 µl for each depth), relative to bregma. We began using the microinjection pump with pilot rat 10. Four weeks later the rats were sacrificed. Cells were transduced in the dorsal hippocampus including CA1 pyramidal cells.

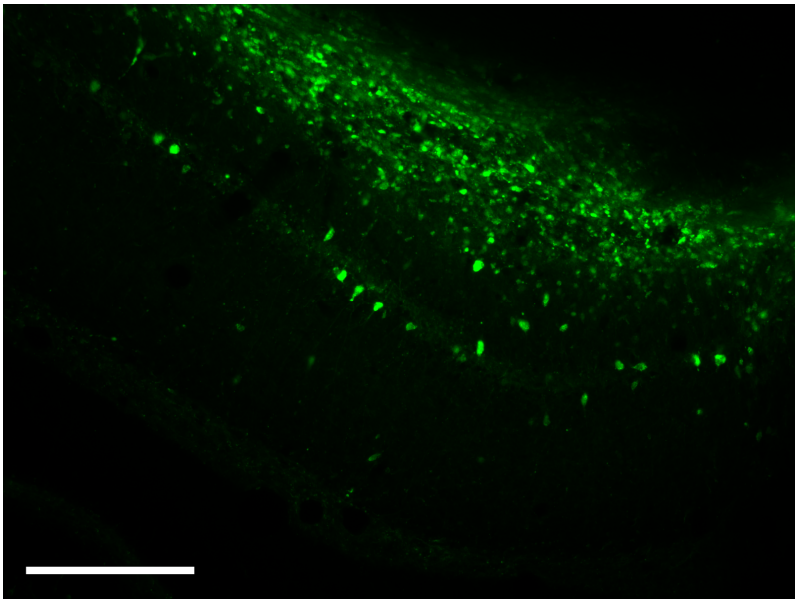

App. B Figure 7. AAV-EGFP transduction in the dorsal hippocampus of pilot rat 9. 10x objective, Scale Bar=250 µm.

Rats 11 and 12

Rats 11 and 12 were injected with 6 µl of AAV-shNogo856 on each side of the hippocampus at coordinates 2 and 2.75 mm lateral, 5.3 mm posterior, and 2.5 and 2.3 mm

ventral (1.5 µl for each depth), relative to bregma. Four weeks later the rats were sacrificed. Transduction was very minimal, and this is the point at which we realized that the virus was leaking at the junction of the metal hub needle and syringe.

Rat 13

Rat 13 was injected with 3 µl of AAV-shNogo856 on each side of the hippocampus at coordinates 2.35 mm lateral, 5.3 mm posterior, and 2.5 and 2.3 mm ventral (1.5 µl for each depth), relative to bregma. One week later the rats were sacrificed. Cells were transduced in the dorsal hippocampus including CA1 pyramidal cells.

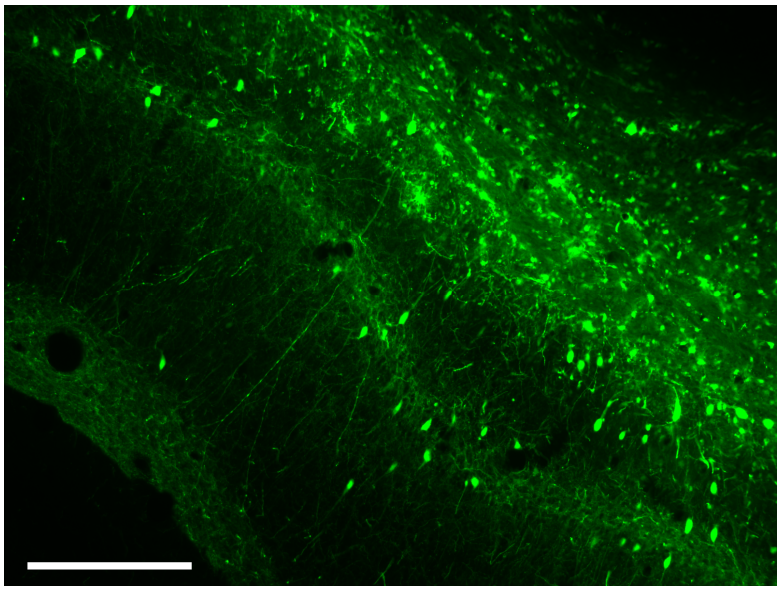

App. B Figure 8. AAV-shNogo856 transduction in the dorsal hippocampus of pilot rat 13. 10x objective, Scale Bar=250 µm.

Conclusion

These pilot experiments allowed us to identify and correct several technical difficulties with injection of AAV into the hippocampus of aged rats. First, we had to adjust our injection coordinates due to the different strain and age of the rats. We also discovered that some types of Hamilton needles can leak at the junction between the needle and the syringe, and this probably caused some of the inconsistencies in our pilot rat injections. In retrospect, we now know that the transduction we saw during the pilot rat experiments was much less than what we saw in the main experiments described in chapter 4. We feel this was due to the leaking needles, and lower titers of the vectors we used for pilot rats 1-8.

APPENDIX B: PILOT EXPERIMENTS

BRAIN PUNCHING AND WESTERN BLOT FOR NOGO-A

Rationale

We sought to determine whether we could detect the Nogo-A protein by western blot in the different subregions of the hippocampus.

Methods

Animal Subjects

Experiments were approved by the Institutional Animal Care and Use Committee of Hines Veterans Affairs Hospital. Subjects were 2 adult female Long Evans black-hooded rats.

Tissue Preparation

Rats were overdosed with pentobarbital (100 mg/kg, i.p.) and the brain was removed and rinsed in ice-cold saline, and cut into 1 mm coronal sections using a rat brain matrix on ice. The sections were placed on glass slide and the slide was placed on dry ice. A brain punch tissue set (The Vibratome Company, St. Louis, MO, USA), was used to take tissue punches from the subregions of the hippocampus (CA1, CA3 and dentate gyrus). For rat 1 we used a punch with a larger internal diameter than what we used for rat 2, and due to the larger size for rat 1 more white matter was included in the punched area. Tissue samples were placed in eppendorf tubes and placed on dry ice, until they were placed in a -80º C freezer for storage.

Immunoblot

Proteins from tissue homogenates from different subregions of the hippocampus were separated by Sodium Dodecyl Sulphate-Polyacrylamide Gel Electrophoresis (SDS-PAGE) (4-12% gradient gel) and then blotted onto a polyvinylidene difluoride (PVDF) membrane. The membrane was then blocked in 5% non-fat milk in 1x TBS/.05% TWEEN 20 (TBST) for 20 minutes, and then incubated overnight at 4º C with the primary antibody (11C7) at 1:20,000 in 5% non-fat milk in TBST. The membrane was then washed in TBST and then incubated with the secondary antibody (goat anti-Mouse IgG horseradish peroxidase (HRP)-conjugated, Pierce, Rockford, IL, USA) at 1:10,000 in 5% non-fat milk in TBST for 2 hours. Then the blot was treated with SuperSignal West Pico Chemiluminescent Substrate (Pierce) for 30 seconds. The blot was developed with Kodak BioMax light films and Kodak M35A X-OMAT processor.

Results

Nogo-A protein expression was detected in both rats in CA1 and in the dentate gyrus (App B Fig 9). Samples from CA3 were not analyzed. Rat 1 appeared to have a higher expression of Nogo-A in CA1 and the dentate gyrus. This may be due to white matter being included in the samples from rat 1.

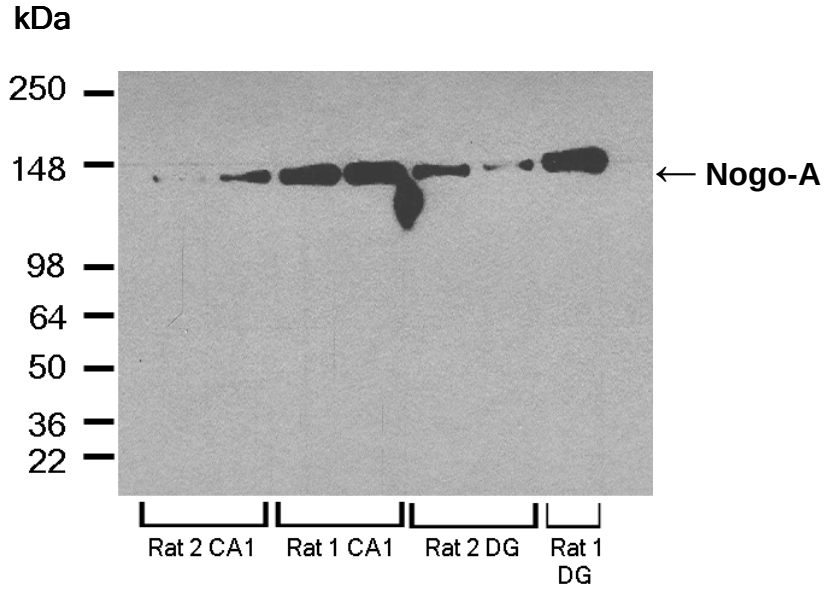

App. B Figure 9. Nogo-A expression in the hippocampus of adult female rats.

Conclusion

Larger punch sizes were used for rat 1, and the tissue was not very well mounted and frozen, thus there may have been white matter and other brain regions included in the punches. For the second rat we were able to improve our technique by using paint brushes to mount the sections before freezing them and by using smaller punch sizes. The lower level of Nogo-A protein expression in rat 2 may reflect lower contamination of the punches by white matter. The lack of degradation products suggests that using cold saline to rinse the brain and freezing the sections to slides with dry ice worked well to prevent protein degradation. Further studies may be able to differentiate differing Nogo-A protein expression in the different subregions of the hippocampus.

REFERENCE LIST

(1999) Recommendations for Standards Regarding Preclinical Neuroprotective and Restorative Drug Development. Stroke 30:2752-2758.

Adams HP, Zoppo GJD, Kummer RV (2006) Rehabilitation after Stroke. In: Management of Stroke: A Practical Guide for the Prevention, Evaluation, and Treatment of Stroke, 3 Edition, pp 315-319. West Islip, NY: Professional Communications.

Aloy EM, Weinmann O, Pot C, Kasper H, Dodd DA, Rülicke T, Rossi F, Schwab ME (2006) Synaptic destabilization by neuronal Nogo-A. Brain Cell Biology 35:137-157.

Andersen M, Zimmer J, Sams-Dodd F (1999) Specific behavioral effects related to age and cerebral ischemia in rats. Pharmacol Biochem Behav 62:673-682.

Atwal JK, Pinkston-Gosse J, Syken J, Stawicki S, Wu Y, Shatz C, Tessier-Lavigne M (2008) PirB is a Functional Receptor for Myelin Inhibitors of Axonal Regeneration. Science 322:967-970.

Badan I, Buchhold B, Hamm A, Gratz M, Walker LC, Platt D, Kessler C, Popa-Wagner A (2003a) Accelerated glial reactivity to stroke in aged rats correlates with reduced functional recovery. J Cereb Blood Flow Metab 23:845-854.

Badan I, Buchhold B, Hamm A, Gratz M, Walker L, Platt D, Kessler C, Popa-Wagner A (2003b) Accelerated glial reactivity to stroke in aged rats correlates with reduced functional recovery. J Cereb Blood Flow Metab 23:845-854.

Bandtlow CE, Schmidt MF, Hassinger TD, Schwab ME, Kater SB (1993) Role of intracellular calcium in NI-35-evoked collapse of neuronal growth cones. Science 259:80-83.

Bandtlow CE, Dlaska M, Pirker S, Czech T, Baumgartner C, Sperk G (2004) Increased expression of Nogo-A in hippocampal neurons of patients with temporal lobe epilepsy. European Journal of Neuroscience 20:195-20

Bareyre FM, Kerschensteiner M, Raineteau O, Mettenleiter TC, Weinmann O, Schwab ME (2004) The injured spinal cord spontaneously forms a new intraspinal circuit in adult rats. Nat Neurosci 7:269-277.

Barth TM, Stanfield BB (1990) The recovery of forelimb-placing behavior in rats with neonatal unilateral cortical damage involves the remaining hemisphere. J Neurosci 10:3449-3459.

Beaud ML, Schmidlin E, Wannier T, Freund P, Bloch J, Mir A, Schwab ME, Rouiller EM (2008) Anti-Nogo-A antibody treatment does not prevent cell body shrinkage in the motor cortex in adult monkeys subjected to unilateral cervical cord lesion. BMC Neurosci 9:5.

Benson MD, Romero MI, Lush ME, Lu QR, Henkemeyer M, Parada LF (2005) Ephrin-B3 is a myelin-based inhibitor of neurite outgrowth. PNAS 102:10694-10699.

Blochlinger S, Weinmann O, Schwab ME, Thallmair M (2001) Neuronal plasticity and formation of new synaptic contacts follow pyramidal lesions and neutralization of Nogo-A: a light and electron microscopic study in the pontine nuclei of adult rats. J Comp Neurol 433:426-436.

Bourne J, Harris KM (2007) Do thin spines learn to be mushroom spines that remember? Curr Opin Neurobiol 17:381-386.

Bourne JN, Harris KM (2008) Balancing Structure and Function at Hippocampal Dendritic Spines. Annu Rev Neurosci 31:47-67.

Bregman BS, Kunkel-Bagden E, Schnell L, Dai HN, Gao D, Schwab ME (1995) Recovery from spinal cord injury mediated by antibodies to neurite growth inhibitors. 378:498-501.

Brenneman M, Wagner S, Cheatwood J, Heldt S, Corwin J, Reep R, Kartje G, Mir A, Schwab M (2008a) Nogo-A inhibition induces recovery from neglect in rats. Behav Brain Res 187:262-272.

Brenneman MM, Wagner SJ, Cheatwood JL, Heldt SA, Corwin JV, Reep RL, Kartje GL, Mir AK, Schwab ME (2008b) Nogo-A inhibition induces recovery from neglect in rats. Behav Brain Res 187:262-272.

Briones T, Suh E, Jozsa L, Woods J (2006) Behaviorally induced synaptogenesis and dendritic growth in the hippocampal region following transient global cerebral ischemia are accompanied by improvement in spatial learning. Exp Neurol 198:530-538.

Broekman M, Comer L, Hyman B, Sena-Esteves M (2006) Adeno-associated virus vectors serotyped with AAV8 capsid are more efficient than AAV-1 or -2 serotypes for widespread gene delivery to the neonatal mouse brain. Neuroscience 138:501-510.

Brosamle C, Halpern ME (2009) Nogo-Nogo receptor signalling in PNS axon outgrowth and pathfinding. Mol Cell Neurosci 40:401-409.

Brosamle C, Huber AB, Fiedler M, Skerra A, Schwab ME (2000) Regeneration of Lesioned Corticospinal Tract Fibers in the Adult Rat Induced by a Recombinant, Humanized IN-1 Antibody Fragment. J Neurosci 20:8061-8068.

Brown AW, Marlowe KJ, Bjelke B (2003) Age effect on motor recovery in a post-acute animal stroke model. Neurobiol Aging 24:607-614.

Brown R, Bardo M, Mace D, Phillips S, Kraemer P (2000) D-amphetamine facilitation of morris water task performance is blocked by eticlopride and correlated with increased dopamine synthesis in the prefrontal cortex. Behav Brain Res 114:135-143.

Budel S, Padukkavidana T, Liu BP, Feng Z, Hu F, Johnson S, Lauren J, Park JH, McGee AW, Liao J, Stillman A, Kim J-E, Yang B-Z, Sodi S, Gelernter J, Zhao H, Hisama F, Arnsten AFT, Strittmatter SM (2008) Genetic Variants of Nogo-66 Receptor with Possible Association to Schizophrenia Block Myelin Inhibition of Axon Growth. J Neurosci 28:13161-13172.

Buss A, Sellhaus B, Wolmsley A, Noth J, Schwab ME, Brook GA (2005) Expression pattern of NOGO-A protein in the human nervous system. Acta Neuropathologica 110:113-119.

Cadelli D, Schwab M (1991a) Regeneration of Lesioned Septohippocampal Acetylcholinesterase-positive Axons is Improved by Antibodies Against the Myelin-associated Neurite Growth Inhibitors NI-35/250. Eur J Neurosci 3:825-832.

Cadelli D, Schwab ME (1991b) Regeneration of Lesioned Septohippocampal Acetylcholinesterase-positive Axons is Improved by Antibodies Against the Myelin-associated Neurite Growth Inhibitors NI-35/250. Eur J Neurosci 3:825-832.

Cafferty WBJ, Strittmatter SM (2006) The Nogo-Nogo Receptor Pathway Limits a Spectrum of Adult CNS Axonal Growth. J Neurosci 26:12242-12250.

Caltharp S, Pira C, Mishima N, Youngdale E, McNeill D, Liwnicz B, Oberg K (2007) NOGO-A induction and localization during chick brain development indicate a role disparate from neurite outgrowth inhibition. BMC Dev Biol 7:32.

Caroni P, Schwab ME (1988a) Antibody against myelin associated inhibitor of neurite growth neutralizes nonpermissive substrate properties of CNS white matter. Neuron 1:85-96.

Caroni P, Schwab M (1988b) Two membrane protein fractions from rat central myelin with inhibitory properties for neurite growth and fibroblast spreading. J Cell Biol 106:1281-1288.

Caroni P, Schwab ME (1988c) Two membrane protein fractions from rat central myelin with inhibitory properties for neurite growth and fibroblast spreading. J Cell Biol 106:1281-1288.

Castanotto D, Rossi J (2009a) The promises and pitfalls of RNA-interference-based therapeutics. Nature 457:426-433.

Castanotto D, Rossi JJ (2009b) The promises and pitfalls of RNA-interference-based therapeutics. Nature 457:426-433.

Cheatwood JL, Emerick AJ, Schwab ME, Kartje GL (2008) Nogo-A Expression After Focal Ischemic Stroke in the Adult Rat. Stroke 39:2091-2098.

Chen LY, Rex CS, Casale MS, Gall CM, Lynch G (2007) Changes in Synaptic Morphology Accompany Actin Signaling during LTP. J Neurosci 27:5363-5372.

Chen M, Huber A, van der Haar M, Frank M, Schnell L, Spillmann A, Christ F, Schwab M (2000a) Nogo-A is a myelin-associated neurite outgrowth inhibitor and an antigen for monoclonal antibody IN-1. Nature 403:434-439.

Chen MS, Huber AB, van der Haar ME, Frank M, Schnell L, Spillmann AA, Christ F, Schwab ME (2000b) Nogo-A is a myelin-associated neurite outgrowth inhibitor and an antigen for monoclonal antibody IN-1. Nature 403:434-439.

Chen S, Hsu C, Hogan E, Maricq H, Balentine J (1986) A model of focal ischemic stroke in the rat: reproducible extensive cortical infarction. Stroke 17:738-743.

Chen W, Gu N, Duan S, Sun Y, Zheng Y, Li C, Pan Y, Xu Y, Feng G, He L (2004) No association between the genetic polymorphisms within RTN4 and schizophrenia in the Chinese population. Neurosci Lett 365:23-27.

Clementz M, Kanjanahaluethai A, O'Brien T, Baker S (2008) Mutation in murine coronavirus replication protein nsp4 alters assembly of double membrane vesicles. Virology 375:118-129.

Cotman CW, Lewis ER, Hand D (1981) The critical afferent theory: a mechanism to account for septohippocampal developmental plasticity. In: Lesion-induced Neuronal Plasticity in Sensorimotor systems (Flohr H, Precht W, eds), pp 13-26. New York: Springer.

Covault J, Lee J, Jensen K, Kranzler H (2004) Nogo 3'-untranslated region CAA insertion: failure to replicate association with schizophrenia and demonstration of marked population difference in frequency of the insertion. Brain Res Mol Brain Res 120:197-200.

Cramer SC (2008) Repairing the human brain after stroke: I. Mechanisms of spontaneous recovery. Ann Neurol 63:272-287.

Craveiro L, Hakkoum D, Weinmann O, Montani L, Stoppini L, Schwab M (2008a) Neutralization of the membrane protein Nogo-A enhances growth and reactive sprouting in established organotypic hippocampal slice cultures. Eur J Neurosci 28:1808-1824.

Craveiro LM, Hakkoum D, Weinmann O, Montani L, Stoppini L, Schwab ME (2008b) Neutralization of the membrane protein Nogo-A enhances growth and reactive sprouting in established organotypic hippocampal slice cultures. Eur J Neurosci 28:1808-1824.

Dahlqvist P, Ronnback A, Bergstrom S, Soderstrom I, Olsson T (2004) Environmental enrichment reverses learning impairment in the Morris water maze after focal cerebral ischemia in rats. Eur J Neurosci 19:2288-2298.

Darian-Smith C, Gilbert CD (1995) Topographic reorganization in the striate cortex of the adult cat and monkey is cortically mediated. J Neurosci 15:1631-1647.

das Nair R, Lincoln N (2007) Cognitive rehabilitation for memory deficits following stroke. In: Cochrane Database of Systematic Reviews: Reviews 2007, 3 Edition. Chichester, UK: John Wiley & Sons, Ltd.

David S, Aguayo AJ (1981) Axonal Elongation into Peripheral Nervous System ``Bridges'' after Central Nervous System Injury in Adult Rats. Science 214:931-933.

Davies SJA, Field PM, Raisman G (1996) Regeneration of Cut Adult Axons Fails Even in the Presence of Continuous Aligned Glial Pathways. Exp Neurol 142:203-216.

Daya S, Berns KI (2008) Gene Therapy Using Adeno-Associated Virus Vectors. Clin Microbiol Rev 21:583-593.

Dergham P, Ellezam B, Essagian C, Avedissian H, Lubell WD, McKerracher L (2002) Rho Signaling Pathway Targeted to Promote Spinal Cord Repair. J Neurosci 22:6570-6577.

D'Hooge R, De Deyn P (2001a) Applications of the Morris water maze in the study of learning and memory. Brain Res Brain Res Rev 36:60-90.

D'Hooge R, De Deyn PP (2001b) Applications of the Morris water maze in the study of learning and memory. Brain Res Brain Res Rev 36:60-90.

Dimou L, Schnell L, Montani L, Duncan C, Simonen M, Schneider R, Liebscher T, Gullo M, Schwab ME (2006) Nogo-A-Deficient Mice Reveal Strain-Dependent Differences in Axonal Regeneration. J Neurosci 26:5591-5603.

Dodd DA, Niederoest B, Bloechlinger S, Dupuis L, Loeffler J-P, Schwab ME (2005) Nogo-A, -B, and -C Are Found on the Cell Surface and Interact Together in Many Different Cell Types. J Biol Chem 280:12494-12502.

Domeniconi M, Cao Z, Spencer T, Sivasankaran R, Wang KC, Nikulina E, Kimura N, Cai H, Deng K, Gao Y (2002) Myelin-Associated Glycoprotein Interacts with the Nogo66 Receptor to Inhibit Neurite Outgrowth. Neuron 35:283-290.

Dupuis L, Gonzalez de Aguil... JL, di Scala F, Rene F, de Tapia M, Pradat PF, Lacomblez L, Seihlan D, Prinjha R, Walsh FS, Meininger V, Loeffler JP (2002) Nogo provides a molecular marker for diagnosis of amyotrophic lateral sclerosis. Neurobiol Dis 10:358-365.

Dupuis L, Pehar M, Cassina P, Rene F, Castellanos R, Rouaux C, Gandelman M, Dimou L, Schwab ME, Loeffler J-P, Barbeito L, Gonzalez de Aguilar J-L (2008) Nogo receptor antagonizes p75NTR-dependent motor neuron death. PNAS 105:740-745.

Elbashir SM, Harborth J, Lendeckel W, Yalcin A, Weber K, Tuschl T (2001) Duplexes of 21-nucleotide RNAs mediate RNA interference in cultured mammalian cells. Nature 411:494-498.

Emerick A, Kartje G (2004) Behavioral recovery and anatomical plasticity in adult rats after cortical lesion and treatment with monoclonal antibody IN-1. Behav Brain Res 152:315-325.

Emerick AJ, Neafsey EJ, Schwab ME, Kartje GL (2003) Functional Reorganization of the Motor Cortex in Adult Rats after Cortical Lesion and Treatment with Monoclonal Antibody IN-1. J Neurosci 23:4826-4830.

Ferretti P, Zhang F, O'Neill P (2003) Changes in spinal cord regenerative ability through phylogenesis and development: lessons to be learnt. Dev Dyn 226:245-256.

Fire A, Xu S, Montgomery MK, Kostas SA, Driver SE, Mello CC (1998) Potent and specific genetic interference by double-stranded RNA in Caenorhabditis elegans. Nature 391:806-811.

Fischer D, He Z, Benowitz LI (2004) Counteracting the Nogo Receptor Enhances Optic Nerve Regeneration If Retinal Ganglion Cells Are in an Active Growth State. J Neurosci 24:1646-1651.

Fouad K, Klusman I, Schwab ME (2004) Regenerating corticospinal fibers in the Marmoset (Callitrix jacchus) after spinal cord lesion and treatment with the anti-Nogo-A antibody IN-1. Eur J Neurosci 20:2479-2482.

Fournier AE, GrandPre T, Strittmatter SM (2001) Identification of a receptor mediating Nogo-66 inhibition of axonal regeneration. 409:341-346.

Fournier AE, Takizawa BT, Strittmatter SM (2003) Rho Kinase Inhibition Enhances Axonal Regeneration in the Injured CNS. J Neurosci 23:1416-1423.

Freund P, Schmidlin E, Wannier T, Bloch J, Mir A, Schwab ME, Rouiller EM (2006) Nogo-A-specific antibody treatment enhances sprouting and functional recovery after cervical lesion in adult primates. Nature Medicine 12:790-792.

Freund P, Wannier T, Schmidlin E, Bloch J, Mir A, Schwab ME, Rouiller EM (2007a) Anti-Nogo-A antibody treatment enhances sprouting of corticospinal axons rostral to a unilateral cervical spinal cord lesion in adult macaque monkey. J Comp Neurol 502:644-659.

Freund P, Wannier T, Schmidlin E, Bloch J, Mir A, Schwab M, Rouiller E (2007b) Anti-Nogo-A antibody treatment enhances sprouting of corticospinal axons rostral to a unilateral cervical spinal cord lesion in adult macaque monkey. J Comp Neurol 502:644-659.

Freund P, Schmidlin E, Wannier T, Bloch J, Mir A, Schwab ME, Rouiller EM (2009) Anti-Nogo-A antibody treatment promotes recovery of manual dexterity after unilateral cervical lesion in adult primates--re-examination and extension of behavioral data. Eur J Neurosci 29:983-996.

Gibb R, Kolb B (1998) A method for vibratome sectioning of Golgi-Cox stained whole rat brain. J Neurosci Methods 79:1-4.

Giger RJ, Venkatesh K, Chivatakarn O, Raiker SJ, Robak L, Hofer T, Lee H, Rader C (2008) Mechanisms of CNS myelin inhibition: evidence for distinct and neuronal cell type specific receptor systems. Restor Neurol Neurosci 26:97-115.

Gil V, Nicolas O, Mingorance A, Urena JM, Tang BL, Hirata T, Saez-Valero J, Ferrer I, Soriano E, del Rio JA (2006a) Nogo-A expression in the human hippocampus in normal aging and in Alzheimer disease. J Neuropathol Exp Neurol 65:433-444.

Gil V, Nicolas O, Mingorance A, Urena J, Tang B, Hirata T, Saez-Valero J, Ferrer I, Soriano E, del Rio J (2006b) Nogo-A expression in the human hippocampus in normal aging and in Alzheimer disease. J Neuropathol Exp Neurol 65:433-444.

Glaser E, Van der Loos H (1981) Analysis of thick brain sections by obverse-reverse computer microscopy: application of a new, high clarity Golgi-Nissl stain. J Neurosci Methods 4:117-125.

Goldman S, Plum F (1997) Compensatory regeneration of the damaged adult human brain: neuroplasticity in a clinical perspective. In: Brain Plasticity, Advances in Neurology (Freund H, Sabel B, Witte O, eds), pp 99-107. Philadelphia: Lippincott-Raven.

Gonzenbach RR, Schwab ME (2008) Disinhibition of neurite growth to repair the injured adult CNS: Focusing on Nogo. Cell Mol Life Sci 65:161-176.

GrandPre T, Li S, Strittmatter SM (2002) Nogo-66 receptor antagonist peptide promotes axonal regeneration. Nature 417:547.

GrandPre T, Nakamura F, Vartanian T, Strittmatter S (2000) Identification of the Nogo inhibitor of axon regeneration as a Reticulon protein. Nature 403:439-444.

Gregorio SP, Mury FB, Ojopi EB, Sallet PC, Moreno DH, Yacubian J, Tavares H, Santos FR, Gattaz WF, Dias-Neto E (2005) Nogo CAA 3'UTR Insertion polymorphism is not associated with Schizophrenia nor with bipolar disorder. Schizophr Res 75:5-9.

Grotta JC, Jacobs TP, Koroshetz WJ, Moskowitz MA (2008) Stroke Program Review Group: An Interim Report. Stroke 39:1364-1370.

Hacke W, Kaste M, Bluhmki E, Brozman M, Davalos A, Guidetti D, Larrue V, Lees KR, Medeghri Z, Machnig T, Schneider D, von Kummer R, Wahlgren N, Toni D, the ECASS Investigators (2008) Thrombolysis with Alteplase 3 to 4.5 Hours after Acute Ischemic Stroke. N Engl J Med 359:1317-1329.

Haines L, O'Brien T (2004) Kurtosis and curvature measures for nonlinear regression models. Statistica Sinica 14:547-570.

Hankey GJ, Spiesser J, Hakimi Z, Bego G, Carita P, Gabriel S (2007) Rate, degree, and predictors of recovery from disability following ischemic stroke. Neurology 68:1583-1587.

Harding T, Dickinson P, Roberts B, Yendluri S, Gonzalez-Edick M, Lecouteur R, Jooss K (2006) Enhanced gene transfer efficiency in the murine striatum and an orthotopic glioblastoma tumor model, using AAV-7- and AAV-8-pseudotyped vectors. Hum Gene Ther 17:807-820.

Hasegawa Y, Fujitani M, Hata K, Tohyama M, Yamagishi S, Yamashita T (2004) Promotion of Axon Regeneration by Myelin-Associated Glycoprotein and Nogo through Divergent Signals Downstream of Gi/G. J Neurosci 24:6826-6832.

He W, Lu Y, Qahwash I, Hu XY, Chang A, Yan R (2004) Reticulon family members modulate BACE1 activity and amyloid-beta peptide generation. Nat Med 10:959-965.

He W, Hu X, Shi Q, Zhou X, Lu Y, Fisher C, Yan R (2006) Mapping of interaction domains mediating binding between BACE1 and RTN/Nogo proteins. J Mol Biol 363:625-634.

Hornung V, Guenthner-Biller M, Bourquin C, Ablasser A, Schlee M, Uematsu S, Noronha A, Manoharan M, Akira S, de Fougerolles A, Endres S, Hartmann G (2005) Sequence-specific potent induction of IFN-alpha by short interfering RNA in plasmacytoid dendritic cells through TLR7. Nat Med 11:263-270.

Hsieh SH-K, Ferraro GB, Fournier AE (2006) Myelin-Associated Inhibitors Regulate Cofilin Phosphorylation and Neuronal Inhibition through LIM Kinase and Slingshot Phosphatase. J Neurosci 26:1006-1015.

Hsu R, Woodroffe A, Lai WS, Cook MN, Mukai J, Dunning JP, Swanson DJ, Roos JL, Abecasis GR, Karayiorgou M, Gogos JA (2007) Nogo Receptor 1 (RTN4R) as a candidate gene for schizophrenia: analysis using human and mouse genetic approaches. PLoS ONE 2:e1234.

Hu F, Strittmatter SM (2008) The N-Terminal Domain of Nogo-A Inhibits Cell Adhesion and Axonal Outgrowth by an Integrin-Specific Mechanism. J Neurosci 28:1262-1269.

Huber AB, Weinmann O, Brosamle C, Oertle T, Schwab ME (2002) Patterns of Nogo mRNA and Protein Expression in the Developing and Adult Rat and After CNS Lesions. J Neurosci 22:3553-3567.

Hunt D, Coffin RS, Prinjha RK, Campbell G, Anderson PN (2003) Nogo-A expression in the intact and injured nervous system. Molecular and Cellular Neuroscience 24:1083-1102.

Ji B, Li M, Wu W-T, Yick L-W, Lee X, Shao Z, Wang J, So K-F, McCoy JM, Blake Pepinsky R, Mi S, Relton JK (2006) LINGO-1 antagonist promotes functional recovery and axonal sprouting after spinal cord injury. Molecular and Cellular Neuroscience 33:311-320.

Jin W, Liu Y, Liu H, Yang H, Wang Y, Jiao X, Ju G (2003a) Intraneuronal localization of Nogo-A in the rat. J Comp Neurol 458:1-10.

Jin WL, Liu YY, Liu HL, Yang H, Wang Y, Jiao XY, Ju G (2003b) Intraneuronal localization of Nogo-A in the rat. J Comp Neurol 458:1-10.

Jokic N, Gonzalez de Aguil... JL, Dimou L, Lin S, Fergani A, Ruegg MA, Schwab ME, Dupuis L, Loeffler JP (2006) The neurite outgrowth inhibitor Nogo-A promotes denervation in an amyotrophic lateral sclerosis model. EMBO Rep 7:1162-1167.

Jokic N, Gonzalez de Aguil... JL, Pradat PF, Dupuis L, Echaniz-Laguna A, Muller A, Dubourg O, Seilhean D, Hauw JJ, Loeffler JP, Meininger V (2005) Nogo expression in muscle correlates with amyotrophic lateral sclerosis severity. Ann Neurol 57:553-556.

Josephson A, Widenfalk J, Widmer HW, Olson L, Spenger C (2001) NOGO mRNA expression in adult and fetal human and rat nervous tissue and in weight drop injury. Exp Neurol 169:319-328.

Jurewicz A, Matysiak M, Raine CS, Selmaj K (2007) Soluble Nogo-A, an inhibitor of axonal regeneration, as a biomarker for multiple sclerosis. Neurology 68:283-287.

Kallai J, Makany T, Karadi K, Jacobs WJ (2005) Spatial orientation strategies in Morris-type virtual water task for humans. Behav Brain Res 159:187-196.

Kallai J, Makany T, Csatho A, Karadi K, Horvath D, Kovacs-Labadi B, Jarai R, Nadel L, Jacobs JW (2007) Cognitive and affective aspects of thigmotaxis strategy in humans. Behav Neurosci 121:21-30.

Karnezis T, Mandemakers W, McQualter JL, Zheng B, Ho PP, Jordan KA, Murray BM, Barres B, Tessier-Lavigne M, Bernard CCA (2004) The neurite outgrowth inhibitor Nogo A is involved in autoimmune-mediated demyelination. 7:736-744.

Kartje G, Schulz M, Lopez-Yunez A, Schnell L, Schwab M (1999) Corticostriatal plasticity is restricted by myelin-associated neurite growth inhibitors in the adult rat. Ann Neurol 45:778-786.

Kartje-Tillotson G, O'Donoghue DL, Dauzvardis MF, Castro AJ (1987) Pyramidotomy abolishes the abnormal movements evoked by intracortical microstimulation in adult rats that sustained neonatal cortical lesions. Brain Res 415:172-177.

Kelly-Hayes M, Beiser A, Kase CS, Scaramucci A, D'Agostino RB, Wolf PA (2003) The influence of gender and age on disability following ischemic stroke: the Framingham study. Journal of Stroke and Cerebrovascular Diseases 12:119-126.

Kennard MA (1936) Age and other factors in motor recovery from precentral lesions in monkeys. Am J Physiol -- Legacy Content 115:138-146.

Kennard MA (1938) Reorganization of motor function in the cerebral cortex of monkeys deprived of motor and premotor areas in infancy. J Neurophysiol 1:477-496.

Kim J-E, Liu BP, Park JH, Strittmatter SM (2004) Nogo-66 Receptor Prevents Raphespinal and Rubrospinal Axon Regeneration and Limits Functional Recovery from Spinal Cord Injury. Neuron 44:439-451.

Kim J-E, Li S, GrandPré T, Qiu D, Strittmatter SM (2003) Axon Regeneration in Young Adult Mice Lacking Nogo-A/B. Neuron 38:187-199.

Klein R, Dayton R, Tatom J, Henderson K, Henning P (2008) AAV8, 9, Rh10, Rh43 vector gene transfer in the rat brain: effects of serotype, promoter and purification method. Mol Ther 16:89-96.

Klein R, Dayton R, Leidenheimer N, Jansen K, Golde T, Zweig R (2006a) Efficient neuronal gene transfer with AAV8 leads to neurotoxic levels of tau or green fluorescent proteins. Mol Ther 13:517-527.

Klein RL, Dayton RD, Leidenheimer NJ, Jansen K, Golde TE, Zweig RM (2006b) Efficient neuronal gene transfer with AAV8 leads to neurotoxic levels of tau or green fluorescent proteins. Mol Ther 13:517-527.

Knierim JJ (2006) Neural representations of location outside the hippocampus. Learn Mem 13:405-415.

Kolb B, Whishaw IQ (1989) Plasticity in the neocortex: mechanisms underlying recovery from early brain damage. Prog Neurobiol 32:235-276.

Koprivica V, Cho K-S, Park JB, Yiu G, Atwal J, Gore B, Kim JA, Lin E, Tessier-Lavigne M, Chen DF, He Z (2005) EGFR Activation Mediates Inhibition of Axon Regeneration by Myelin and Chondroitin Sulfate Proteoglycans. Science 310:106-110.

Lavebratt C, Trifunovski A, Persson AS, Wang FH, Klason T, Ohman I, Josephsson A, Olson L, Spenger C, Schalling M (2006) Carbamazepine protects against megencephaly and abnormal expression of BDNF and Nogo signaling components in the mceph/mceph mouse. Neurobiol Dis 24:374-383.

Lee H, Raiker SJ, Venkatesh K, Geary R, Robak LA, Zhang Y, Yeh HH, Shrager P, Giger RJ (2008) Synaptic Function for the Nogo-66 Receptor NgR1: Regulation of Dendritic Spine Morphology and Activity-Dependent Synaptic Strength. J Neurosci 28:2753-2765.

Lee J-K, Kim J-E, Sivula M, Strittmatter SM (2004) Nogo Receptor Antagonism Promotes Stroke Recovery by Enhancing Axonal Plasticity. J Neurosci 24:6209-6217.

Lehmann M, Fournier A, Selles-Navarro I, Dergham P, Sebok A, Leclerc N, Tigyi G, McKerracher L (1999) Inactivation of Rho Signaling Pathway Promotes CNS Axon Regeneration. J Neurosci 19:7537-7547.

Lenzlinger P, Shimizu S, Marklund N, Thompson H, Schwab M, Saatman K, Hoover R, Bareyre F, Motta M, Luginbuhl A, Pape R, Clouse A, Morganti-Kossmann C, McIntosh T (2005a) Delayed inhibition of Nogo-A does not alter injury-induced axonal sprouting but enhances recovery of cognitive function following experimental traumatic brain injury in rats. Neuroscience 134:1047-1056.

Lenzlinger PM, Shimizu S, Marklund N, Thompson HJ, Schwab ME, Saatman KE, Hoover RC, Bareyre FM, Motta M, Luginbuhl A, Pape R, Clouse AK, Morganti-Kossmann C, McIntosh TK (2005b) Delayed inhibition of Nogo-A does not alter injury-induced axonal sprouting but enhances recovery of cognitive function following experimental traumatic brain injury in rats. Neuroscience 134:1047-1056.

Li S, Strittmatter SM (2003) Delayed Systemic Nogo-66 Receptor Antagonist Promotes Recovery from Spinal Cord Injury. J Neurosci 23:4219-4227.

Li S, Carmichael ST (2006) Growth-associated gene and protein expression in the region of axonal sprouting in the aged brain after stroke. Neurobiology of Disease 23:362-373.

Li S, Zheng J, Carmichael ST (2005a) Increased oxidative protein and DNA damage but decreased stress response in the aged brain following experimental stroke. Neurobiology of Disease 18:432-440.

Li S, Kim J-E, Budel S, Hampton TG, Strittmatter SM (2005b) Transgenic inhibition of Nogo-66 receptor function allows axonal sprouting and improved locomotion after spinal injury. Molecular and Cellular Neuroscience 29:26-39.

Li S, Liu BP, Budel S, Li M, Ji B, Walus L, Li W, Jirik A, Rabacchi S, Choi E, Worley D, Sah DWY, Pepinsky B, Lee D, Relton J, Strittmatter SM (2004) Blockade of Nogo-66, Myelin-Associated Glycoprotein, and Oligodendrocyte Myelin Glycoprotein by Soluble Nogo-66 Receptor Promotes Axonal Sprouting and Recovery after Spinal Injury. J Neurosci 24:10511-10520.

Liebscher T, Schnell L, Schnell D, Scholl J, Schneider R, Gullo M, Fouad K, Mir A, Rausch M, Kindler D, Hamers FPT, Schwab ME (2005) Nogo-A antibody improves regeneration and locomotion of spinal cord-injured rats. Ann Neurol 58:706-719.

Lindner M (1997) Reliability, distribution, and validity of age-related cognitive deficits in the Morris water maze. Neurobiol Learn Mem 68:203-220.

Lindsey JW, Crawford MP, Hatfield LM (2008) Soluble Nogo-A in CSF is not a useful biomarker for multiple sclerosis. Neurology 71:35-37.

Liu H, Abecasis GaR, Heath SC, Knowles A, Demars S, Chen Y-J, Roos JL, Rapoport JL, Gogos JA, Karayiorgou M (2002) Genetic variation in the 22q11 locus and susceptibility to schizophrenia. Proc Natl Acad Sci U S A 99:16859-16864.

Liu Y-Y, Jin W-L, Liu H-L, Ju G (2003) Electron microscopic localization of Nogo-A at the postsynaptic active zone of the rat. Neuroscience Letters 346:153-156.

Lloyd-Jones D, et al. (2009) Heart Disease and Stroke Statistics--2009 Update: A Report From the American Heart Association Statistics Committee and Stroke Statistics Subcommittee. Circulation 119:e21-181.

Marklund N, Bareyre FM, Royo NC, Thompson HJ, Mir AK, Grady MS, Schwab ME, McIntosh TK (2007a) Cognitive outcome following brain injury and treatment with an inhibitor of Nogo-A in association with an attenuated downregulation of hippocampal growth-associated protein-43 expression. J Neurosurg 107:844-853.

Marklund N, Bareyre F, Royo N, Thompson H, Mir A, Grady M, Schwab M, McIntosh T (2007b) Cognitive outcome following brain injury and treatment with an inhibitor of Nogo-A in association with an attenuated downregulation of hippocampal growth-associated protein-43 expression. J Neurosurg 107:844-853.

Markus T, Tsai S, Bollnow M, Farrer R, O'Brien T, Kindler-Baumann D, Rausch M, Rudin M, Wiessner C, Mir A, Schwab M, Kartje G (2005a) Recovery and brain reorganization after stroke in adult and aged rats. Ann Neurol 58:950-953.

Markus TM, Tsai S, Bollnow MR, Farrer RG, O'Brien TE, Kindler-Baumann DR, Rausch M, Rudin M, Wiessner C, Mir AK, Schwab ME, Kartje GL (2005b)

Recovery and brain reorganization after stroke in adult and aged rats. Ann Neurol 58:950-953.

McCaffrey AP, Meuse L, Pham TT, Conklin DS, Hannon GJ, Kay MA (2002) RNA interference in adult mice. Nature 418:38-39.

McGee AW, Yang Y, Fischer QS, Daw NW, Strittmatter SM (2005) Experience-Driven Plasticity of Visual Cortex Limited by Myelin and Nogo Receptor. Science 309:2222-2226.

McKerracher L, David S, Jackson DL, Kottis V, Dunn RJ, Braun P (1994) Identification of myelin-associated glycoprotein as a major myelin-derived inhibitor of neurite growth. Neuron 13:805-811.

Meier S, Brauer AU, Heimrich B, Schwab ME, Nitsch R, Savaskan NE (2003) Molecular analysis of Nogo expression in the hippocampus during development and following lesion and seizure. FASEB J:02-0453fje.

Meng Y, Zhang Y, Tregoubov V, Janus C, Cruz L, Jackson M, Lu WY, MacDonald JF, Wang JY, Falls DL, Jia Z (2002) Abnormal spine morphology and enhanced LTP in LIMK-1 knockout mice. Neuron 35:121-133.

Merkler D, Metz GAS, Raineteau O, Dietz V, Schwab ME, Fouad K (2001) Locomotor Recovery in Spinal Cord-Injured Rats Treated with an Antibody Neutralizing the Myelin-Associated Neurite Growth Inhibitor Nogo-A. J Neurosci 21:3665-3673.

Mi S, Lee X, Shao Z, Thill G, Ji B, Relton J, Levesque M, Allaire N, Perrin S, Sands B, Crowell T, Cate RL, McCoy JM, Pepinsky RB (2004) LINGO-1 is a component of the Nogo-66 receptor/p75 signaling complex. Nat Neurosci 7:221-228.

Mingorance A, Fontana X, Sole M, Burgaya F, Urena JM, Teng FY, Tang BL, Hunt D, Anderson PN, Bethea JR, Schwab ME, Soriano E, del Rio JA (2004a) Regulation of Nogo and Nogo receptor during the development of the entorhino-hippocampal pathway and after adult hippocampal lesions. Mol Cell Neurosci 26:34-49.

Mingorance A, Fontana X, Sole M, Burgaya F, Urena J, Teng F, Tang B, Hunt D, Anderson P, Bethea J, Schwab M, Soriano E, del Rio J (2004b) Regulation of Nogo and Nogo receptor during the development of the entorhino-hippocampal pathway and after adult hippocampal lesions. Mol Cell Neurosci 26:34-49.

Mingorance-Le Meur A, Zheng B, Soriano E, del Rio JA (2007) Involvement of the Myelin-Associated Inhibitor Nogo-A in Early Cortical Development and Neuronal Maturation. Cereb Cortex 17:2375-2386.

Montani L, Gerrits B, Gehrig P, Dimou L, Wollscheid B, Schwab ME (2009) Neuronal Nogo-A modulates growth cone motility via RhoGTP/LIMK1/cofilin in the unlesioned adult nervous system. J Biol Chem:M808297200.

Moreau-Fauvarque C, Kumanogoh A, Camand E, Jaillard C, Barbin G, Boquet I, Love C, Jones EY, Kikutani H, Lubetzki C, Dusart I, Chedotal A (2003) The Transmembrane Semaphorin Sema4D/CD100, an Inhibitor of Axonal Growth, Is Expressed on Oligodendrocytes and Upregulated after CNS Lesion. J Neurosci 23:9229-9239.

Morris RGM (1981) Spatial localization does not require the presence of local cues. Learn Motiv 12:239-260.

Mukhopadhyay G, Doherty P, Walsh FS, Crocker PR, Filbin MT (1994) A novel role for myelin-associated glycoprotein as an inhibitor of axonal regeneration. Neuron 13:757-767.

Niederost B, Oertle T, Fritsche J, McKinney RA, Bandtlow CE (2002) Nogo-A and Myelin-Associated Glycoprotein Mediate Neurite Growth Inhibition by Antagonistic Regulation of RhoA and Rac1. J Neurosci 22:10368-10376.

Niederost BP, Zimmermann DR, Schwab ME, Bandtlow CE (1999) Bovine CNS Myelin Contains Neurite Growth-Inhibitory Activity Associated with Chondroitin Sulfate Proteoglycans. J Neurosci 19:8979-8989.

Novak G, Tallerico T (2006) Nogo A, B and C expression in schizophrenia, depression and bipolar frontal cortex, and correlation of Nogo expression with CAA/TATC polymorphism in 3'-UTR. Brain Res 1120:161-171.

Novak G, Kim D, Seeman P, Tallerico T (2002) Schizophrenia and Nogo: elevated mRNA in cortex, and high prevalence of a homozygous CAA insert. Brain Res Mol Brain Res 107:183-189.

Oertle T, van der Haar ME, Bandtlow CE, Robeva A, Burfeind P, Buss A, Huber AB, Simonen M, Schnell L, Brosamle C, Kaupmann K, Vallon R, Schwab ME (2003) Nogo-A Inhibits Neurite Outgrowth and Cell Spreading with Three Discrete Regions. J Neurosci 23:5393-5406.

Okada M, Nakanishi H, Tamura A, Urae A, Mine K, Yamamoto K, Fujiwara M (1995) Long-term spatial cognitive impairment after middle cerebral artery occlusion in rats: no involvement of the hippocampus. J Cereb Blood Flow Metab 15:1012-1021.

Onoue H, Satoh J-I, Ogawa M, Tabunoki H, Yamamura T (2007) Detection of anti-Nogo receptor autoantibody in the serum of multiple sclerosis and controls. Acta Neurol Scand 115:153-160.

Papadopoulos C, Tsai S, Alsbiei T, O'Brien T, Schwab M, Kartje G (2002a) Functional recovery and neuroanatomical plasticity following middle cerebral artery occlusion and IN-1 antibody treatment in the adult rat. Ann Neurol 51:433-441.

Papadopoulos CM, Tsai S, Alsbiei T, O'Brien TE, Schwab ME, Kartje GL (2002b) Functional recovery and neuroanatomical plasticity following middle cerebral artery occlusion and IN-1 antibody treatment in the adult rat. Ann Neurol 51:433-441.

Papadopoulos CM, Tsai S-Y, Cheatwood JL, Bollnow MR, Kolb BE, Schwab ME, Kartje GL (2006) Dendritic Plasticity in the Adult Rat Following Middle Cerebral Artery Occlusion and Nogo-A Neutralization. Cereb Cortex 16:529-536.

Park JB, Yiu G, Kaneko S, Wang J, Chang J, He XL, Garcia KC, He Z (2005) A TNF receptor family member, TROY, is a coreceptor with Nogo receptor in mediating the inhibitory activity of myelin inhibitors. Neuron 45:345-351.

Park JH, Strittmatter SM (2007) Nogo receptor interacts with brain APP and Abeta to reduce pathologic changes in Alzheimer's transgenic mice. Curr Alzheimer Res 4:568-570.

Park JH, Widi GA, Gimbel DA, Harel NY, Lee DHS, Strittmatter SM (2006a) Subcutaneous Nogo Receptor Removes Brain Amyloid-{beta} and Improves Spatial Memory in Alzheimer's Transgenic Mice. J Neurosci 26:13279-13286.

Park JH, Gimbel DA, GrandPre T, Lee J-K, Kim J-E, Li W, Lee DHS, Strittmatter SM (2006b) Alzheimer Precursor Protein Interaction with the Nogo-66 Receptor Reduces Amyloid-beta Plaque Deposition. J Neurosci 26:1386-1395.

Paxinos GW, Charles (2005) The Rat Brain in Stereotaxic Coordinates, 5th Edition: Academic Press.

Pernet V, Joly S, Christ F, Dimou L, Schwab ME (2008) Nogo-A and Myelin-Associated Glycoprotein Differently Regulate Oligodendrocyte Maturation and Myelin Formation. J Neurosci 28:7435-7444.

Pleis J, Lethbridge-Çejku M (2007) Summary health statistics for U.S. Adults: National Health Interview Survey, 2006. National Center for Health Statistics. Vital Health Stat 10.

Pool M, Niino M, Rambaldi I, Robson K, Bar-Or A, Fournier AE (2009) Myelin regulates immune cell adhesion and motility. Exp Neurol In Press, Uncorrected Proof.

Popa-Wagner A, Carmichael S, Kokaia Z, Kessler C, Walker L (2007a) The response of the aged brain to stroke: too much, too soon? Curr Neurovasc Res 4:216-227.

Popa-Wagner A, Carmichael ST, Kokaia Z, Kessler C, Walker LC (2007b) The response of the aged brain to stroke: too much, too soon? Curr Neurovasc Res 4:216-227.

Popa-Wagner A, Badan I, Walker L, Groppa S, Patrana N, Kessler C (2007c) Accelerated infarct development, cytogenesis and apoptosis following transient cerebral ischemia in aged rats. Acta Neuropathol 113:277-293.

Pradat PF, Bruneteau G, Gonzalez de Aguil... JL, Dupuis L, Jokic N, Salachas F, Le Forestier N, Echaniz-Laguna A, Dubourg O, Hauw JJ, Tranchant C, Loeffler JP, Meininger V (2007) Muscle Nogo-A expression is a prognostic marker in lower motor neuron syndromes. Ann Neurol 62:15-20.

Pradhan AD (2007) Role of neuronal Nogo-A in postnatal dendritic spine morphogenesis. Loyola University Chicago dissertation.

Prinjha R, Moore SE, Vinson M, Blake S, Morrow R, Christie G, Michalovich D, Simmons DL, Walsh FS (2000) Neurobiology: Inhibitor of neurite outgrowth in humans. Nature 403:383-384.

Raineteau O, Fouad K, Noth P, Thallmair M, Schwab ME (2001) Functional switch between motor tracts in the presence of the mAb IN-1 in the adult rat. Proc Natl Acad Sci U S A 98:6929-6934.

Reep RL, Corwin JV (2009) Posterior parietal cortex as part of a neural network for directed attention in rats. Neurobiol Learn Mem 91:104-113.

Reindl M, Khantane S, Ehling R, Schanda K, Lutterotti A, Brinkhoff C, Oertle T, Schwab ME, Deisenhammer F, Berger T, Bandtlow CE (2003) Serum and cerebrospinal fluid antibodies to Nogo-A in patients with multiple sclerosis and acute neurological disorders. J Neuroimmunol 145:139-147.

Reitz C, Luchsinger JA, Tang M-X, Manly J, Mayeux R (2006) Stroke and Memory Performance in Elderly Persons Without Dementia. Arch Neurol 63:571-576.

Richard M, Giannetti N, Saucier D, Sacquet J, Jourdan F, Pellier-Monnin V (2005) Neuronal expression of Nogo-A mRNA and protein during neurite outgrowth in the developing rat olfactory system. Eur J Neurosci 22:2145-2158.

Rosen CL, Dinapoli VA, Nagamine T, Crocco T (2005) Influence of age on stroke outcome following transient focal ischemia. J Neurosurg 103:687-694.

Satoh J, Onoue H, Arima K, Yamamura T (2005) Nogo-A and nogo receptor expression in demyelinating lesions of multiple sclerosis. J Neuropathol Exp Neurol 64:129-138.

Saucier D, Cain D (1995) Spatial learning without NMDA receptor-dependent long-term potentiation. Nature 378:186-189.

Schaechter JD, Moore CI, Connell BD, Rosen BR, Dijkhuizen RM (2006) Structural and functional plasticity in the somatosensory cortex of chronic stroke patients. Brain 129:2722-2733.

Schmalfeldt M, Bandtlow CE, Dours-Zimmermann MT, Winterhalter KH, Zimmermann DR (2000) Brain derived versican V2 is a potent inhibitor of axonal growth. J Cell Sci 113:807-816.

Schneider GE (1979) Is it really better to have your brain lesion early? A revision of the "Kennard principle". Neuropsychologia 17:557-583.

Schnell L, Schwab ME (1990) Axonal regeneration in the rat spinal cord produced by an antibody against myelin-associated neurite growth inhibitors. Nature 343:269.

Schnell L, Schwab ME (1993) Sprouting and Regeneration of Lesioned Corticospinal Tract Fibres in the Adult Rat Spinal Cord. Eur J Neurosci 5:1156-1171.

Schnell SA, Staines WA, Wessendorf MW (1999) Reduction of Lipofuscin-like Autofluorescence in Fluorescently Labeled Tissue. J Histochem Cytochem 47:719-730.

Schratt GM, Tuebing F, Nigh EA, Kane CG, Sabatini ME, Kiebler M, Greenberg ME (2006) A brain-specific microRNA regulates dendritic spine development. Nature 439:283-289.

Schulz MK, Schnell L, Castro AJ, Schwab ME, Kartje GL (1998) Cholinergic innervation of fetal neocortical transplants is increased after neutralization of myelin-associated neurite growth inhibitors. Exp Neurol 149:390-397.

Schwab ME, Thoenen H (1985) Dissociated neurons regenerate into sciatic but not optic nerve explants in culture irrespective of neurotrophic factors. J Neurosci 5:2415-2423.

Schwab ME, Caroni P (1988) Oligodendrocytes and CNS myelin are nonpermissive substrates for neurite growth and fibroblast spreading in vitro. J Neurosci 8:2381-2393.

Schweigreiter R, Walmsley AR, Niederost B, Zimmermann DR, Oertle T, Casademunt E, Frentzel S, Dechant G, Mir A, Bandtlow CE (2004) Versican V2 and the central inhibitory domain of Nogo-A inhibit neurite growth via p75NTR/NgR-independent pathways that converge at RhoA. Molecular and Cellular Neuroscience 27:163-174.

Seymour A, Andrews E, Tsai S, Markus T, Bollnow M, Brenneman M, O'Brien T, Castro A, Schwab M, Kartje G (2005a) Delayed treatment with monoclonal antibody IN-1 1 week after stroke results in recovery of function and corticorubral plasticity in adult rats. J Cereb Blood Flow Metab 25:1366-1375.

Seymour AB, Andrews EM, Tsai S, Markus TM, Bollnow MR, Brenneman MM, O'Brien TE, Castro AJ, Schwab ME, Kartje GL (2005b) Delayed treatment with monoclonal antibody IN-1 1 week after stroke results in recovery of function and corticorubral plasticity in adult rats. J Cereb Blood Flow Metab 25:1366-1375.

Simonen M, Pedersen V, Weinmann O, Schnell L, Buss A, Ledermann B, Christ F, Sansig G, van der Putten H, Schwab ME (2003) Systemic Deletion of the Myelin-Associated Outgrowth Inhibitor Nogo-A Improves Regenerative and Plastic Responses after Spinal Cord Injury. Neuron 38:201-211.

Sinibaldi L, De Luca A, Bellacchio E, Conti E, Pasini A, Paloscia C, Spalletta G, Caltagirone C, Pizzuti A, Dallapiccola B (2004) Mutations of the Nogo-66 receptor (RTN4R) gene in schizophrenia. Hum Mutat 24:534-535.

Sivasankaran R, Jiong Pei R, Wang KC, Yi Ping Zhang KC, Shields CB, Xu X-M, He Z (2004) PKC mediates inhibitory effects of myelin and chondroitin sulfate proteoglycans on axonal regeneration. Nat Neurosci 7:261-268.

Spillmann AA, Bandtlow CE, Lottspeich F, Keller F, Schwab ME (1998) Identification and Characterization of a Bovine Neurite Growth Inhibitor (bNI-220). J Biol Chem 273:19283-19293.

Spruston N, McBain C (2006) Structural and Functional Properties of Hippocampal Neurons. In: The Hippocampus Book, 1 Edition (Andersen P, Morris R, Amaral D, Bliss T, O'Keefe J, eds), pp 133-202. New York: Oxford University Press.

Tada T, Sheng M (2006) Molecular mechanisms of dendritic spine morphogenesis. Curr Opin Neurobiol 16:95-101.

Takeda Y, Kamida T, Fujiki M, Kobayashi H (2007) Hippocampal Nogo-A and neo-Timm's staining in amygdala kindling rats. Neurol Res 29:199-203.

Tan EC, Chong SA, Wang H, Chew-Ping Lim E, Teo YY (2005) Gender-specific association of insertion/deletion polymorphisms in the nogo gene and chronic schizophrenia. Brain Res Mol Brain Res 139:212-216.

Tarulli AW (2007) Other causes of stroke. In: The Stroke Book (Torbey MT, Selim MH, eds), pp 71-91. New York: Cambridge University Press.

Tashiro A, Yuste R (2008) Role of Rho GTPases in the morphogenesis and motility of dendritic spines. Methods Enzymol 439:285-302.

Tatagiba M, Rosahl S, Gharabaghi A, Blomer U, Brandis A, Skerra A, Samii M, Schwab ME (2002) Regeneration of auditory nerve following complete sectioning and intrathecal application of the IN-1 antibody. Acta Neurochir (Wien) 144:181-187.

Teng FY, Tang BL (2008) Nogo-A and Nogo-66 receptor in amyotrophic lateral sclerosis. J Cell Mol Med 12:1199-1204.

Thallmair M, Metz GA, Z'Graggen WJ, Raineteau O, Kartje GL, Schwab ME (1998) Neurite growth inhibitors restrict plasticity and functional recovery following corticospinal tract lesions. Nat Neurosci 1:124-131.

Tsai S-Y, Markus T, Andrews E, Cheatwood J, Emerick A, Mir A, Schwab M, Kartje G (2007) Intrathecal treatment with anti-Nogo-A antibody improves functional recovery in adult rats after stroke. Experimental Brain Research 182:261-266.

Voeltz GK, Prinz WA, Shibata Y, Rist JM, Rapoport TA (2006) A Class of Membrane Proteins Shaping the Tubular Endoplasmic Reticulum. Cell 124:573-586.

Wallace DG, Martin MM, Winter SS (2008) Fractionating dead reckoning: role of the compass, odometer, logbook, and home base establishment in spatial orientation. Naturwissenschaften 95:1011-1026.

Wallace DG, Hines DJ, Pellis SM, Whishaw IQ (2002) Vestibular Information Is Required for Dead Reckoning in the Rat. J Neurosci 22:10009-10017.

Wang KC, Kim JA, Sivasankaran R, Segal R, He Z (2002a) P75 interacts with the Nogo receptor as a co-receptor for Nogo, MAG and OMgp. Nature 420:74-78.

Wang KC, Koprivica V, Kim JA, Sivasankaran R, Guo Y, Neve RL, He Z (2002b) Oligodendrocyte-myelin glycoprotein is a Nogo receptor ligand that inhibits neurite outgrowth. Nature 417:941-944.

Wang X, Chun S-J, Treloar H, Vartanian T, Greer CA, Strittmatter SM (2002c) Localization of Nogo-A and Nogo-66 Receptor Proteins at Sites of Axon-Myelin and Synaptic Contact. J Neurosci 22:5505-5515.

Wannier-Morino P, Schmidlin E, Freund P, Belhaj-Saif A, Bloch J, Mir A, Schwab ME, Rouiller EM, Wannier T (2008) Fate of rubrospinal neurons after unilateral section of the cervical spinal cord in adult macaque monkeys: effects of an antibody treatment neutralizing Nogo-A. Brain Res 1217:96-109.

Webb DJ, Zhang H, Majumdar D, Horwitz AF (2007) {alpha}5 Integrin Signaling Regulates the Formation of Spines and Synapses in Hippocampal Neurons. J Biol Chem 282:6929-6935.

Weibel D, Cadelli D, Schwab ME (1994) Regeneration of lesioned rat optic nerve fibers is improved after neutralization of myelin-associated neurite growth inhibitors. Brain Res 642:259-266.

Weinmann O, Schnell L, Ghosh A, Montani L, Wiessner C, Wannier T, Rouiller E, Mir A, Schwab ME (2006) Intrathecally infused antibodies against Nogo-A penetrate the CNS and downregulate the endogenous neurite growth inhibitor Nogo-A. Molecular and Cellular Neuroscience 32:161-173.

Wenk C, Thallmair M, Kartje G, Schwab M (1999) Increased corticofugal plasticity after unilateral cortical lesions combined with neutralization of the IN-1 antigen in adult rats. J Comp Neurol 410:143-157.

Whishaw IQ (1998) Place learning in hippocampal rats and the path integration hypothesis. Neurosci Biobehav Rev 22:209-220.

Wiessner C, Bareyre F, Allegrini P, Mir A, Frentzel S, Zurini M, Schnell L, Oertle T, Schwab M (2003a) Anti-Nogo-A antibody infusion 24 hours after experimental stroke improved behavioral outcome and corticospinal plasticity in normotensive and spontaneously hypertensive rats. J Cereb Blood Flow Metab 23:154-165.

Wiessner C, Bareyre FM, Allegrini PR, Mir AK, Frentzel S, Zurini M, Schnell L, Oertle T, Schwab ME (2003b) Anti-Nogo-A antibody infusion 24 hours after experimental stroke improved behavioral outcome and corticospinal plasticity in normotensive and spontaneously hypertensive rats. J Cereb Blood Flow Metab 23:154-165.

Willi R, Aloy E, Yee B, Feldon J, Schwab M (2008a) Behavioral characterization of mice lacking the neurite outgrowth inhibitor Nogo-A. Genes Brain Behav.

Willi R, Aloy EM, Yee BK, Feldon J, Schwab ME (2008b) Behavioral characterization of mice lacking the neurite outgrowth inhibitor Nogo-A. Genes Brain Behav.

Wojcik S, Engel WK, Askanas V (2006) Increased expression of Noga-A in ALS muscle biopsies is not unique for this disease. Acta Myol 25:116-118.

Wong ST, Henley JR, Kanning KC, Huang K-h, Bothwell M, Poo M-m (2002) A p75NTR and Nogo receptor complex mediates repulsive signaling by myelin-associated glycoprotein. 5:1302-1308.

Xiong L, Rouleau GA, Delisi LE, St-Onge J, Najafee R, Riviere JB, Benkelfat C, Tabbane K, Fathalli F, Danics Z, Labelle A, Lal S, Joober R (2005) CAA insertion polymorphism in the 3'UTR of Nogo gene on 2p14 is not associated with schizophrenia. Brain Res Mol Brain Res 133:153-156.

Yamashita T, Tohyama M (2003) The p75 receptor acts as a displacement factor that releases Rho from Rho-GDI. Nat Neurosci 6:461-467.

Yiu G, He Z (2006) Glial inhibition of CNS axon regeneration. Nature Reviews Neuroscience 7:617-627.

Yonemori F, Yamaguchi T, Yamada H, Tamura A (1999) Spatial cognitive performance after chronic focal cerebral ischemia in rats. J Cereb Blood Flow Metab 19:483-494.

Z'Graggen WJ, Metz GAS, Kartje GL, Thallmair M, Schwab ME (1998) Functional Recovery and Enhanced Corticofugal Plasticity after Unilateral Pyramidal Tract Lesion and Blockade of Myelin-Associated Neurite Growth Inhibitors in Adult Rats. J Neurosci 18:4744-4757.

Zhang L, Zhang RL, Wang Y, Zhang C, Zhang ZG, Meng H, Chopp M (2005) Functional Recovery in Aged and Young Rats After Embolic Stroke: Treatment With a Phosphodiesterase Type 5 Inhibitor. Stroke 36:847-852.

Zheng B, Ho C, Li S, Keirstead H, Steward O, Tessier-Lavigne M (2003) Lack of Enhanced Spinal Regeneration in Nogo-Deficient Mice. Neuron 38:213-224.

Zheng B, Atwal J, Ho C, Case L, He X-l, Garcia KC, Steward O, Tessier-Lavigne M (2005) Genetic deletion of the Nogo receptor does not reduce neurite inhibition in vitro or promote corticospinal tract regeneration in vivo. Proc Natl Acad Sci U S A 102:1205-1210.

Zhu HY, Guo HF, Hou HL, Liu YJ, Sheng SL, Zhou JN (2007) Increased expression of the Nogo receptor in the hippocampus and its relation to the neuropathology in Alzheimer's disease. Hum Pathol 38:426-434.

VITA

Rebecca Lynn Gillani was born February 23, 1982 in Wheatland, Wyoming to William and Jo Ann Smith. She graduated from Woodstown High School in Woodstown, New Jersey in 2000. At the University of Illinois at Urbana-Champaign, Ms. Gillani majored in Cell and Structural Biology and graduated in December 2003 as a James Scholar and with University Honors. From 2001-2003 Ms. Gillani worked as an undergraduate researcher in the laboratory of Dr. William T. Greenough and was awarded a Cell and Structural Biology Senior Distinction in 2003 for her work on the role of Fragile X Mental Retardation Protein in dendritic pruning.

In December 2003 Ms. Gillani joined the laboratory of Dr. Paul E. Gold at the University of Illinois at Urbana-Champaign as a research assistant for projects studying the modulation of learning and memory by hormones, and the neurochemical basis of learning and memory.

In 2004 Ms. Gillani began her MD/PhD training at Loyola University Chicago, and joined the laboratory of Dr. Gwendolyn L. Kartje to study the therapeutic potential of anti-Nogo-A immunotherapy for cognitive impairments after stroke in the aged. Ms. Gillani was awarded a Ruth L. Kirschstein National Research Service Award from the National Institute of Neurological Disorders and Stroke in June 2007 to support her training. Ms. Gillani is a student member of the Society for Neuroscience.

DISSERTATION APPROVAL SHEET

The dissertation submitted by Rebecca Lynn Gillani has been read and approved by the following committee:

Gwendolyn L. Kartje, M.D., Ph.D. (Dissertation Advisor and Committee Chair)
Professor of Cell Biology, Neurobiology and Anatomy, and Neurology
Associate Director of the Neuroscience Institute
Loyola University Chicago
Chief of Neuroscience Research
Edward Hines Jr. V.A. Hospital

Kathryn J. Jones, Ph.D.
Professor of Cell Biology, Neurobiology and Anatomy, and Otolaryngology
Director of the Neuroscience Institute
Loyola University Chicago
Research Career Scientist
Edward Hines Jr. V.A. Hospital

Jody L. Martin, Ph.D.
Associate Professor of Medicine
Graduate Faculty of Physiology
Loyola University Chicago

Edward J. Neafsey, Ph.D.
Professor of Cell Biology, Neurobiology and Anatomy
Director of the Neuroscience Graduate Program
Loyola University Chicago

Michael J. Schneck, M.D.
Associate Professor of Neurology and Neurological Surgery
Loyola University Chicago

Douglas G. Wallace, Ph.D.
Assistant Professor of Psychology
Northern Illinois University

The final copies have been examined by the director of the dissertation and the signature which appears below verifies the fact that any necessary changes have been incorporated and that the dissertation is now given final approval by the committee with reference to content and form.

The dissertation is therefore accepted in partial fulfillment of the requirements for the degree of Doctor of Philosophy.

_____ _____

Date Director's Signature